

11-7-2006

Red Tides In the Gulf of Mexico: Where, When, and Why?

J. J. Walsh

University of South Florida, jwalsh@seas.marine.usf.edu

J. K. Jolliff

University of South Florida

B. P. Darrow

University of South Florida

J. M. Lenes

University of South Florida

S.P. Milroy

University of South Florida

See next page for additional authors

Follow this and additional works at: https://aquila.usm.edu/fac_pubs



Part of the [Marine Biology Commons](#)

Recommended Citation

Walsh, J., Jolliff, J., Darrow, B., Lenes, J., Milroy, S., Remsen, A., Dieterle, D., Carder, K., Chen, F., Chen, F., Vargo, G., Weisberg, R., Fanning, K., Muller-Karger, F., Shinn, E., Steidinger, K., Heil, C., Tomas, C., Prospero, J., Lee, T., Kirkpatrick, G., Whittedge, T., Stockwell, D., Villareal, T., Jochens, A., Bontempi, P. (2006). Red Tides In the Gulf of Mexico: Where, When, and Why?. *Journal of Geophysical Research-Oceans*, 111(C11).

Available at: https://aquila.usm.edu/fac_pubs/2168

Authors

J. J. Walsh, J. K. Jolliff, B. P. Darrow, J. M. Lenex, S.P. Milroy, A. Remsen, D.A. Dieterle, K.L. Carder, F.R. Chen, F.R. Chen, G.A. Vargo, R.H. Weisberg, K.A. Fanning, F.E. Muller-Karger, E. Shinn, K.A. Steidinger, C.A. Heil, C.R. Tomas, J.S. Prospero, T.N. Lee, G.J. Kirkpatrick, T.E. Whitledge, D.A. Stockwell, T.A. Villareal, A.E. Jochens, and P.S. Bontempi

Red tides in the Gulf of Mexico: Where, when, and why?

J. J. Walsh,¹ J. K. Jolliff,^{1,2} B. P. Darrow,¹ J. M. Lenes,¹ S. P. Milroy,¹ A. Remsen,¹ D. A. Dieterle,¹ K. L. Carder,¹ F. R. Chen,¹ G. A. Vargo,¹ R. H. Weisberg,¹ K. A. Fanning,¹ F. E. Muller-Karger,¹ E. Shinn,¹ K. A. Steidinger,³ C. A. Heil,³ C. R. Tomas,⁴ J. S. Prospero,⁵ T. N. Lee,⁵ G. J. Kirkpatrick,⁶ T. E. Whitledge,⁷ D. A. Stockwell,⁷ T. A. Villareal,⁸ A. E. Jochens,⁹ and P. S. Bontempi¹⁰

Received 22 November 2004; revised 14 June 2006; accepted 3 July 2006; published 7 November 2006.

[1] Independent data from the Gulf of Mexico are used to develop and test the hypothesis that the same sequence of physical and ecological events each year allows the toxic dinoflagellate *Karenia brevis* to become dominant. A phosphorus-rich nutrient supply initiates phytoplankton succession, once deposition events of Saharan iron-rich dust allow *Trichodesmium* blooms to utilize ubiquitous dissolved nitrogen gas within otherwise nitrogen-poor sea water. They and the co-occurring *K. brevis* are positioned within the bottom Ekman layers, as a consequence of their similar diel vertical migration patterns on the middle shelf. Upon onshore upwelling of these near-bottom seed populations to CDOM-rich surface waters of coastal regions, light-inhibition of the small red tide of $\sim 1 \text{ ug chl l}^{-1}$ of ichthyotoxic *K. brevis* is alleviated. Thence, dead fish serve as a supplementary nutrient source, yielding large, self-shaded red tides of $\sim 10 \text{ ug chl l}^{-1}$. The source of phosphorus is mainly of fossil origin off west Florida, where past nutrient additions from the eutrophied Lake Okeechobee had minimal impact. In contrast, the P-sources are of mainly anthropogenic origin off Texas, since both the nutrient loadings of Mississippi River and the spatial extent of the downstream red tides have increased over the last 100 years. During the past century and particularly within the last decade, previously cryptic *Karenia spp.* have caused toxic red tides in similar coastal habitats of other western boundary currents off Japan, China, New Zealand, Australia, and South Africa, downstream of the Gobi, Simpson, Great Western, and Kalahari Deserts, in a global response to both desertification and eutrophication.

Citation: Walsh, J. J., et al. (2006), Red tides in the Gulf of Mexico: Where, when, and why?, *J. Geophys. Res.*, *111*, C11003, doi:10.1029/2004JC002813.

1. Introduction

[2] “I collected a little packet of this brown-colored fine dust ... From the direction of the wind whenever it has

¹College of Marine Science, University of South Florida, St. Petersburg, Florida, USA.

²Now at Naval Research Laboratory, Stennis Space Center, Mississippi, USA.

³Florida Marine Research Institute, Florida Fish and Wildlife Conservation Commission, St. Petersburg, Florida, USA.

⁴Center for Marine Science, University of North Carolina, Wilmington, North Carolina, USA.

⁵Rosenstiel School of Marine and Atmospheric Science, University of Miami, Miami, Florida, USA.

⁶Mote Marine Laboratory, Sarasota, Florida, USA.

⁷School of Fisheries and Ocean Sciences, University of Alaska, Fairbanks, Alaska, USA.

⁸Department of Marine Science, University of Texas, Port Aransas, Texas, USA.

⁹Department of Oceanography, Texas A&M University, College Station, Texas, USA.

¹⁰Department of Marine Science, University of Southern Mississippi, Stennis Space Center, Mississippi, USA.

fallen, ... we may be sure that it all comes from Africa ... It has often fallen on ships ... even more than a thousand miles from the coast of Africa and at points sixteen hundred miles distant in a north and south direction” ... on 18 March 1832 “not far from the Abrolhos Islets” [$\sim 13^\circ\text{S}$, 38°W], close to the Brazil coast ... “my attention was called to a reddish-brown appearance in the sea ... these are small bundles of *Trichodesmium erythraeum* ... found in the Red Sea [Montagne, 1844]. In almost every long voyage some account is given ... They appear especially common near Australia; and off Cape Leeuwin” at the West Australian coast [$\sim 35^\circ\text{S}$, 115°W] “... Captain Cook, in his third voyage, remarks that sailors ... gave the name of sea-sawdust” - Darwin [1839]. “Darwin [1846]” later “reported that in the Cape Verde Islands region, the North Star very often disappeared at about 30° above the horizon, due to high atmospheric turbidity, which led to problems in local navigation” [Schutz et al., 1981].

[3] Red tides of the ichthyotoxic *Karenia brevis* have been previously described as blooms of *Gymnodinium breve* or *Ptychodiscus brevis*, and are closely related to, if not synonymous with those of *Gyrodinium aureolum*,

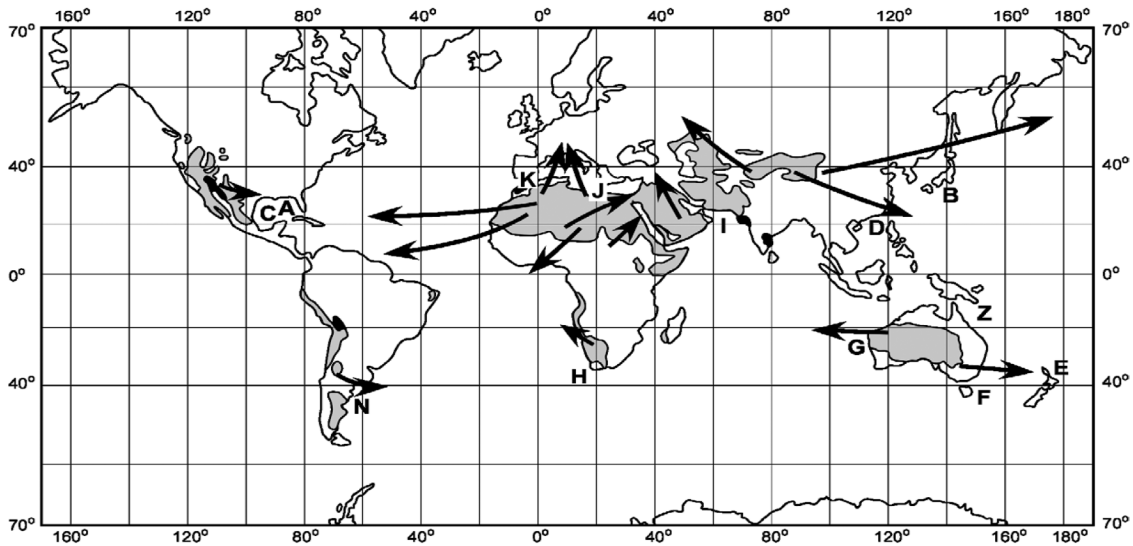


Figure 1. Locations of the Saharan, Saudi Arabian, Gobi, Simpson, Great Western, Kalahari, Atacama, and Patagonian Deserts and their downstream trajectories of aeolian dust [after Meigs, 1953; Pewe, 1981] in relation to red tides of *Karenia brevis/mikimotoi* off Florida (A) and Japan (B) over the last century, and off Texas (C), Hong Kong (D), New Zealand (E), Tasmania (F), Western Australia (G), South Africa (H), Kuwait (I), Greece (J), and Tunisia (K), over the last decade. The Argentine shelf (N) may have recent undetected red tides of *Karenia*, since *Trichodesmium* blooms and dust hazes prevail here, as well, while blooms of *Karenia* have been found off southern Chile. The Great Barrier Reef (Z) represents the null case of background populations of *Trichodesmium*, without dust influxes and low residual phosphate stocks, that yield small blooms of other dinoflagellates, instead of red tides of *Karenia*.

Gymnodinium nagasakiense, and *K. mikimotoi*. They have now become frequent events along the south Texas coast (Figure 1), meriting a discussion of their occurrence off Padre Island in Frommer’s latest guidebook [Baird et al., 2003]. Their past impact can perhaps be inferred from observations first recorded along Galveston Island in

1528–1534, when shellfish harvest was suspended seasonally [Cabeza de Vaca, 1871]. The annual occurrence of these toxic red tides of *K. brevis* off Texas (Figure 2a) is now similar to those in the eastern Gulf of Mexico, off Florida (Figure 2b). A knowledge of their common origin, in terms of the same environmental conditions that foster

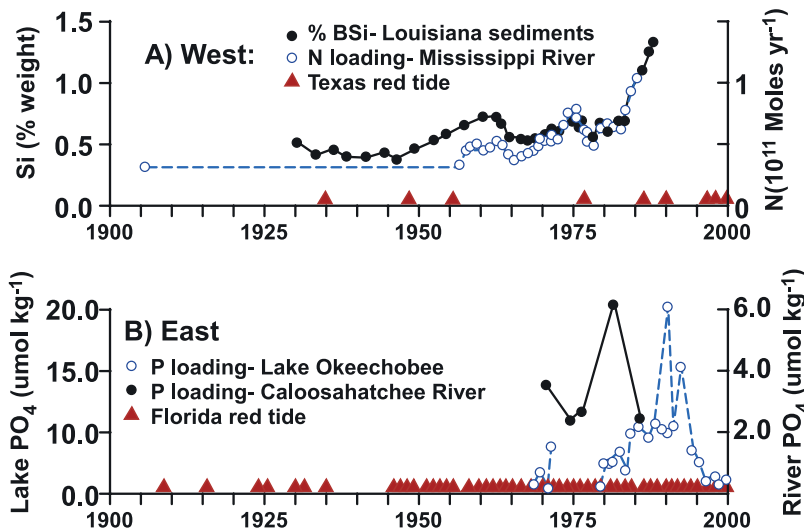


Figure 2. The occurrence over the last century of modern red tides of *K. brevis* (triangles) off (a) the Texas coast in relation to nutrient (N) loading of the Mississippi River (open circles) and accumulation of biogenic silica in Louisiana shelf sediments (solid circles), west of the Mississippi River delta [after Turner and Rabelais, 1994], and (b) the Florida coast in relation to the seasonally averaged nutrient content (P) of Lake Okeechobee at Moore Haven (open circles) and the Caloosahatchee River at Fort Myers (solid circles).

Table 1. First Occurrences of Red Tides of *Karenia spp./Gyrodinium aureolum* Within Coastal Habitats, Adjacent to Populations of *Trichodesmium* Within Warm Western Boundary Currents, and Downstream of Arid Regions

Species	Year	Region	Boundary Current ^a	Desert
<i>K. brevis</i>	1844	West Florida Shelf	Loop	Sahara
<i>K. mikimoto</i>	1893	Toba, Ise Bay, Japan	Kuroshio	Gobi
<i>K. brevis</i>	1935	South Texas Shelf	Loop	Sahara
<i>K. mikimotoi</i>	1998	Hong Kong, southern China	Kuroshio	Gobi
<i>K. digitata</i>	2000	Hong Kong	Kuroshio	Gobi
<i>K. longicanalis</i>	2001	Hong Kong	Kuroshio	Gobi
<i>Gyrodinium aureolum</i>	1966	Southern Norway	Gulf Stream	Sahara
<i>G. aureolum</i>	1968	Western Denmark	Gulf Stream	Sahara
<i>G. aureolum</i>	1971	Eastern Irish Sea	Gulf Stream	Sahara
<i>G. aureolum</i>	1976	Southern Ireland	Gulf Stream	Sahara
<i>G. aureolum</i>	1978	Western France	Gulf Stream	Sahara
<i>G. aureolum</i>	1981	Southern Brazil	Brazil	-
<i>G. aureolum</i>	1988	Northern Argentina	Brazil	Patagonia
<i>K. spp.</i>	1999	Southern Chile Shelf	El Nino/Humboldt ^a	Altacama
<i>G. aureolum</i>	1991	Tunisia		Sahara
<i>K. selliformis</i>	1999	Kuwait		Arabia
<i>K. bicuneiformis</i>	2003	Gordon's Bay, S. Africa	Agulhas	Kalahari
<i>K. cristata</i>	2003	Walker Bay, S. Africa	Agulhas	Kalahari
<i>G. aureolum</i>	1987	Hauraki Gulf	East Auckland	Simpson
<i>K. mikimotoi</i>	1992	Hauraki Gulf	East Auckland	Simpson
<i>K. brevisulcata</i>	2000	Wellington Harbor	East Auckland	Simpson
<i>K. concordia</i>	2004	Hauraki Gulf	East Auckland	Simpson
<i>K. papilionacea</i>	2004	New Zealand	East Auckland	Simpson
<i>K. asterichroma</i>	2004	Tasmania	East Australian	Simpson
<i>K. umbella</i>	2004	Tasmania	East Australian	Simpson
<i>K. umbella</i>	2004	Western Australia	Leeuwin ^a	Great Western

^aThe Humboldt and Leeuwin habitats are eastern boundary currents along South America and West Australia that at times flow polewards, in response to respective interannual and seasonal changes of alongshore pressure gradients.

their onset and maintenance of their blooms within both regions of Gulf of Mexico would aid both monitoring and amelioration of their present local harmful impacts - neurotoxic shellfish poisoning (NSP) and asthma symptoms - on humans who now live near Florida and Texas coastal waters.

[4] Indeed, if our hypothesis for the common origin of *K. brevis* on both sides of the Gulf of Mexico, i.e. in response to iron fertilization by Saharan dust of precursor blooms of the nitrogen-fixer, *Trichodesmium* [Walsh and Steidinger, 2001] on the outer shelf, adjacent to the western boundary current source of diazotrophs, is correct, it would have far-reaching implications. It could also explain the recent global outbreaks of other previously cryptic *Karenia spp.* within similar coastal habitats, adjacent to other western boundary currents and downstream of other arid areas, subjected to increased desertification over the last century (Table 1).

[5] The first modern South Texas red tide of *K. brevis*, inferred from aerosol impacts on humans, was a small one of short duration in 1935 [Lund, 1936]. The associated fish kills that year were also attributed to low salinity, fish gill clogging by diatoms, and toxic gasses of volcanic and/or anthropogenic origins [Buskey et al., 1996]. Earlier fish kills within Laguna Madre, off Corpus Christi during 1880, were similarly attributed to cold temperature and low salinity [Johnson, 1881]. After identification of the toxic dinoflagellate [Davis, 1948], however, a small second red tide was observed (Figure 2a) off south Texas during 1948 [Gunter, 1952].

[6] A third, larger red tide (Figure 2a) was found there in September 1955 at Port Isabel, TX [Wilson and Ray, 1956]. Another extensive Texas red tide was monitored during

1986 (Figure 2a) by aircraft [Trebatoski, 1988; Buskey et al., 1996], exhibiting the same alongshore trajectory as in 2000, from off Galveston on 4 September 1986 to the Mexican border by 16 October of that year. Here, another red tide was seen in 2000 by both the MODIS satellite (Figure 3) and coastal observers (Figure 4a). This 2000 red tide was then the largest of the four observed off Texas in 1996, 1997, 1999, and 2000. The economic consequences amounted to a loss of ~10.7 million dollars during 2000 within just Galveston county [Evans and Jones, 2001].

[7] Based on records of the Texas Parks and Wildlife Department [Denton and Contreras, 2004], the 2000 red tide began in early August off Port Arthur, TX (Figure 4a). By 9 September 2000, shellfish harvesting was closed in Galveston Bay. On 13 September 2000, a large fish kill was reported in Matagorda Bay. Red tides were later found in Corpus Christi Bay during October 2000, and by November 2000 all bay ecosystems, from Galveston to Port Isabel, had been impacted by *K. brevis* and associated fish kills.

[8] Furthermore, based upon other records of the Texas Department of Health, the Mexican Directorate for Environmental Health, and the Servicios de Salud de Vera Cruz [Tester et al., 2004], elevated brevetoxin levels within shellfish tissue extended as far south as the Mexican state of Vera Cruz, where the red tide persisted until February 2001. All together ~500 water samples documented the alongshore chronology of the red tide within Texas and Mexican coastal waters during 2000 [Denton and Contreras, 2004; Tester et al., 2004].

[9] In contrast, harmful algal blooms of *K. brevis* were usually more frequent events over the last century off Florida (Figure 1), with the first red tide of presumably *K. brevis* documented in 1844 [Feinstein, 1956]. Other

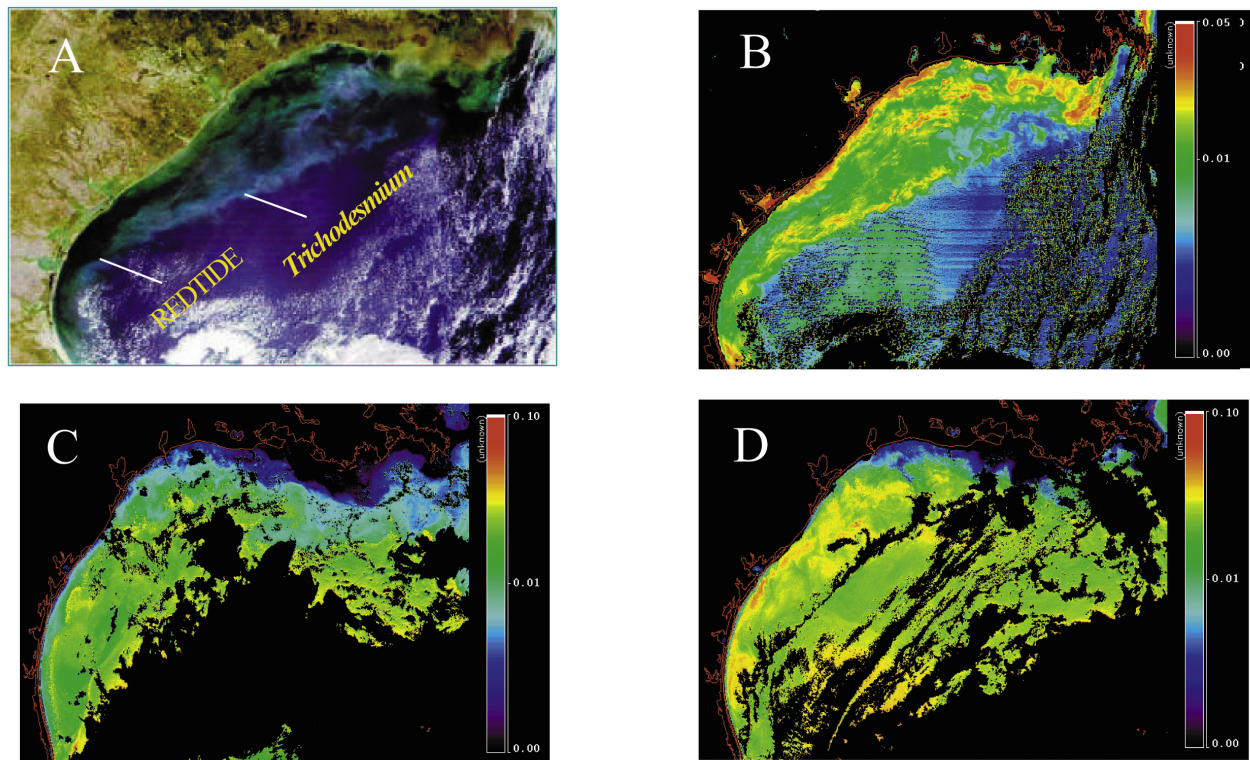


Figure 3. A MODIS Terra satellite estimate of red tide and *Trichodesmium* within the western Gulf of Mexico during July–September 2000. Based upon a backscatter algorithm [Cannizzaro *et al.*, 2004], the reddish-black color is a red tide of *Karenia brevis* and the pale blue color is co-occurring nitrogen fixers at depth, *Trichodesmium*, within offshore waters (a) on 29 September 2000. The high resolution RGB bands are 470, 555, and 659 nm. The other panels are the satellite estimates of backscatter per unit chlorophyll, on (b) the same day, and earlier on (c) 28 July 2000 and (d) 17 August 2000.

red tides followed during 1854, 1878–1879, and 1886, described as “dead fish in ... poisoned water ... of a reddish” and “red brick color” with “oysters ... in Tampa ... spoiled” ... “and clams ... of Sarasota Bay ... of a repulsive green hue at their edges” [Porter, 1879; Glazier, 1880; Ingersoll, 1881]. During 1957, before much phosphorus loading of Lake Okeechobee from agricultural runoff (Figure 2b), some red tides moved from south to north, along the west coast of Florida, from Naples to Tampa (Figure 4b), in a mirror image of the Texas red tides (Figure 4a).

[10] Based upon $\sim 10,000$ samples of red tides along the West Florida coast during 1957 to 1997 (Figure 2b) [Walsh and Steidinger, 2001], toxic levels of $>1 \times 10^5$ cells l^{-1} , or >1 μg chl l^{-1} , of *K. brevis* were usually first observed near shore at $\sim 27^\circ N$ latitude, between Tampa Bay and Charlotte Harbor (Figure 5). This region was thus selected as the study site for the ECOHAB (ECology and Oceanography of Harmful Algal Blooms) project on the West Florida Shelf (WFS) during 1998–2001. The NOAA/EPA supported ECOHAB program served as the catalyst for collaboration among other concurrent programs. They were: MMS NEGOM (NorthEastern Gulf Of Mexico); ONR FSLE (Florida Shelf Lagrangian Experiment); ONR HyCODE (Hyperspectral Coastal Ocean Dynamics Experiment); NSF DOTGOM (Details {Daughters} Of *Trichodesmium*

Gulf Of Mexico); and state-supported FMRI/MOTE projects of the Coastal Production cruises and the Sarasota cross-shelf time series (Figure 6).

[11] Extensive blooms of *K. brevis* were found off both Florida and Texas during September 2005 by the Florida Fish and Wildlife Conservation Commission and the Texas Parks and Wildlife Department, posing the question “do they form the same way, representing one phytoplankton niche in the Gulf of Mexico?” Indeed, based upon ribosomal DNA sequences, they are the same species of *Karenia brevis*, despite clonal differences in maximum growth rate and salinity tolerance [Loret *et al.*, 2002], on both sides of the Gulf.

[12] The answers to this question depend upon a subset of other questions. Given that these laboratory cultures of *K. brevis* can use most forms of inorganic nitrogen (nitrate, ammonium, nitrite) and at least urea [Baden and Mende, 1979; Steidinger *et al.*, 1998a], like other phytoplankton, but that they do not fix dinitrogen gas, N_2 , how do they accumulate 20–40 μg chl l^{-1} , or 8–16 μmol PN kg^{-1} , on the WFS at a PN/Chl ratio ($\mu mol/\mu g$) of 0.4 for these shade-adapted phytoplankton [Shanley and Vargo, 1993], if the ambient stocks of new nitrogen are <0.25 μmol NO_3 kg^{-1} [Masserini and Fanning, 2000]?

[13] Given that their field populations on the West Florida shelf have a maximum growth rate of only 0.4 day^{-1} at

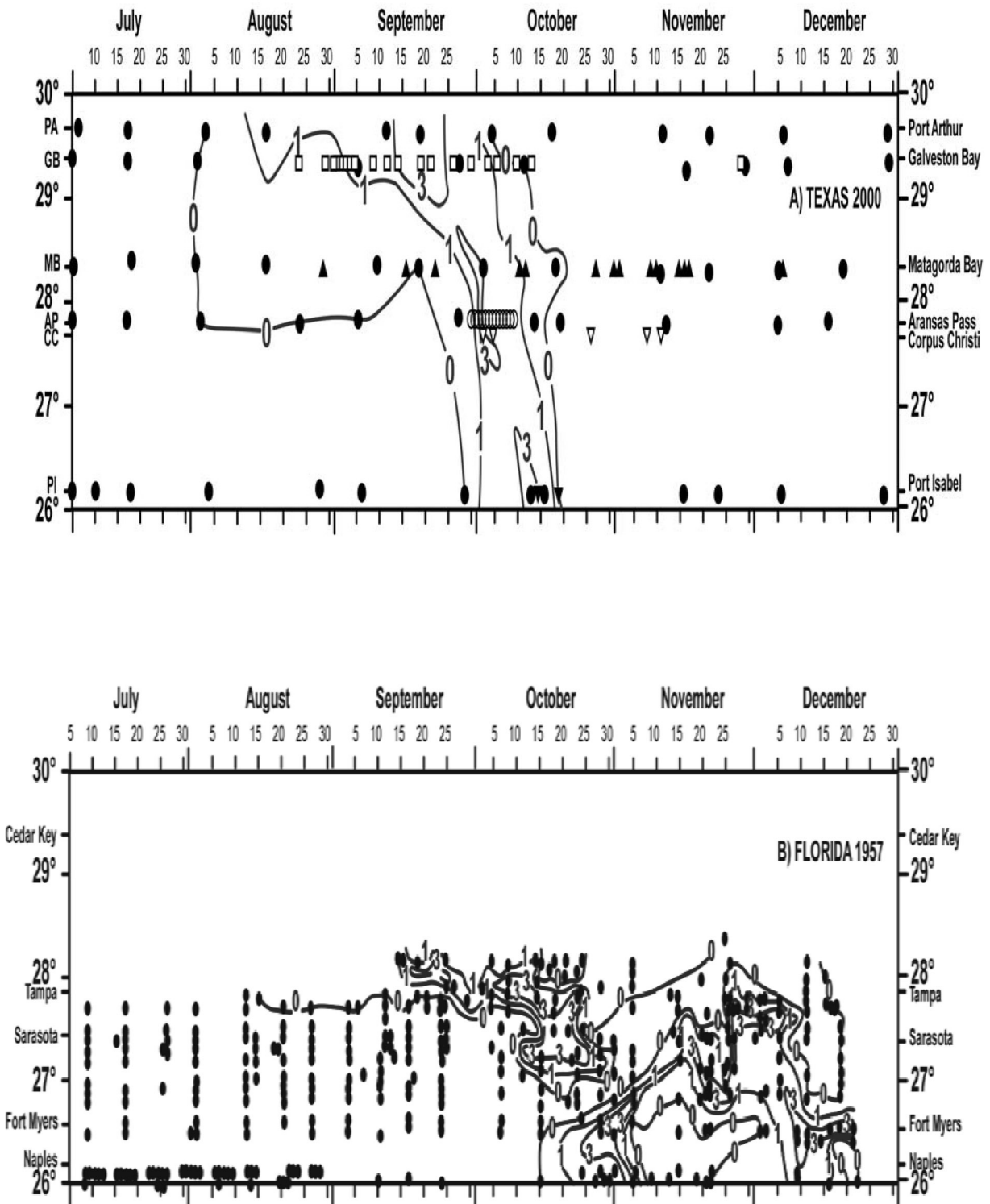


Figure 4. The surface observations of equivalent chlorophyll stocks ($\mu\text{g chl l}^{-1}$) of *K. brevis* abundance (assuming $10^{-5} \mu\text{g chl cell}^{-1}$) during (a) July–December 2000 off Texas [Denton and Contreras, 2004], where the red tide propagated southwards, from Port Arthur to Port Isabel, and (b) October–December 1957 off Florida [Dragovich et al., 1961; Dragovich, 1963], where the red tide mainly propagated northwards, from Naples to Tampa.

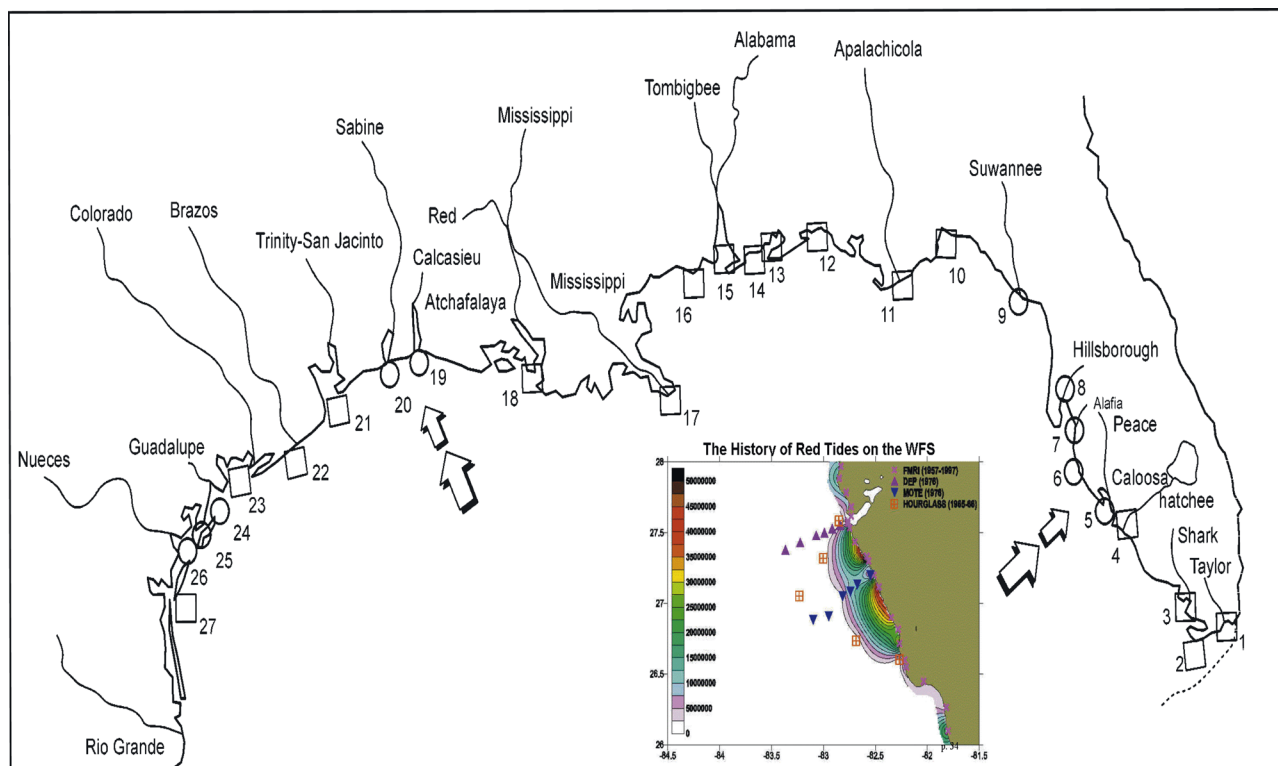


Figure 5. The cumulative distribution of the toxic dinoflagellate, *Karenia brevis*, on the West Florida shelf during 1957 to 1997, in relation to molar ratios of the total N/P stocks within 27 estuaries of the northern Gulf of Mexico [after Nordlie, 1990; Philips and Badylak, 1996; Turner and Rabalais, 1999; Rudnick et al., 1999]. When the river TDN/TDP ratios are less than 16, they are designated by open circles, with the numerals: (5) for Charlotte Harbor off the Peace River; (7) for Tampa Bay off Alafia River; (8) for Tampa Bay off Hillsborough River; and (9) for the Suwannee River. Areas identified as higher ratios than the Redfield one of 16 are instead indicated by open squares, with the numerals: (4) for San Carlos Bay off Caloosahatchee River; and (11) for the Apalachicola River. In other locations, number (1) designates eastern Florida Bay at the mouth of Taylor Slough; (2) western Florida Bay; (3) Ponce De Leon Bay off Shark River Slough; (6) Sarasota Bay; (10) Apalachee Bay; (12) Choctawhatchee Bay; (13) Pensacola Bay; (14) Perdido Bay; (15) Mobile Bay at the mouths of the Tombigbee and Alabama Rivers; (16) Mississippi Sound; (17) Mississippi River delta; (18) Atchafalaya Bay; (19) Calcasieu Lake off Calcasieu River; (20) Sabine Lake off Sabine River, (21) Galveston Bay off Trinity/San Jacinto Rivers; (22) Brazos River; (23) Matagorda Bay off Colorado River; (24) San Antonio Bay off Guadalupe River; (25) Aransas Bay; (26) Corpus Christi Bay off Nueces River; and (27) Laguna Madre, north of Rio Grande at Brownsville, TX. The large arrows denote epicenters of red tide initiation of *K. brevis*, within propitious physical and chemical habitats, off Florida and Texas.

ambient temperatures of $\sim 20^{\circ}\text{C}$, compared to three-fold larger mean growth rates of $\sim 1.2 \text{ day}^{-1}$ for diatoms, coccolithophores, coccoid cyanophytes, and microflagellates at the same temperature [Van Dolah and Leighfield, 1999; Walsh et al., 2001], how do red tides ever out compete other phytoplankton to accumulate stocks of $>20 \text{ ug chl l}^{-1}$ in the Gulf of Mexico? Indeed, when very strong upwelling prevails on the WFS, nitrate-assimilating diatoms are the dominant group of phytoplankton in both the “real world” and in models [Walsh et al., 2003], as within eastern boundary currents of usually more persistent upwelling [Walsh, 1996].

[14] Furthermore, given the relatively minimal thermal impact on solubility of dissolved nitrogen gas of $383\text{--}429 \text{ umol N}_2 \text{ kg}^{-1}$ [Weiss, 1970] within seasonal temperature changes of surface sea water of $\sim 18\text{--}25^{\circ}\text{C}$ at 35 per mil salinity on the WFS [Walsh et al., 2003], and the slow

growth rate for *Trichodesmium* of 0.4 day^{-1} at $\sim 20^{\circ}\text{C}$ [Walsh et al., 2001], should iron and/or phosphorus [Rueter et al., 1990, 1992; Paerl et al., 1994; Sanudo-Wilhelmy et al., 2001], more than N_2 , limit either nitrogen fixation, or transfer of DON to the rest of the food web in the Gulf of Mexico - as suggested many years ago for a nutrient source of Florida red tides [Lasker and Smith, 1954]?

[15] Finally, during the past century and particularly within the last decade, previously cryptic *Karenia spp.* have caused toxic red tides in similar coastal habitats of other western boundary currents off Japan, China, New Zealand, Australia, and South Africa, downstream of the Gobi, Simpson, Great Western, and Kalahari Deserts. Given these recent blooms, do they represent an expansion of the fish-killing niche of *Karenia*, in a global response to both desertification and eutrophication?



Figure 6. Locations of water samples of nutrients during Coastal Production (hearts), NEGOM (solid squares), FSLE (open quadrilateral polygons), and ECOHAB/HyCODE (pluses) cruises to the West Florida shelf in relation to Miocene phosphate-rich deposits of the underlying sediments and adjacent land. The estimated land (shaded) and marine (solid curve) extent of the fossil phosphorus was based on well cores [Ryder, 1985], sediment phosphorite percentages [Bates, 1963; Birdsall, 1979], and logs of quartz sand deposits [Cunningham *et al.*, 1990].

[16] We thus begin this analysis with the 20-fold larger data set on red tides and associated environmental variables within the eastern Gulf of Mexico (Figure 6), than in the western Gulf (Figure 7), to construct our hypothesis that blooms of *K. brevis* on both the western and eastern sides of the Gulf have the same origin of energy transfer between two groups of slow-growing, vertically migrating phytoplankton, allowing them both to out compete the faster growing diatoms that utilize nitrate during most boreal spring blooms.

[17] One group is Sun-adapted diazotrophs within the Gulf of Mexico, reflecting a nutrient supply of iron from Saharan dust at the sea surface of a high incident radiation regime, to synthesize nitrogenase enzymes used in nitrogen-fixation. Such synthesis involves a ten-fold larger iron-demand than during formation of nitrate reductase by diatoms and flagellates [Rueter *et al.*, 1992; Sunda and Huntsman, 1995; Orcutt *et al.*, 2001]. The other group is shade-adapted toxic dinoflagellates, reflecting a nutrient supply of phosphorus in either phosphorite, phosphate, or organic form from the sea bottom of a low incident radiation regime, to synthesize enzymes involved in ammonium-assimilation.

[18] Specifically, we use observations from the eastern Gulf of Mexico to develop the hypothesis that a full sequence of physical and ecological events is required each year for *K. brevis* to become the dominant feature of coastal food webs: (1) phosphorus-rich nutrient supply at low DIN/PO₄ ratios, relative to the Redfield ratio of ~ 16 for balanced phytoplankton growth, from initial and recycled estuarine/ground water origins to eliminate competitors;

(2) aerosol delivery of iron-rich desert dust (Figure 1) there to alleviate iron-limitation of nitrogen fixers on the outer shelf; (3) allowing a subsequent *Trichodesmium* bloom; (4) above phosphate-rich midshelf waters; (5) with co-aggregation of slow growing, Sun-adapted diazotrophs and shade-adapted toxic dinoflagellates that both vertically migrate to the bottom of the midshelf euphotic zone, such that they are positioned within subsequent near-bottom

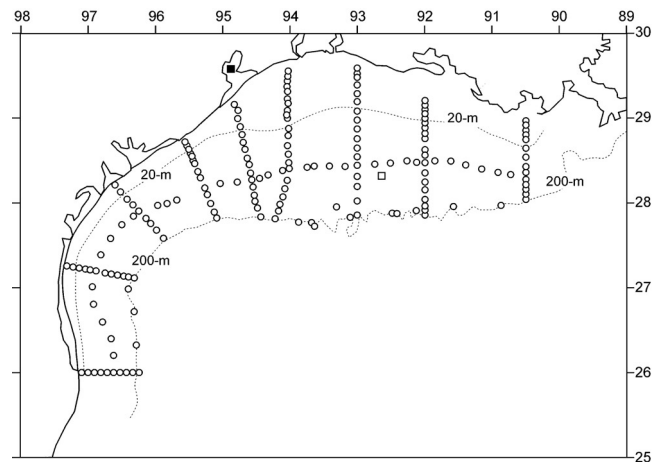


Figure 7. Locations of water samples (open circles) of nutrients and pigments during the LATEX survey of 26 July–8 August 1993, in relation to a vertical profile of 226radium (open square) obtained in July 1975 [Reid, 1984].

Ekman layers; (6) for onshore currents to upwell at the seaward side of near-bottom convergence fronts their seed populations of near-aphotic waters to CDOM-rich surface waters of coastal regions, easing light-inhibition here of; (7) small initial red tides of ichthyotoxic *K. brevis*; (8) grown from DON release upon demise of the precursor diazotroph bloom, (9) and then dead fish serving as supplementary nutrient source; (10) to yield a self-shaded, large red tide, fed from decaying diazotrophs and fish.

[19] We then validate each of the ten steps of this hypothesis with independent observations on the origins of both diazotroph blooms and red tides of the same species of *Karenia* and *Trichodesmium* within the western Gulf of Mexico. Finally, a robust hypothesis should work for any coastal ecosystem similar to those of the Gulf of Mexico, i.e. western boundary currents, downstream of desert supplies of dust, in which *K. brevis*, or a cognate species is now dominant. We thus assemble information (Table 1) on recent outbreaks of *Karenia spp* in relation to dust supplies of iron and known distributions of *Trichodesmium* within western boundary currents, adjacent to aerosol plumes emanating from the Sahara, Gobi, Simpson, Great Western, Kalahari, Arabian, and Patagonian Deserts, as well as the inferred rare reversal of an eastern boundary current downstream of the Atacama Desert of Chile (Figure 1).

2. Methods

2.1. Eastern Gulf Observations

[20] During March 1998–December 2001, 175 cruises of R/V *Eugenie Clark*, *Gyre*, *Suncoaster*, *Bellows*, *Sea Diver*, *Walton Smith*, and *Pelican* collected extensive data sets along the west coast of Florida (Figure 6). Observations consisted of: hydrography; turbidity; spectral dependence of light absorption; backscatter; water-leaving radiance; light attenuation; Saharan dust; dissolved nutrients [nitrate-NO₃, ammonium-NH₄, urea, phosphate-PO₄, silicate-SiO₄, iron-Fe, Dissolved Organic Phosphorus (DOP), Dissolved Organic Nitrogen (DON), Dissolved Inorganic Carbon (DIC), Dissolved Organic Carbon (DOC)]; Colored Dissolved Organic Matter (CDOM); brevetoxins; particulate constituents [chlorophyll, phaeopigments, Particulate Nitrogen (PN), Particulate Carbon (PC), Particulate Phosphorus (PP), del¹⁵N of PN as the ratio of nitrogen isotopes]; and counts of the dominant phytoplankton and zooplankton species. Moored arrays of current, temperature/salinity, and optical sensors were deployed at some locations on the WFS to monitor the physical habitat hourly, before and after the less frequent monthly shipboard surveys.

[21] Additionally, during 10–11 September 2002, the diel vertical distribution of *Trichodesmium* colonies over a 24-hour period above the 50 m isobath of the WFS at 27.2°N, 83.5°W was investigated with a plankton imaging sensor, using SIPPER, the Shadowed Image Particle Profiling and Evaluation Recorder [Remsen *et al.*, 2004]. During a time series of seven 2-hour deployments of HRS, the USF High Resolution Sampler [Sutton *et al.*, 2001] provided vertical profiles of the water column. Of the 1.2 million plankton images collected by SIPPER from 208 m³ of seawater, a total of 60,350 *Trichodesmium* colony images were identified, using a multiple-class support vector machine classifier [Luo *et al.*, 2004, 2005]. The accuracy

of the classifier in correctly identifying *Trichodesmium* colonies was 81.4%. We shall find that they vertically migrate on the WFS, like noxious red tides of *K. brevis* [Walsh *et al.*, 2002].

[22] A pressing need for management of such harmful algal blooms (HABs) is the development of numerical models for prediction of the onset and dispersal of coastal marine HABs [Franks, 1997; Donahy and Osborn, 1997; Walsh *et al.*, 2001]. Such models require accurate initial and boundary conditions to become realistic forecast tools. We use this recent information to identify the environmental factors that lead to initiation and maintenance of one specific HAB, that of *K. brevis* in the Gulf of Mexico. Given a “known” epicenter in the eastern Gulf (Figure 5), our model then explores the consequences of both fossil and anthropogenic sources of nutrients for this Gulf-wide HAB.

[23] Thus, we first consider the observational evidence for eventual formation of red tides of *K. brevis* at near-bottom convergence fronts in the eastern Gulf of Mexico. Here, we knew that near shore supplies of nutrients in a low molar N/P ratio intersected with offshore seed populations of this toxic dinoflagellate and co-occurring diazotrophs [Walsh and Steidinger, 2001]. Prior coupled, three-dimensional physical and ecological models had considered the importance of estuarine sources of CDOM as a light shield [Walsh *et al.*, 2003] and as an organic nutrient source [Jolliff *et al.*, 2003], but ignored the associated influxes of inorganic nutrients from rivers.

[24] Thus, the consequences of DIN/PO₄ loadings from 30 estuaries of the eastern Gulf of Mexico are now examined, based on their freshwater discharges and end member concentrations of the inorganic nutrients. Among these boundary conditions (Table 2), we chose DIN/PO₄ ratios: of 3.4–6.2 for the Caloosahatchee River, Charlotte Harbor, Sarasota and Tampa Bays to emphasize fossil nutrient loadings from the southern estuaries; of 79.2–96.3 for the Apalachicola, Perdido, Biloxi Rivers and Mobile Bay to stress anthropogenic nutrient supplies from the northern estuaries; and of 15.6 for the deep-sea supplies at depths of ≥300 m on the shelf-break boundary of the WFS model, based upon NEGOM data (Figure 6).

[25] Our numerical model analyses are concerned with the impact of both deep-sea supplies and these estuarine fluxes of inorganic nitrogen and phosphorus on the origin of red tides on the WFS. We then see how well our hypothesis of onset of red tides of *K. brevis* in the eastern and western Gulf of Mexico works for other shelves, where red tides of *Karenia spp* are found downstream of arid regions (Table 1). One caveat common to either side of the Gulf of Mexico, as well as for Hong Kong and southern Chile waters, is that for maintenance of the larger red tides, a supplemental nutrient source is required for the ichthyotoxic *K. brevis* of decomposing dead fish [Walsh *et al.*, 2006].

[26] To evaluate our complex hypothesis that estuarine nutrient conditioning at the landward side of near-shore, near-bottom convergence fronts begins a series of events, which determines the type and sequence of algal blooms in the Gulf of Mexico, we also examine the prior data on element ratios of Florida river end members. We relate the combined organic and inorganic forms of nitrogen and phosphorus within the eastern Gulf of Mexico estuaries (Figure 5) to both known phosphorite deposits on land

Table 2. Coastal Boundary Conditions of a Coupled Physical/Ecological Model of Carbon, Nitrogen, and Phosphorus Cycling on the West Florida Shelf

River/Estuary System	DOC, mg C/L	NO ₃ , μ M N	NH ₄ , μ M N	PO ₄ , μ M P	SS, mg/L	DIN/PO ₄ , molar
Mississippi River Delta	2.83	107.00	1.00	2.80	240.00	38.6
Pearl + B.Chitto R.	6.60	16.79	4.21	1.29	63.70	22.7
Mobile Bay	9.06	50.00	2.86	0.65	61.80	81.9
Pascagoula River	15.09	19.29	5.00	0.84	211.00	29.0
Wolf River	6.98	19.29	0.71	0.32	50.90	62.0
Biloxi River ^a	4.15	24.29	1.25	0.32	50.45	79.2
Perdido River	5.66	29.29	1.79	0.32	50.00	96.3
Choctawhatchee Bay	5.66	15.20	0.71	0.72	34.44	22.1
Pennascola Bay	4.97	8.57	2.86	0.30	18.89	37.8
St. Andrew Bay	6.58	8.21	2.14	0.32	9.50	32.1
Appalachicola River	3.58	23.21	1.79	0.31	43.50	80.0
Ochlockonee	9.81	7.86	2.86	0.77	5.00	13.8
St. Marks River	17.55	5.21	2.36	1.10	3.62	6.9
Econfina River	16.42	2.36	0.71	0.32	28.00	9.5
Aucilla River	22.64	3.43	2.86	1.39	5.00	4.5
Fenholloway River	18.49	4.14	4.29	3.55	5.00	2.4
Steinhatchee River	22.83	2.64	2.86	1.42	9.85	3.9
Suwanee River	23.02	35.46	2.85	4.32	9.07	8.9
Waccassassa R.	22.83	40.25	0.71	3.01	6.15	13.6
Withlacoochee River	22.83	6.66	2.98	2.13	3.08	4.5
Crystal R./Springs	1.13	21.43	2.86	1.35	2.00	17.9
Pithlascotee	9.25	3.57	3.57	1.87	9.07	3.8
Anlcote River	9.25	10.71	5.00	3.23	9.07	4.9
Tampa Bay and Vicinity	9.25	58.93	67.22	22.26	5.00	5.7
Sarasota Bay	7.36	8.90	8.47	10.48	5.10	4.5
Charlotte Harbor	25.28	63.12	4.77	20.18	22.70	3.4
Caloosahatchee River	5.47	21.43	5.00	4.26	10.00	6.2
Big Cypress Basin	15.66	1.40	1.93	0.52	2.00	6.4
Everglades Basin	15.66	1.68	9.69	0.65	7.35	17.6
Florida Bay	15.66	25.09	1.49	0.05	–	501.5

^aNo data available in the NWIS database for the Biloxi River; the boundary values were geographically interpolated to the nearest watersheds.

(Figure 6), tagged by high Ra-226 activity [Fanning *et al.*, 1982], and deep-sea pools of phosphate [Walsh *et al.*, 2003].

[27] Finally, with additional estimates of freshwater flows in the eastern Gulf of Mexico and the inorganic nutrient content of some river end members (Table 2), we then consider the fate of estuarine and deep-sea external supplies of nitrate, ammonium, and phosphate in the present three-dimensional, coupled biophysical model of the WFS. Without the estuarine influxes of NO₃, NH₄, and PO₄, it was previously employed in separate analyses of both shelf-break supplies of nitrate [Walsh *et al.*, 2003] and river supplies of labile DON [Jolliff *et al.*, 2003]. Details of the new model's assumptions, especially the boundary conditions and lack of iron limitation, are provided in Appendix A.

[28] We are not aware of any phosphorite deposits in south Texas soils, but there are uranium sources [U.S. Department of Energy, 2003] for the high Ra-226 activity of ~ 530 dpm m⁻³ found (the solid square of Figure 7) within Galveston Bay [Reid, 1984]. Farther offshore, a surface salinity of 29.68 psu in July 1975 was similar to that observed in July–August 1993. The associated radium-226 activity of ~ 164 dpm m⁻³ above the ~ 60 -m isobath in July 1975 [Reid, 1984] rules out the Mississippi River as the proximate major source of surface nutrients within this shelf region during 1993.

[29] Since the half-life of ²²⁶Ra is ~ 1600 years, it is conservative on the time scale of either seasonal fresh water discharges, or of the ~ 20 years separating the two sets of Texas observations. Thus, we use a regression of these salinity and ²²⁶Ra activity data [Reid, 1984] on the east Texas

shelf (the open square of Figure 7), with a r^2 of 0.95, to estimate a possible ²²⁶Ra freshwater source of ~ 402 dpm m⁻³ in either 1985, or 1993. Recall that the radium content of the Mississippi River is only ~ 100 dpm m⁻³ [Moore, 1967], but that of Galveston Bay is ~ 530 dpm m⁻³ [Reid, 1984]. Thus the radium tracer on the middle Texas shelf (Figure 7) suggests a local Texas origin, where the original nutrients of Mississippi River origin are recycled, altering their stoichiometry as a consequence of faster bacterial recycling of phosphorus from planktonic diatom debris [Grill and Richards, 1964]. Whatever the source of phosphorus: recycled and/or fossil Miocene supplies, it would appear that cell lysis of diazotrophs and thence fish are the major sources of red tides in the Gulf of Mexico, and elsewhere.

[30] The evidence for additional internal recycled nutrient sources from decaying fish at the same convergence fronts are thus explored. At each of the ten steps of our hypothesis evaluation, the various assumptions are tested with other independent data within the western Gulf of Mexico. There, we shall find that another “unknown” epicenter of red tide initiation at low N/P ratios is located underneath the plume of the Mississippi River on the shelf near the Louisiana-Texas border. The nutrient initial conditions of this northwestern epicenter are now apparently of mainly anthropogenic origin, rather than the mainly fossil origin of the southeastern epicenter off Florida. These observations are placed within the context of a century of red tide observations off the Florida and Texas coasts (Figure 2), in relation to phosphate mining and farming within the

drainage basins of the Kissimmee, Caloosahatchee, and Mississippi Rivers (Figure 5).

2.2. Western Gulf Observations

[31] Within the western Gulf of Mexico, field observations during 1986–87, 1992–1994, and 1998–2000 constitute tests of our hypothesis of red tide origin. A series of seven cross-shelf sections between the coast and the 50-m isobath, from off Brownsville, TX to Cameron, LA during the LATEX cruises of April 1992–December 1994 (Figure 7) provided estimates of near shore nutrient stocks [Jochens *et al.*, 1998], as well as phytoplankton biomass [Neuhard, 1994] and species composition [Bontempi, 1995]. Subsequent biweekly fin fish surveys of the Texas Parks and Wildlife Department yielded additional nutrient and phytoplankton samples at five locations within 15 km of the Texas coastline (Sabine Pass off Port Arthur, Bolivar Roads Pass off Galveston, Cavallo Pass off Matagorda Bay, Port Aransas Pass, and Brazos Santiago Pass off Brownsville) for an assessment of initial conditions of red tides between November 1998 and December 2000 [Villareal *et al.*, 2001].

[32] A third time series of aerosol iron measurements in relation to more frequent cell counts of *K. brevis* was obtained off Aransas Pass, TX during March–December 2000 [Biegalski and Villareal, 2005]. Furthermore, a fourth time series of in situ observations of red tide abundance was collected during 5 July–27 December 2000 along the Texas coast (Figure 4a), from Port Arthur to Port Isabel [Denton and Contreras, 2004]. At the end of this 2000 red tide, satellite imagery on 29 September captured a phytoplankton plume in surface waters of the Texas shelf (Figure 3), with a low backscatter signature (Figure 3b) of *K. brevis* (the black color of Figure 3a) [Cannizzaro *et al.*, 2004] in shelf waters off Brownsville, TX.

[33] Here, the MODIS satellite algorithm suggested a total phytoplankton biomass of ~ 10 $\mu\text{g chl l}^{-1}$ in 2000 - as observed there in 1999 [Villareal *et al.*, 2001]. Farther offshore, high backscatter estimates from space instead suggested [Subramanian *et al.*, 1999] populations of ~ 1 $\mu\text{g chl l}^{-1}$ of *Trichodesmium* in slope waters (the pale blue color of Figure 3a), with high backscatter per unit chlorophyll (Figure 3b). Were these nitrogen-fixers also present at the beginning of the 2000 red tide off Port Arthur, TX in July–August?

[34] Our concurrent ship surveys of slope waters at $\sim 95.3^\circ$, 26.8°N within the western Gulf of Mexico on 24 July 2000 then found a mean of 21 colonies l^{-1} of *Trichodesmium*. Their background chlorophyll stock was ~ 0.8 $\mu\text{g chl l}^{-1}$, assuming a colony size of $\sim 3 \times 10^4$ cells [Carpenter, 1983] and a chlorophyll content of $\sim 1.2 \times 10^{-6}$ $\mu\text{g chl cell}^{-1}$ [Borstad, 1982] for these diazotrophs. The MODIS imagery suggested a similar range of 0.1–1.0 $\mu\text{g chl l}^{-1}$ within this region of high backscatter per unit chlorophyll, a few days later on 28 July 2000 (Figure 3c).

2.3. Other Western Boundary Currents

[35] We conclude our analyses, with a discussion of the global implications of eutrophication and desertification on the recent emergence of previously cryptic *Karenia* species and associated fish kills within similar coastal habitats to those of the Gulf of Mexico: the East China Sea, with

respect to red tides off Japan and Hong Kong; and the Coral, Timor, and Tasman Seas, in relation to red tides off Australia and New Zealand; as well as in the Persian Gulf; the western Indian Ocean; the Argentine Sea; the Mediterranean Sea; and even the Irish and North Seas (Table 1).

3. Results

3.1. Estuarine Nutrient Supplies

[36] Total Dissolved Nitrogen (TDN) is defined as DIN + DON and Total Dissolved Phosphorus (TDP) is the sum of $\text{PO}_4 + \text{DOP}$, where DIN (dissolved inorganic nitrogen) is nitrite + $\text{NO}_3 + \text{NH}_4$. We thus ignore the most abundant component of inorganic nitrogen in the form of ~ 400 $\mu\text{mol N}_2 \text{ kg}^{-1}$ as a dissolved gas, used only by the nitrogen fixers. Bulk measurements of TDN and TDP are more frequent for the Gulf of Mexico estuaries [Nordlie, 1990; Turner and Rabalais, 1999; Rudnick *et al.*, 1999; Brand, 2002] than their components. Accordingly, we begin with TDN/TDP ratios and then consider mainly the inorganic forms in the model (Tables 2 and 3). When appropriate, each subsection describes our results from the eastern side of the Gulf, followed by those from Texas waters and other western boundary current systems.

[37] The average molar TDN/TDP ratio of the Peace River (Figure 5), draining the Florida Miocene Hawthorn phosphorite [Dragovich *et al.*, 1968] deposits (Figure 6), is 3.0, compared to those of 10.2 of the Hillsborough River at the head of Tampa Bay and of 11.1 in the Suwannee River to the north [Nordlie, 1990]. The Caloosahatchee River in the southwest Florida region drains Lake Okeechobee and the Everglades Agricultural Area [Havens *et al.*, 1996], but it instead has a TDN/TDP ratio of 57.7, like that of 52.4 found in the Apalachicola River farther to the north [Nordlie, 1990]. In contrast, the DIN/ PO_4 ratios of the Caloosahatchee and Apalachicola Rivers are 6.2 and 80.0 (Table 2), reflecting the fossil inorganic source of their respective drainage basins (Figure 5), not dissolved organic debris left behind after modification by bacteria and phytoplankton.

[38] DON is more refractory than DOP. For example, DON/DOP molar ratios of 51.2 were observed, after a phytoplankton population of mainly diatoms, with an initial molar PN/PP ratio of 16.8, was allowed to decay in the dark [Grill and Richards, 1964]. Thus, the estuarine TDN/TDP molar ratio is of most interest, when it is also lower than the Redfield ratio of 16 [Klausmeier *et al.*, 2004], in three regions of the Gulf of Mexico (#s 5–9, #s 19–20, and #s 24–26 of Figure 5), adjacent respectively to the Florida, Louisiana, and Texas shelves.

[39] Such an inferred N-limitation of phytoplankton growth from low N/P ratios within the eastern Gulf of Mexico - except, of course for the diazotrophic nitrogen fixers using N_2 - is confirmed by nutrient bioassays of the phytoplankton on the southern WFS off the Ten Thousand Islands [Brand, 2002]. A similar result was obtained from bioassays within western Florida Bay [Tomas *et al.*, 1999]. Since the N/P molar ratio of fertilizers applied to drainage basins of the Gulf of Mexico is ~ 8 [Turner and Rabalais, 1999], however, the P excess of the central west Florida region (Figure 5) could be attributed to both fossil phos-

Table 3. Model Parameters

Symbol	Parameter	Value/Units/Reference
θ_1	molar N to C ratio Phytoplankton	0.1509 mol N (mol C) ⁻¹ [Redfield et al., 1963]
θ_2	molar N to C ratio Bacteria	0.2000 mol N (mol C) ⁻¹ [Kirchman, 2000]
θ_3	molar N to C ratio DOM	0.0667 mol N (mol C) ⁻¹ [Benner et al., 1992]
θ_4	molar N to C ratio Phytodetritus	0.1333 mol N (mol C) ⁻¹ [Walsh et al., 1999]
θ_5	molar N to C ratio TCDOC	0.0250 mol N (mol C) ⁻¹ [Ertel et al., 1986]
ϑ_1	molar P to C ratio Phytoplankton	0.0094 mol P (mol C) ⁻¹ [Redfield et al., 1963]
ϑ_2	molar P to C ratio Bacteria	0.0189 mol P (mol C) ⁻¹ [Kirchman, 2000]
ϑ_3	molar P to C ratio DOM ^a	mol P (mol C) ⁻¹ [Lucea et al., 2003]
ϑ_4	molar P to C ratio Phytodetritus	0.0040 mol P (mol C) ⁻¹ [Paytan et al., 2003]
b	coefficient of NH ₃ uptake	1.5 (dimensionless) [Walsh et al., 1999]
κ	Particulate detritus solubilization rate	0.132 day ⁻¹ [Walsh et al., 1999]
GGE	bacterial Gross Growth Efficiency	0.3 Corg ass (Corg uptake) ⁻¹ [del Giorgio and Cole, 2000]
β	Fraction of TCDOC photolysis yield to labile DOC	0.1 mole C DOC (mole C photo) ⁻¹ (calibrated ^b)
η_1	photosynthetic quotient NO ₃ assimilation	1.3 mol O ₂ per mol C ass.[Laws, 1991; Redfield et al., 1963]
η_2	photosynthetic quotient NH ₄ assimilation	1.0 mol O ₂ per mol C assimilated [Laws, 1991]
η_3	phytoplankton respiration quotient	1.0 mol O ₂ per mol C respired [Laws, 1991]
η_4	bacteria respiration quotient	1.0 mol O ₂ per mol C respired [Laws, 1991]
η_5	photolytic remin quotient	1.0 mol O ₂ per mol C photochem. altered [Amon and Benner, 1996]
η_6	Nitrification O ₂ ratio	2.0 mol O ₂ per mol NH ₄ to NO ₃ (stoichiometry ^c)
Φ_C	Carbon specific quantum yield of Photosynthesis	0.075 mol C (mol photons) ⁻¹ [Wozniak et al., 2002]
g_{m20}	maximum gross assimilation rate for phytoplankton @ 20°C	0.12 hr ⁻¹ [Walsh et al., 1999]
g_{mb20}	maximum gross assimilation rate for bacteria @ 20°C	0.24 hr ⁻¹ [Kemp et al., 1993]
n_1	MM half saturation constant phytoplankton DIN	0.5 mmol C m ⁻³ [Walsh et al., 1999]
n_2	MM half saturation constant phytoplankton DIP	0.25 mmol P m ⁻³ [Riegman et al., 2000]
n_3	MM half saturation constant bacterial DOC	0.83 mmol C m ⁻³ [Walsh et al., 1999]
n_4	MM half saturation constant bacterial DIN	0.10 mmol N m ⁻³ [Vallino et al., 1996]
n_5	MM half saturation constant bacterial DIP	0.10 mmol P m ⁻³ [Holm and Armstrong, 1981]
Dr	maximum denitrification rate	0.01 day ⁻¹ [Herzfeld and Hamilton, 2000]
Nr	maximum nitrification rate	0.05 day ⁻¹ [Herzfeld and Hamilton, 2000]
w_{d1}	small detritus sinking rate	0.25 m day ⁻¹ (estimated)
w_{d2}	large detritus sinking rate	2.50 m day ⁻¹ [Walsh et al., 1999]
w_{d3}	sediment sinking rate	5.00 m day ⁻¹ [Walsh et al., 1999]
Kt	temperature coefficient	0.063°C ⁻¹ (calibrated to Q10)
ϵ_1	maintenance respiration rate of Phytoplankton	0.015 day ⁻¹ [Geider, 1992]
ϵ_2	maintenance respiration rate of Bacteria	0.015 day ⁻¹ [Geider, 1992]
α_1	fraction of grazed P carbon respired	0.35 [Walsh et al., 1999]
α_2	fraction of grazed P carbon to DOC	0.50 [Walsh et al., 1999]
α_3	fraction of grazed P carbon to SDET	0.10(2/3 of 0.15)
α_4	fraction of grazed P carbon to LDET	0.05(1/3 of 0.15)
α_5	fraction of solubilized particulate detritus	0.212 (calibrated ^d)
C:Chl	Carbon to Chlorophyll ratio	~50–150 mg C (mg Chl-a) ⁻¹ (Redalje unpublished ^e)
Pt	Minimum (threshold) phytoplankton carbon ^f	0.2 mmol C m ⁻³ (0.1 ug Chl-a L ⁻¹) [Ducklow, 2000]
Bt	Minimum (threshold) bacterioplankton carbon	0.2 mmol C m ⁻³ [Ducklow, 2000]

^aDOP/DOC ratios in coastal marine environments are often $\ll 0.00067$ [Hopkinson et al., 1997; Lucea et al., 2003; Hopkinson et al., 2002]. It is assumed that particulate organic phosphorus is remineralized whenever carbon is transferred to the DOC pool.

^bCalibrated from apparent quantum yield studies of terrigenous humics for NH₄ yield and labile organic carbon yield.

^cThe ideal stoichiometry for ammonium nitrification is $\text{NH}_4^+ + 1.5\text{O}_2 = \text{NO}_2^- + \text{H}_2\text{O} + 2\text{H}^+$; nitrite nitrification is $\text{NO}_2^- + 0.5\text{O}_2 = \text{NO}_3^-$; for a total yield of 2 moles O₂. If photosynthetic nitrate assimilation yields 8.6 moles O₂ (per mole N), while respiration of phytoplankton carbon yields 7.6 moles O₂ (per mole N) – then 2 moles O₂ consumption per nitrified mole N are required for Redfield stoichiometry (C:N:P:O₂ = 106:16:1:-138).

^dAssuming the remineralization of phytodetritus is due to particle adhesive bacteria of a C:P ratio = 53 and that DOM contains negligible DOP, then the bacteria must remineralize ~21% of the solubilized phytodetritus.

^eMean C:Chl ratio for the northern Gulf of Mexico ~50, as cited in Dagg [1995]; the range is adjusted to account for low light conditions.

^fThreshold carbon values are required for numerical stability; no loss processes occur below the threshold values.

phorus supplies [Dragovich et al., 1968] and more recent agriculture [Hammet, 1988].

[40] Sugar cane fields had been initiated around Lake Okeechobee by 1890. During the same period, phosphate mining began in the Peace River region [Derr, 1998]. Indeed, application of fertilizers to the fields around the Lake basically led to an anthropogenic eastward shift of the Miocene phosphorite deposits (Figure 6). Rapid expansion of the extent of sugar cane farms within the Everglades Agricultural Area [Snyder and Davidson, 1994] and subsequent back pumping of nutrient-rich waters into Lake Okeechobee [Havens et al., 1996], as well as the Caloosa-

hatchee River, did not occur, however, until after the Cuban revolution in 1959. Recall that the alongshore trajectory of a Florida red tide, past the mouth of the Caloosahatchee River (Figure 4b) is that of 1957, before significant phosphorus loading of this estuary (Figure 2a).

[41] A four-fold increase of sugar cane fields around Lake Okeechobee then occurred between 1960 and 1968 [Flaig and Havens, 1995]. In response, the phosphorus loadings to cattle ranches and dairy farms in the drainage basin of the Kissimmee River to the north of the Lake, and to sugar cane and vegetable corps within the Everglades Agricultural Area to the south, both doubled between 1973 and 1978 [Flaig

and Havens, 1995]. Over a 10 year prior after 1973, the phosphorus and nitrogen contents [Havens et al., 1996] of the Lake Okeechobee had also doubled. Using records of the United States Geological Survey (<http://nwis.waterdata.usgs.gov>) and the South Florida Water Management District (<http://sfwmd.gov/dbhdyrdo>), we compiled a time series over 1974–2000 (Figure 2b) of the seasonally averaged phosphate content near Moore Haven, FL on the west side of Lake Okeechobee.

[42] By 1884, a canal had been constructed, linking the downstream Caloosahatchee River with Lake Okeechobee [Gunter and Hall, 1965]. As early as 1965, the effluents of this river were thought to be unlikely sources of red tides on the WFS [Gunter and Hall, 1965], despite earlier advocacy of altering the drainage basin of the Caloosahatchee estuary [Slobodkin, 1953]. The mean phosphorus stock of the Caloosahatchee River at Fort Myers, FL (Figure 2b) over a 20 year period of 1966–1985 was then $3.8 \text{ umol PO}_4 \text{ kg}^{-1}$ (see USGS database). Are there any other earlier measurements of phosphorus on the WFS, since our assumption of the value of this boundary condition will be a major factor in alongshore propagation of this estuarine signal?

[43] Previously in July 1947, estimates of Total Phosphorus (TP) for this region of the 1947 red tide [Gunter et al., 1948] were a mean of $8.6 \text{ umol TP kg}^{-1}$ at a nearshore salinity of 32.6 psu off Sarasota, FL [Ketchum and Keen, 1948]. During January–July 1947, patches of as much as $1.4\text{--}6.0 \times 10^7 \text{ cells l}^{-1}$, or $140\text{--}600 \text{ ug chl l}^{-1}$ of *K. brevis*, were then found off Fort Myers and Venice, FL [Davis, 1948]. We assume a conservative mean stock for *K. brevis* of a ten-fold smaller amount of 37 ug chl l^{-1} , between these high patches. It yields a red tide estimate of $0.9 \text{ umol PP kg}^{-1}$ during January–July 1947, using a PN/chl ratio of 0.4 umol/ug for *K. brevis* [Shanley and Vargo, 1993] and a PN/PP ratio of 16. Because $\text{TP} = \text{PP} + \text{TDP}$, a mean phytoplankton biomass of $0.9 \text{ umol PP kg}^{-1}$ suggests that at least $7.7 \text{ umol TDP kg}^{-1}$ may have then been left behind by the phytoplankton in July 1947 off Sarasota, FL.

[44] During October 1952, another red tide (Figure 2b) was first noticed between Gasparilla and Sanibel Islands [Slobodkin, 1953]. In November 1952 along the 10-m isobath off Fort Myers, this red tide was sampled for nutrient and hydrographic observations [Chew, 1953]. By then, it extended from Naples north to Venice [Feinstein et al., 1955]. At a depth-averaged salinity of 33.68 psu, where only “moderate red water” was observed, the total phosphorus content was $0.73 \text{ umol TP kg}^{-1}$ near the mouth of the Caloosahatchee River [Chew, 1953]. A few km farther downstream at a mean salinity of 34.72 psu, the total phosphorus stock increased to $1.43 \text{ umol TP kg}^{-1}$, where “heavy red water” was found above the same isobath.

[45] Since the respective depth-averaged temperatures were 23.29°C and 23.76°C , most of the increase of mean supersaturation of oxygen, from 143.4% to 166.1% at the same stations, was attributed to photosynthesis of the red tide [Chew, 1953]. If the downstream increment of $0.70 \text{ umol TP kg}^{-1}$ was also due to growth of *K. brevis*, with a PN/PP molar ratio of 16 and a PN/chl weight/molar of 0.4 [Shanley and Vargo, 1993], it was equivalent to a red tide increase of 28 ug chl l^{-1} during November 1952. This red tide of $0.70 \text{ umol PP kg}^{-1}$ was described as “medium to

heavy” that year around Sanibel Island [Kusek et al., 1999], off Fort Myers. With initial ichthyotoxic levels of instead $\sim 1 \text{ ug chl l}^{-1}$, or $\sim 0.04 \text{ umol PP kg}^{-1}$, of *K. brevis* and $0.73 \text{ umol TP kg}^{-1}$ near the mouth of the Caloosahatchee River in November 1952, we conclude that 0.7 TDP kg^{-1} was the estuarine boundary condition that year.

[46] Later during the red tide of November–December 1954 (Figure 2b), above the $\sim 6\text{-m}$ isobath to the south of Sarasota off Gasparilla Island, a mean total phosphorus of $2.5 \text{ umol TP kg}^{-1}$ and $1.6 \times 10^5 \text{ cells l}^{-1}$ of *K. brevis* were also found at the same mean salinity of 32.6 psu [Hela, 1955]. Diurnal migration of *K. brevis* was then observed, with higher stocks of $1 \times 10^7 \text{ cells l}^{-1}$ of this toxic dinoflagellate found associated with dead and dying fish. However, a much smaller mean phytoplankton biomass of $1.6 \text{ ug chl l}^{-1}$, or $0.04 \text{ umol PP kg}^{-1}$, suggests a stock of at least $2.5 \text{ umol TDP kg}^{-1}$ during 1954.

[47] Farther inshore, at near zero salinity and no red tide within the Caloosahatchee River, a mean total phosphorus content of $1.1 \text{ umol TP kg}^{-1}$ was observed during 1952–1954 [Odum et al., 1955]. If no other phytoplankton, nor particulate detritus, were then present, a stock of $1.1 \text{ umol TDP kg}^{-1}$ would also have been inferred for this estuary during the early 1950s. We thus arrive at a mean prefertilization stock of total dissolved phosphorus along the WFS, between Fort Myers and Sarasota of $\sim 3.0 \text{ TDP kg}^{-1}$ during 1947–1954.

[48] Assuming that these earlier near shore DOP and PO_4 pools were then also equivalent - as in September 1998 (Figure 8), we estimate that the coastal phosphate stock during 1947–1954 was $1.5 \text{ umol PO}_4 \text{ kg}^{-1}$ along the southeastern boundary of the WFS. Indeed, within the Caloosahatchee River at Fort Myers during May 1949–August 1950, the mean phosphorus stocks were $1.2 \text{ umol PO}_4 \text{ kg}^{-1}$ and $1.4 \text{ umol DOP kg}^{-1}$, or a sum of 2.6 TDP kg^{-1} [Graham et al., 1954]. The earlier and more recent observations of phosphorus within coastal waters thus suggest a value of $1.5 \text{ umol PO}_4 \text{ kg}^{-1}$ for the background loading of leached Miocene phosphorite deposits (Figure 6) to the near shore WFS. During 1986–1996, the nutrient loadings from the surrounding drainage basin to the north and south of the Caloosahatchee River were two-fold more important than those from Lake Okeechobee to the east, in determining the amounts of phosphate and total phosphorus found in the estuary [Doering and Chamberlain, 1999].

[49] Thus, anthropogenic doubling of phosphate supplies for Florida red tides during 1966–1985, from either farming or mining [Graham et al., 1954], was not a factor promoting the initiations, either of the 1957 red tide (Figure 4b), or of the ones observed earlier during 1946–1947 [Gunter et al., 1948], 1952 [Chew, 1953], and 1954 [Hela, 1955; Odum et al., 1955], as well as of those found between 1854–1886 and 1916–1936 within the eastern Gulf of Mexico (Figure 2b). Furthermore, despite 40–53% reductions in the anthropogenic nitrogen and phosphorus loadings to Lake Okeechobee by 1979 [Havens et al., 1996], red tides have persisted on the adjacent WFS (Figure 2b).

[50] Because fossil pools of phosphorus have not yet been depleted in south central Florida (Figure 6), red tides have been observed every year since 1946 (Figure 2b), reflecting an increase in the number of observers rather than of red

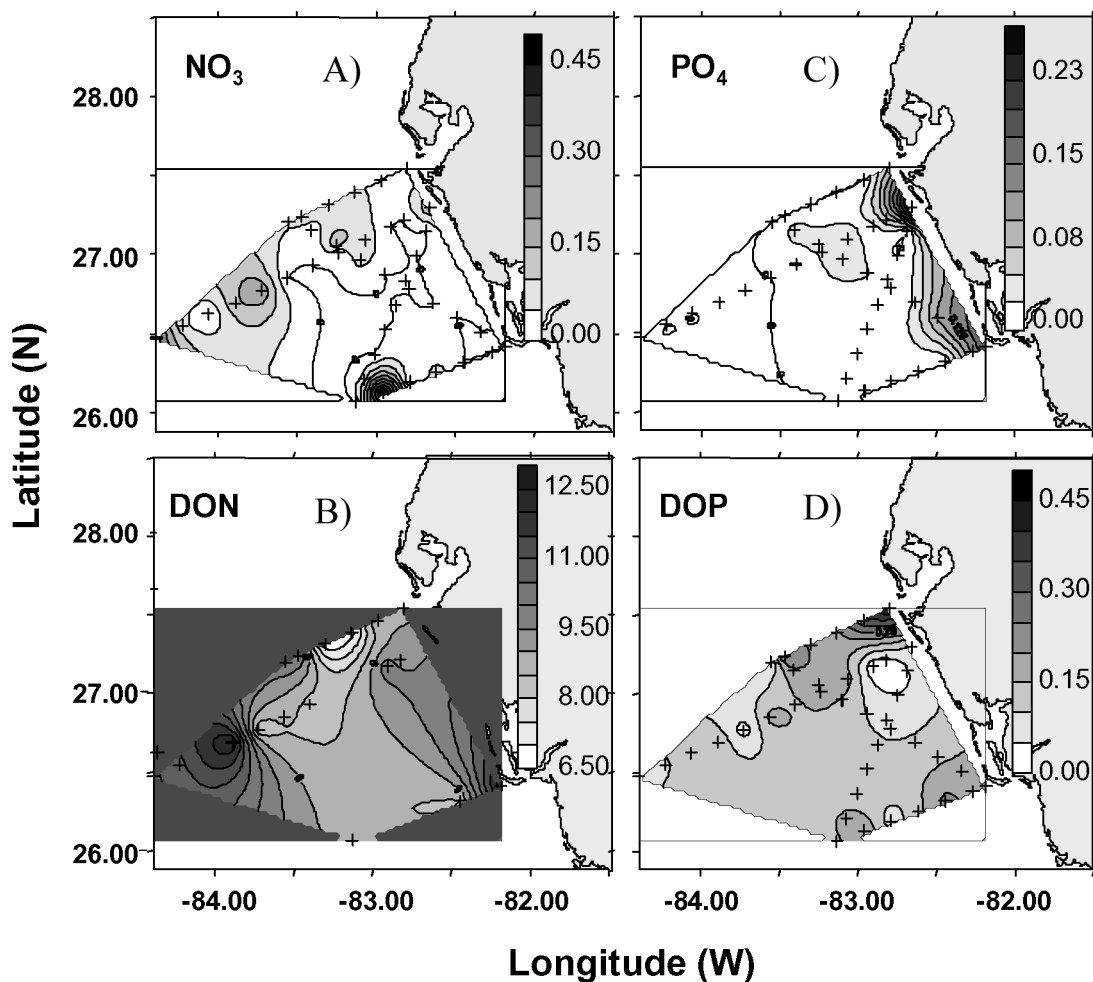


Figure 8. The chemical initial conditions of near-surface distributions of (a) nitrate, (b) dissolved organic nitrogen, (c) phosphate, and (d) dissolved organic phosphorus on the inner West Florida shelf, between Tampa Bay and Charlotte Harbor during 9–12 September 1998.

tides, first described in 1844. These annual events of Florida red tides occurred before and after phosphorus additions to Lake Okeechobee and the Caloosahatchee River in the 1970s (Figure 2b). The fossil supply of phosphorus to the WFS is thus more important than the agricultural legacy.

[51] The Taylor and Shark River Sloughs drain Lake Okeechobee (Figure 5) and the surrounding Everglades Agricultural Area, where a ten-fold expansion of the sugar cane farm area occurred since 1930 [Brand, 2002]. Yet, their TDN/TDP ratios were ≥ 50 after 1987 [Rudnick *et al.*, 1999], not those of 3–10 for either the west central Florida rivers (Figure 5), or fertilizer applied to agricultural regions around the Gulf of Mexico [Turner and Rabalais, 1999].

[52] Furthermore, long residence times of estuarine transit lead to less nitrogen export from Gulf of Mexico estuaries, i.e. smaller N/P ratios - as a result of particle fall out, sedimentary denitrification, and N_2 evasion. About 50% of the initial nitrogen loading is left after 100 days [Turner and Rabalais, 1999]. For example, at the south end of Lake Okeechobee, the molar TDN/TDP ratio is 72.6 [Brand, 2002], compared to that of 50.0 found downstream within Taylor Slough (Figure 5). But these values are still much larger than a Redfield ratio of ~ 16 required for balanced

growth of phytoplankton, and specifically for red tides of *K. brevis* [Wilson, 1966; Vargo and Howard-Shamblott, 1990].

[53] After drainage of the phosphate-rich Hawthorn formation [Dragovich *et al.*, 1968] of central West Florida (Figure 6), the mean nitrate ($50.9 \text{ umol NO}_3 \text{ kg}^{-1}$) and phosphate ($92.6 \text{ umol PO}_4 \text{ kg}^{-1}$) contents of the Peace River at Arcadia, FL are much larger than those of the Apalachicola River at Chattahoochee, FL ($16.7 \text{ umol NO}_3 \text{ kg}^{-1}$ and $0.6 \text{ umol PO}_4 \text{ kg}^{-1}$) in respective NO_3/PO_4 ratios of 0.5 and 27.8. Similarly, high phosphate values were recently found (Table 2) at the mouth of the Caloosahatchee River ($4.3 \text{ umol PO}_4 \text{ kg}^{-1}$ at an intermediate NO_3/PO_4 ratio of 5.0). Inclusion of ammonium stocks from additional USGS data (<http://nwis.waterdata.usgs.gov>) yields the DIN/ PO_4 ratios of 80.0 for the Apalachicola River, 6.2 for the Caloosahatchee River, and 3.4 for Charlotte Harbor, used in our simulation analyses (Table 2).

[54] Like the northern Florida estuaries, the TDN/TDP ratios at the mouths of the Mississippi and Atchafalaya Rivers are >16 (Figure 5), implying initial P-limitation of most phytoplankton, including the nitrogen-fixing diazotrophs. Initial phytoplankton incorporation of the Missis-

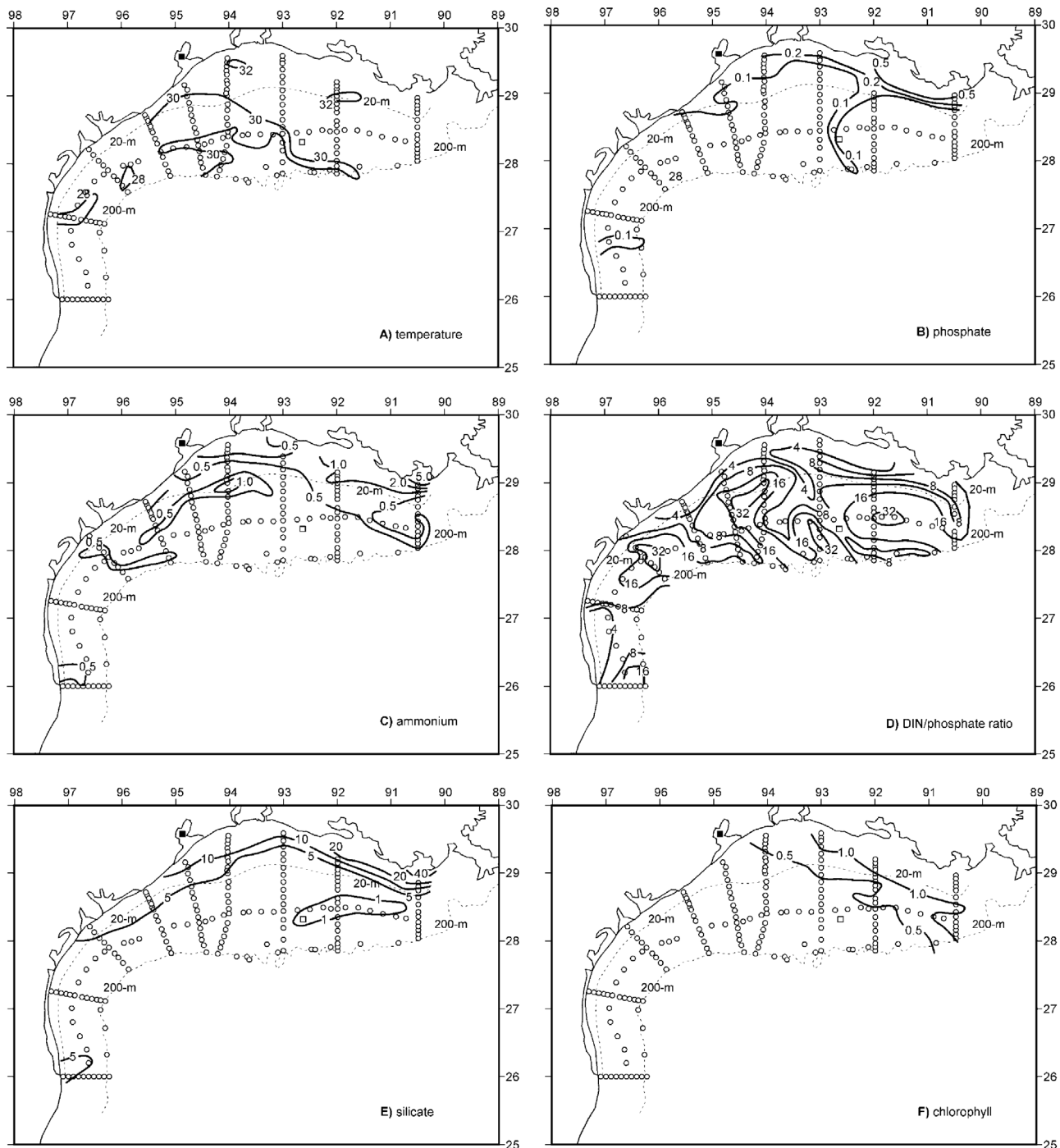


Figure 9. The physico-chemical initial conditions of near-surface distributions of (a) temperature, (b) phosphate, (c) ammonium, (d) DIN/phosphate ratio, (e) silicate, and (f) chlorophyll across the Texas-Louisiana shelf during the LATEX survey of 26 July–8 August 1993.

sippi River nutrient supplies, at the surface (Figure 9) with high N/P ratios, occurs as fast-growing [Fahnenstiel *et al.*, 1995] blooms of diatoms [Turner and Rabelais, 1994; Dortch and Whitledge, 1992]. Indeed, reflecting a long term increased influx of diatoms to surficial sediments [Walsh *et al.*, 1985], a two-fold increment of amorphous silica was observed at the bottom (Figure 2a) of the western Louisiana shelf by 1960 [Turner and Rabelais, 1994], over a 30-year period from \sim 1930. Here, biotic recycling within

near shore sediments leads to release of large amounts of dissolved silicon, ammonium, and phosphorus at low DIN/PO₄ ratios of <4 within near-bottom waters on the western Louisiana shelf (Figure 10). These low DIN/PO₄ ratios of near bottom, recycled marine stocks are the source of low TN/TP ratios found (#s 19–20 of Figure 4) within Sabine and Calcasieu Lakes [Turner and Rabalais, 1999] at the Texas-Louisiana border. During such upwelling, the near-bottom phosphorus-rich waters move onshore to prime

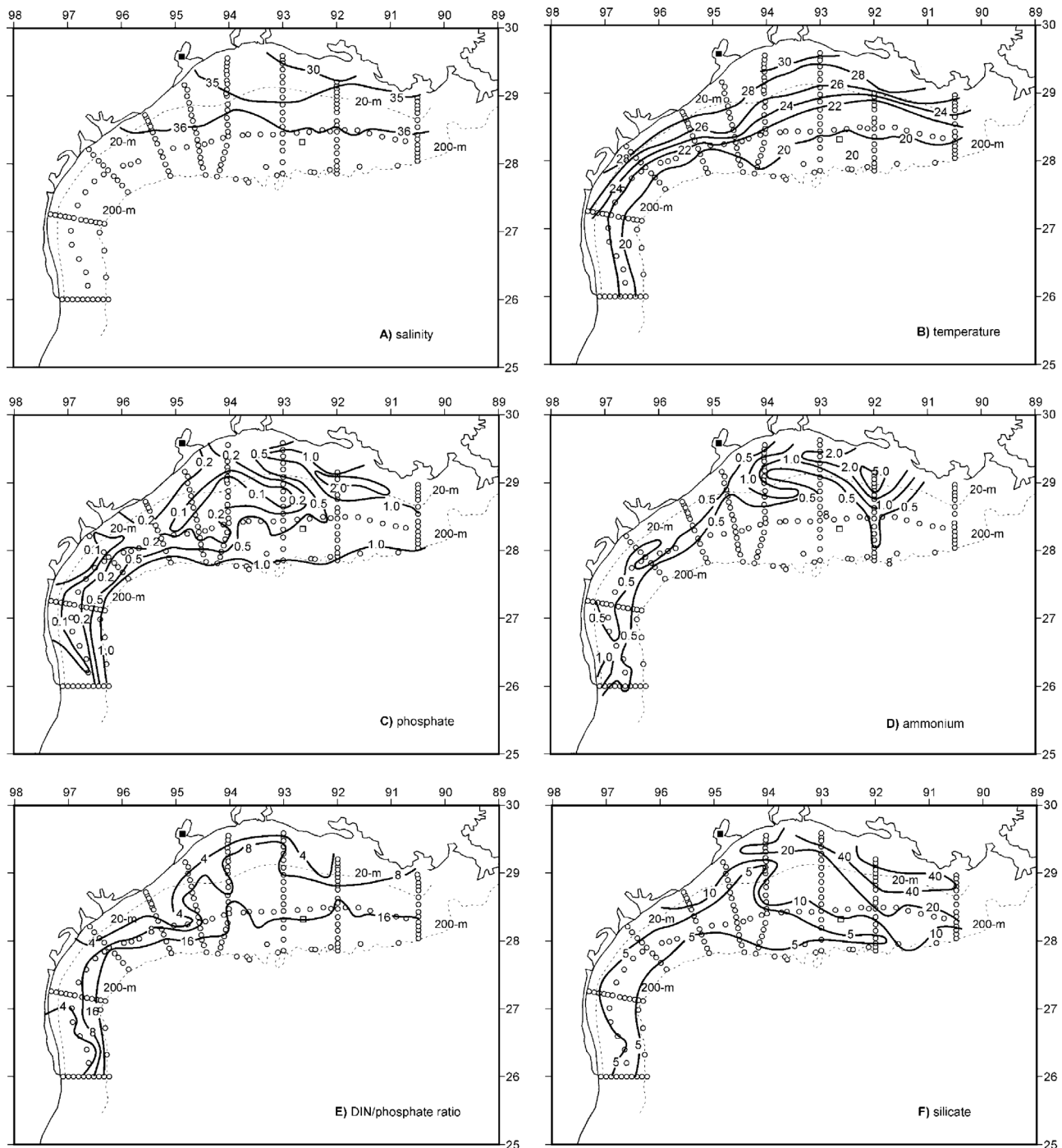


Figure 10. The physico-chemical initial conditions of near-bottom distributions of (a) salinity, (b) temperature, (c) phosphate, (d) ammonium, (e) DIN/phosphate ratio, and (f) silicate across the Texas-Louisiana shelf during the same LATEX survey. A bottom salinity of ~ 36.06 psu was also found in the same region on the outer shelf (open square) during July 1975 [Reid, 1984].

Trichodesmium blooms and thence red tides within downstream Texas waters.

[55] Farther south, the estuaries of the Nueces and Guadalupe Rivers (#s 24 and 26 of Figure 5), contain respective mean DIN/PO₄ ratios of ~ 6.1 [Whitledge, 1989] and 5.1 [Twilley *et al.*, 1999]. Furthermore, the peak runoff of the Nueces River in April–May 1990–1994 led to >250 $\mu\text{mol SiO}_4 \text{ kg}^{-1}$, >20 $\mu\text{mol NO}_3 \text{ kg}^{-1}$, >15 $\mu\text{mol NH}_4 \text{ kg}^{-1}$, and >8 $\mu\text{mol PO}_4 \text{ kg}^{-1}$ in Corpus Christi Bay. Such a DIN/PO₄

ratio of <5 should favor formation of diazotroph blooms and subsequent red tides on the adjacent Texas shelf, where the TN/TP ratio is <16 (Figure 5). Here, diatom and occasional coccoid cyanophyte blooms instead form, with as much as 60 $\mu\text{g chl l}^{-1}$ and primary production of 7 $\text{g C m}^{-2} \text{ day}^{-1}$ measured by us within Corpus Christi Bay.

[56] Despite a mean salinity of 32.1 parts per thousand in Corpus Christi Bay, however, local freshwater discharge is too small to impact the observed salinity structure of near

shore coastal waters [Jochens and Nowlin, 1999]. The southwest Texas situation of low DIN/PO₄ ratios within Corpus Christi Bay thus represents the first null case of our analysis, in which a region of low N/P ratios of adjacent estuaries does not form an epicenter of red tides in the Gulf of Mexico. Here, the additional necessary condition of a physical aggregation process is lacking, because low salinity is not present on the inner shelf [Jochens and Nowlin, 1999]. Thus, near-bottom convergence fronts, i.e. step 6 of our hypothesis - as occur on the Louisiana and central West Florida shelves- are rare off South Texas.

3.2. Chemical Initial Conditions on the Shelf

[57] Rainfall is bimodal in Florida, with a spring rainy season in the north and a summer one in the south. A peak discharge to Apalachicola Bay of $\sim 1300 \text{ m}^3 \text{ s}^{-1}$ in February–April [Gilbes *et al.*, 1996] is about 20-fold larger in the north than that of the Peace River freshwater influx of $\sim 65 \text{ m}^3 \text{ s}^{-1}$ to Charlotte Harbor in the south, during the local summer floods of July–September [McPherson *et al.*, 1990]. At similar respective volumes of ~ 12.6 and $14.0 \times 10^8 \text{ m}^3$ over the 2-m deep Apalachicola and Peace River estuaries [Livingston, 1984; McPherson *et al.*, 1990], the residence times of freshwater during peak river discharge are a maximum of ~ 12 days in the former and ~ 250 days in the latter.

[58] Accordingly, the nutrient signals of the northern river are found on the adjacent shelf during spring, whereas only the residues of phytoplankton and bacterial utilization escape the southern estuary in summer. Since phosphorus is recycled faster by bacteria than nitrogen [Grill and Richards, 1964], moreover, the longer residence time within Charlotte Harbor yields a DIN/PO₄ ratio of 3.4 from the original bulk TDN/TDP ratio of 3.0 [Nordlie, 1990]. In contrast with a much shorter residence time within the estuary of the Apalachicola River, the microbiota have no regenerative impact on the TDN/TDP ratio of 52.4 [Nordlie, 1990], yielding instead a DIN/PO₄ ratio of 80.0 (Table 2), i.e. a loss of phosphorus.

[59] By September, the dissolved TDP at the mouth of Charlotte Harbor consists of $>0.2 \text{ umol P kg}^{-1}$ of both PO₄ and DOP (Figure 8). Using the daily freshwater influxes during the previous summer-fall rainy periods of 1998, we previously estimated the rate of phosphorus-rich estuarine outwelling from Tampa Bay and Charlotte Harbor to the WFS [Vargo *et al.*, 2004]. At NO₃/PO₄ molar ratios of <2 , such effluxes meet most of the daily P-demand, on the adjacent inner WFS out to the 10-m isobath, of an initial small bloom of $\sim 1 \times 10^5 \text{ cells l}^{-1}$, or $\sim 1.0 \text{ ug chl l}^{-1}$, of *K. brevis*. However, the concurrent demands of nitrogen during balanced growth of the red tide are not satisfied.

[60] Yet, by early November 1998, in response to an iron deposition event during September (Figure 11), a red tide of $>0.5 \times 10^5 \text{ cells l}^{-1}$, or $>0.5 \text{ ug chl l}^{-1}$ was first found off the mouth of Charlotte Harbor and then as much as $10.0 \text{ ug chl l}^{-1}$ by December 1998 [Vargo *et al.*, 2004]. Where did all of the nutrients come from - particularly nitrogen - to yield such large red tides off Florida?

[61] *Trichodesmium* spp is a colonial, nitrogen-fixing, diazotroph. It was a co-dominant of the 1947 Florida red tide [Gunter *et al.*, 1948], from which *Gymnodinium breve*, i.e. *Karenia brevis*, was first described [Davis, 1948]. This

diazotroph resides in warm waters of the North Atlantic western boundary current system at the edge of the Brazil [Calef and Grice, 1966], Venezuelan [Margalef, 1965], Texas (Figure 3), Florida [King, 1950], Georgia [Dunstan and Hosford, 1977], and Irish [Farran, 1932] shelves, where it would first encounter high phosphate stocks within near-bottom waters of the outer shelf, e.g. Figure 10. The low N/P ratios of inner shelf waters off Florida (Figure 8) and Texas (Figure 9) prevent diatoms from winning - like they do in the high N/P Louisiana waters of the Mississippi River plume - but they represent the last pools of inorganic nutrients used by the diazotrophs, after onshore movement, in response to upwelling favorable winds.

[62] We believe that the nutrient pools of both near-bottom phosphorus and of atmospheric iron and dinitrogen gas on the outer shelves of the Gulf of Mexico are the first pools of inorganic nutrients, setting the stage for accumulation of initial diazotroph and dinoflagellate stocks there, that vertically migrate [Hela, 1955; Walsh *et al.*, 2002] together into bottom Ekman layers. Thus, their maintenance and ultimate impacts on fish and mammals are instead determined by the factors effecting recycled nutrient conditions of the inner shelves.

[63] The Mississippi River is, of course, the ultimate major source of both surface (Figures 9b–9e) and near-bottom (Figures 10c–10f) nutrients in the western Gulf of Mexico. After significant bacterial alteration of their original stoichiometry, however, the low near-bottom DIN/PO₄ ratios of <4 found during the LATEX cruises on the Louisiana-Texas shelf (Figure 10e) are similar to those of <3 within surficial sediments on the northern WFS [Darrow *et al.*, 2003] and at the mouth of Charlotte Harbor (Figure 8). Thus, in response to upwelling of altered initial chemical conditions at the Texas coast, these surface waters would also be subject to N-limitation of the phytoplankton. For example, the DIN/PO₄ ratio was 2.2 within near shore waters off Port Arthur, TX during 3–16 August 2000 [Villareal and Magana, 2001] at the onset of that red tide (Figure 2a).

3.3. Atmospheric Supplies

[64] *Trichodesmium* is a tropical nitrogen-fixer of Caribbean origin [Margalef, 1965; Calef and Grice, 1966; Borstad, 1982; Walsh, 1996; Lenes *et al.*, 2005] transported by the Loop Current into outer slope surface waters of the Gulf of Mexico, where background iron stocks of $\sim 0.2 \text{ nmol Fe kg}^{-1}$ [Lenes *et al.*, 2001] are ~ 100 -fold less than those at the mouth of Florida Bay [Caccia and Millero, 2003]. These diazotrophs vertically migrate at speeds of $\sim 1\text{--}2 \text{ m hr}^{-1}$ [Walsh *et al.*, 2001, 2002], such that they can daily harvest near-bottom phosphate stocks [Karl *et al.*, 1992] of $>0.25 \text{ umol PO}_4 \text{ kg}^{-1}$ above the 25–50 m isobaths of the WFS. Accordingly, when summer plumes of Saharan dust fall out on the WFS, these diazotrophs have been observed within 75 km of the West Florida coast for more than 50 years of plankton observations [King, 1950].

[65] Indeed, a delayed response of the 1998 red tide to iron fertilization off Florida (Figure 11) is consistent with the ~ 30 -day time lag of (1) first iron-stimulation of the *Trichodesmium* nitrogen fixers and (2) then final accumulation of $>10 \text{ ug chl l}^{-1}$ of the toxic dinoflagellates, found earlier during 1980 [Walsh and Steidinger, 2001]. The half-

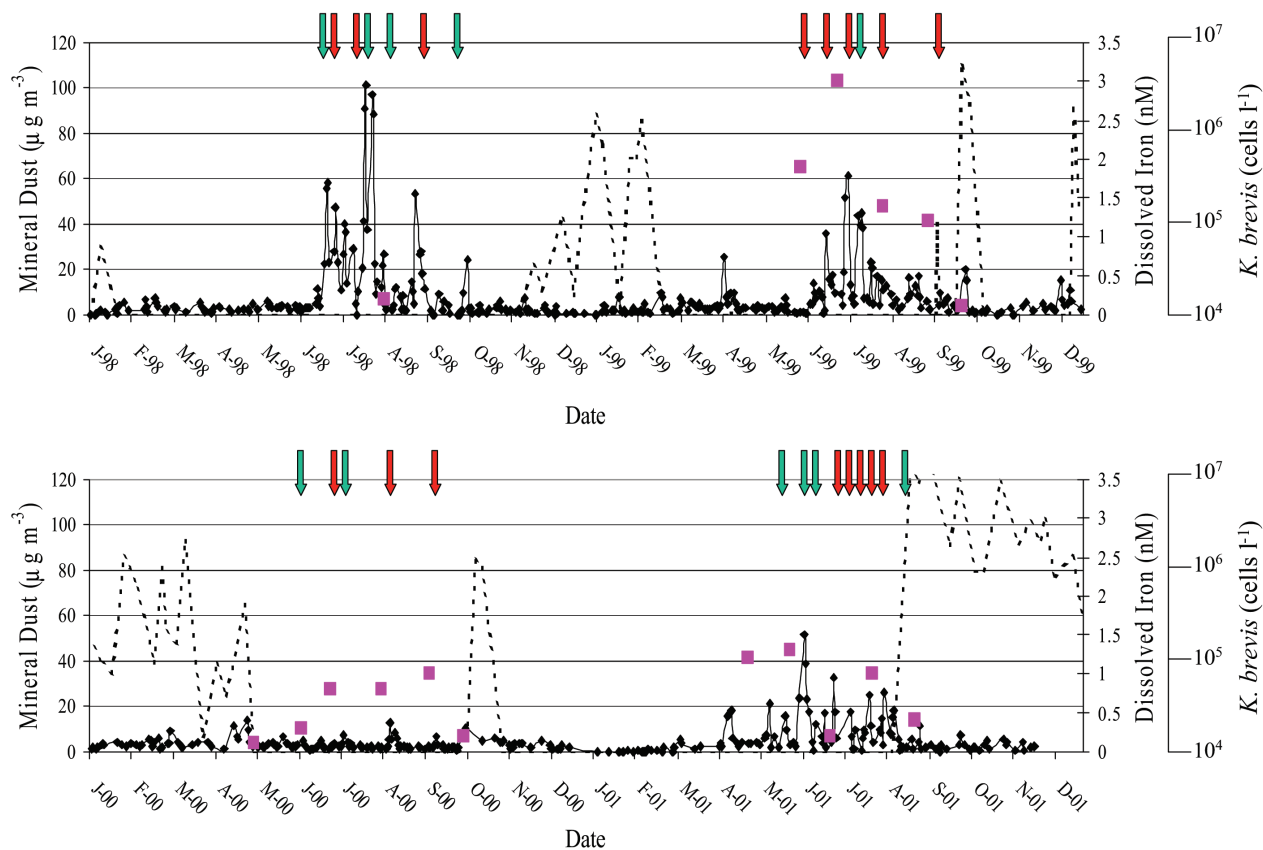


Figure 11. Mineral dust (blue) at Miami and red tides (dashed line) on the West Florida shelf during 1998–2001. Saharan dust events of low non-sea-salt nitrate are denoted by arrows, with the red ones indicating concurrent wet deposition (i.e., 24–48 hr delay) at Tampa Airport of >1.0 mm rainfall. Pink squares indicate mean dissolved Fe concentrations at ECOHAB stations within the surface waters of the outer west Florida shelf (50–200 m isobaths). The weekly means of the daily alongshore integrals of *K. brevis* populations are the dashed line of surface abundances (10^4 – 10^6 cells l^{-1}) within 9 km of the west Florida coast, from off Cedar Key to near Cape Romano.

saturation constant, n_{Fe} , of uptake of iron by phytoplankton is estimated to be 1.0 nmol Fe kg^{-1} for *Trichodesmium* and 0.2 nmol Fe kg^{-1} for either *K. brevis*, or diatoms [Walsh et al., 2001]. Thus, within a P-replete environment, the diazotrophs are Fe-limited and the toxic dinoflagellates are N-limited.

[66] We observed this sequence earlier on the WFS during June–July 1980 [Walsh and Steidinger, 2001]. A simple model of NH_4 and DON transfer between the co-occurring diazotrophs and *K. brevis*, growing at slow respective growth rates of 0.7 and 0.2 day^{-1} , then replicated the 1980 time series. Note further that each of the 1998–2001 fall red tides lagged both the summer influxes of Saharan dust, identified by low concentrations of non-sea-salt (nss) nitrate [Prospero et al., 1987], and increments of dissolved iron to the offshore incubators of *Trichodesmium* on the outer WFS (Figure 11).

[67] These diazotrophs require relatively large amounts of iron to make the enzyme nitrogenase for their fixation of dinitrogen gas, N_2 . They need about ten-fold more Fe than the diatoms demand to form nitrate reductase for their assimilation of nitrate, as reflected in Fe/PN molar ratios

of $\sim 2 \times 10^{-3}$ for *Trichodesmium* [Rueter et al., 1992] and $\sim 2 \times 10^{-4}$ for diatoms [Sunda and Huntsman, 1995]. Within regions of little nitrate, however, the smaller Fe-requirements of the diatoms would be moot.

[68] Furthermore, some dinoflagellates, which are closely related to *K. brevis*, e.g. *Gymnodinium sanguineum*, instead have a Fe/PN molar ratio of $\sim 5 \times 10^{-3}$ within iron-starved cultures, grown on nitrate and ammonium [Doucette and Harrison, 1991]. With a 2–3 fold greater Fe-requirement than *Trichodesmium*, the dinoflagellates are thus not the primary benefactors of initial aeolian supplies of iron. During rainfall events of Saharan dust deposition to the iron-poor surface waters on the outer WFS (Figure 11), the diazotrophs would out compete the red tide inocula for iron. Consequently, since the diazotrophs also use the ubiquitous dissolved dinitrogen gas, not just the ammonium, or urea, required by *K. brevis* [Steidinger et al., 1998a], they initiate the summer-fall succession of nonsiliceous phytoplankton on the WFS.

[69] Other wet deposition events of iron supply to the outer WFS were later observed, with means of ≥ 1.0 nmol Fe kg^{-1} found there in 1999 [Lenes et al., 2001] and 2000

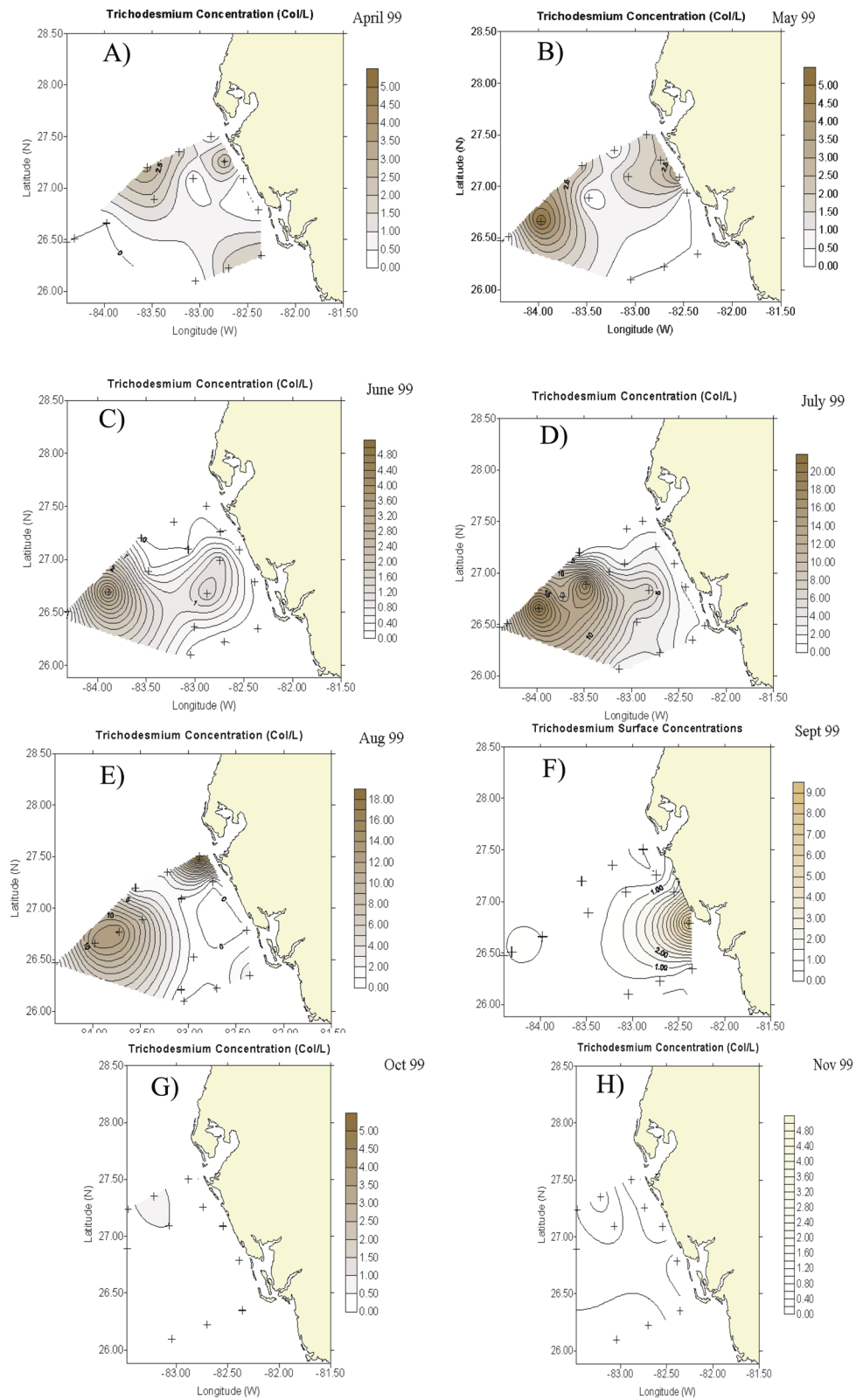


Figure 12. A time series of surface stocks of *Trichodesmium* (colonies l^{-1}) during (a) April through (h) November 1999 on the west Florida shelf.

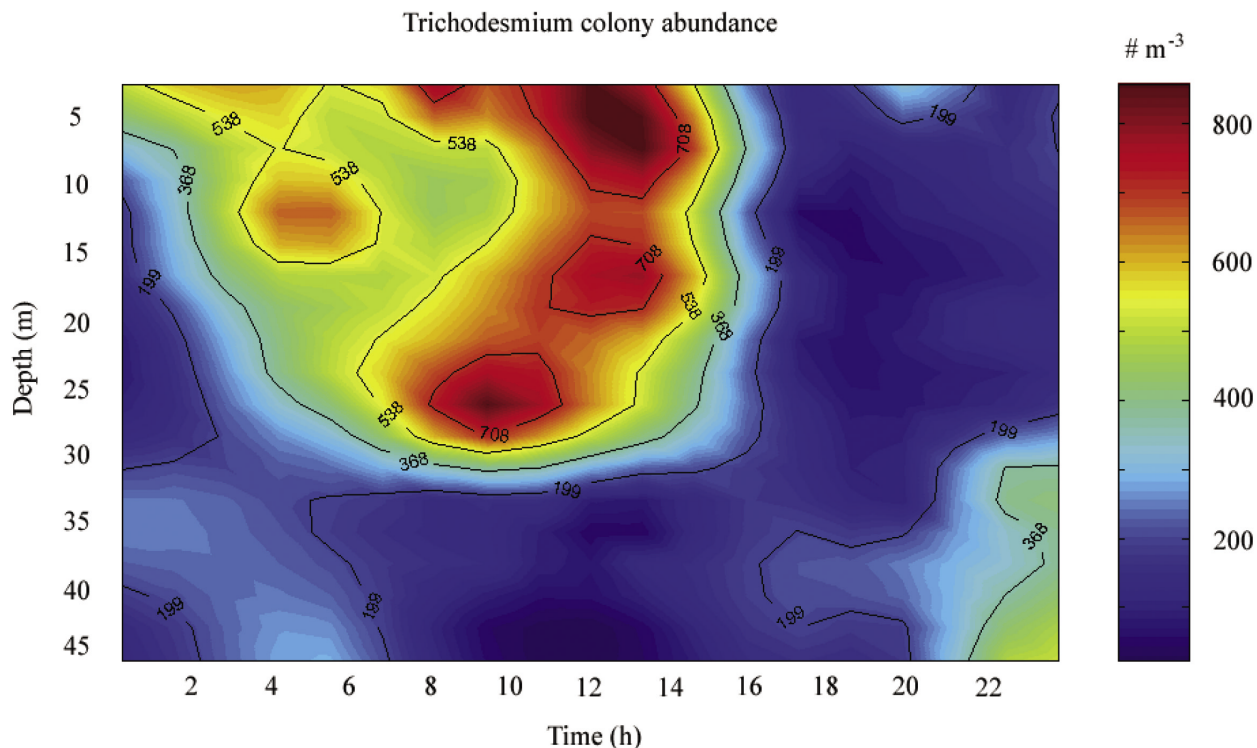


Figure 13. A SIPPER time series of the diel vertical structure of *Trichodesmium* (colonies m^{-3}) above the 50-m isobath of the Sarasota, FL transect across the west Florida shelf during 10–11 September 2002.

(Figure 11). Farther to the east, the aerosol iron concentrations above the eastern Atlantic Ocean are 100-fold larger, within the Saharan dust plume, than at the equator [Sarhou *et al.*, 2003]. On the sea surface, the respective dissolved iron concentrations there are then >1.1 and <0.1 nmol Fe kg^{-1} [Sarhou *et al.*, 2003], similar to the temporal gradients found in the WFS (Figure 11). Furthermore, laboratory cultures of *Trichodesmium* spp. respond favorably to iron additions [Paerl *et al.*, 1994].

[70] After a pulse of iron-rich atmospheric aerosols above Port Aransas, Tx during mid-September 2000, a small red tide of $>2.5 \times 10^5$ cells l^{-1} , or 2.5 $\mu\text{g chl l}^{-1}$, of *K. brevis* was found there ~ 30 days later [Biegalski and Villareal, 2005]. This Texas red tide increment is in response to pulses of nitrogen fixation and DON release by iron-starved diazotrophs, like those observed on the WFS [Mulholland *et al.*, 2004, 2006].

3.4. Accumulation of Particulate Nutrients in the Form of Nitrogen Fixers

[71] When such N_2 -rich, but otherwise nitrogen-depleted, P-rich, and Fe-rich conditions prevail in the Gulf of Mexico, diazotrophs, but not diatoms, flourish [Walsh and Steidinger, 2001; Lenés *et al.*, 2001]. Moreover, once Saharan dust arrives on the WFS and *Trichodesmium* populations are seeded at the shelf-break by the Loop Current, initial and subsequent co-limitation here by both phosphorus and iron [Sanudo-Wilhelmy *et al.*, 2001; Mills *et al.*, 2004] of the nitrogen fixers would be unlikely, where phosphorus supplies of $\gg 0.1$ $\mu\text{mol PO}_4 \text{ kg}^{-1}$ and $\gg 0.2$ $\mu\text{mol DOP kg}^{-1}$ are available, i.e. much larger

ambient phosphorus stocks than their half-saturation constants for uptake of these P-forms [Lenés *et al.*, 2005].

[72] For example, after observations of wet deposition of Saharan dust on 27 June 1999 at Miami, FL mean dissolved iron surface stocks of ~ 3 nmol Fe kg^{-1} were found at the edge of the WFS (Figure 11) - recall that the half-saturation constant for iron uptake by these diazotrophs is estimated to be 1 nmol Fe kg^{-1} [Walsh *et al.*, 2001]. In response, a ten-fold increment of *Trichodesmium* colonies occurred in this region by July 1999 (Figure 12d), compared to their initial conditions found during the preceding ECOHAB surveys of April–June 1999 (Figures 12a–12c). The near-bottom diazotroph populations on the outer shelf (Figure 13) were then harvesting phosphate stocks of >1.0 $\mu\text{mol PO}_4 \text{ kg}^{-1}$ [Lenés *et al.*, 2001].

[73] In October 1999, after prior apparent landward movement of the diazotroph stocks during August–September (Figures 12e and 12f), they were then harvesting near-shore phosphate stocks of >0.5 $\mu\text{mol PO}_4 \text{ kg}^{-1}$ as well [Lenés *et al.*, 2001]. Indeed, at very high levels of *Trichodesmium* discoloration of surface waters in the WFS seen by aircraft off St. Petersburg Beach during July 1995, their biomass amounted to surface stocks of $>4 \times 10^7$ cells l^{-1} , or >50 $\mu\text{g chl l}^{-1}$ along the coast. During April 1949, the city of Sarasota used trucks to haul it away, after stranding of *Trichodesmium* on the beaches of Sarasota Bay.

[74] Recall that these nitrogen-fixers were also present in satellite imagery at the beginning of the 2000 Texas red tide (Figure 3). Then, our concurrent ship surveys of slope waters at $\sim 95.3^\circ$, 26.8°N in the western Gulf of Mexico

found a mean of 21 colonies l^{-1} of *Trichodesmium* on 24 July 2000. Similarly, a precursor bloom of *Trichodesmium* was also found off the Port Aransas jetty on 16 September 1986, when the pre-red tide stocks of *K. brevis* were <50 cells l^{-1} at ~ 2 km offshore of the barrier island [Trebatoski, 1988]. Moreover, a subsequent red tide of 3×10^7 cells l^{-1} was sampled a month later to the south within Corpus Christi Bay on 16 October 1986 [Trebatoski, 1988]. The alongshore trajectories of the 1986 and 2000 (Figure 4a) Texas red tides were also the same.

[75] Using a PC/Chl weight ratio of 220/1 [Carpenter, 1983] and a Redfield PC/PP molar ratio of 106 [Walsh et al., 2001], such an accumulation of Florida diazotroph biomass in 1995 amounted to a storage of >8.6 $\mu\text{mol PP kg}^{-1}$ as particulate phosphorus. Filtered water samples from other blooms of healthy *Trichodesmium* yielded a similar amount of 7.8 $\mu\text{mol PP kg}^{-1}$ off Venice, FL during October 1950, when the inorganic stock was 0.05 $\mu\text{mol PO}_4 \text{ kg}^{-1}$ [Graham et al., 1954]. During their decomposition, these colonial diazotrophs are instead a source of phosphorus, with 0.30 $\mu\text{mol PO}_4 \text{ kg}^{-1}$ found after a bloom of *Trichodesmium* above the 20-m isobath of the central WFS in October 1986 [Walsh and Steidinger, 2001].

[76] Indeed, these diazotrophs are a source of nitrogen during their population growth [Prufert-Bebout et al., 1993], as well as after bloom collapse [Devassy et al., 1978]. Since diatoms, coccolithophores, flagellates, and even some dinoflagellates grow 2–3 fold faster than *K. brevis* [Walsh et al., 2001], how do the slow-growing toxic dinoflagellates on the WFS intercept nitrogen released by *Trichodesmium* [Capone et al., 1994; Mulholland et al., 2004, 2006]?

3.5. Synchrony of Diel Migration

[77] Oxygen is deleterious to nitrogen-fixers, thus explaining: why sites of photosynthesis are distinct from those of nitrogen-fixation in nonheterocystous *Trichodesmium* trichomes [Bryceson and Fay, 1981; Janson et al., 1994]; why there are temporal alternations in N_2 acquisition and O_2 evolution [Berman-Frank et al., 2001]; and why some members of the *Trichodesmium* colony pass excreted nitrogen, in the form of amino acids and ammonium [Capone et al., 1994], to other members via the external medium of sea water. Indeed, during some *Trichodesmium* blooms in May 2000 on the WFS, we found as much as 36.9 $\mu\text{mol DON kg}^{-1}$ and 15.9 $\mu\text{mol NH}_4 \text{ kg}^{-1}$ inside a diazotroph patch, compared to 22.9 $\mu\text{mol DON kg}^{-1}$ and only 4.8 $\mu\text{mol NH}_4 \text{ kg}^{-1}$ outside of its boundaries.

[78] Field populations of *Trichodesmium* from the Timor and Arafura Seas, north of Australia, exhibit midmorning maxima of photosynthesis [Berman-Frank et al., 2001], at the time of day when these WFS diazotrophs, seeded from slope waters (Figure 12), move upward on the middle shelf (Figure 13) to obtain maximal light at the top of the euphotic zone. Based upon the intensive sampling of more than 1.2 million plankton images collected during the SIPPER time series at the ~ 50 -m isobath of the WFS, the diel vertical distribution of *Trichodesmium* colonies during September 2002 exhibits a shoaling of the depth of maximum abundance of colonies towards the sea surface during early morning (Figure 13).

[79] The *Trichodesmium* colonies are Sun-adapted, with light saturation and compensation intensities of ~ 300 and 125 $\mu\text{E m}^{-2} \text{ sec}^{-1}$ [Roenneberg and Carpenter, 1993; Carpenter and Roenneberg, 1995]. In contrast, *Karenia brevis* is shade-adapted, with a light saturation intensity of ~ 65 $\mu\text{E m}^{-2} \text{ sec}^{-1}$ [Shanley and Vargo, 1993]. Yet, even during December, noon surface incident radiation to the WFS is ~ 1200 $\mu\text{E m}^{-2} \text{ sec}^{-1}$ [Walsh et al., 2002].

[80] During the afternoon, when the WFS populations of *Trichodesmium* begin their descent, sinking to below a depth of 40 m after sunset (Figure 13), the Australian populations exhibit instead a maximum in nitrogen-fixation [Berman-Frank et al., 2001], when the demand for stored energy in the form of polyphosphates is also large for diazotrophs off the Bahama Islands [Roenneberg and Carpenter, 1993; Romans et al., 1994]. On the outer WFS, the closest large stocks of phosphate are at depth, rather than at the coast, such that these diazotrophs are in search of phosphorus during their descent, as off Hawaii [Karl et al., 1992].

[81] Basically, as *Trichodesmium* adjusts its carbohydrate ballast [Walsby, 1992; Romans et al., 1994] to float up and sink down each day (Figure 13), seeking light at the surface and nutrients at depth, we speculate that initial small stocks of *K. brevis* swim alongside the diazotroph colonies. They exhibit the same vertical pattern of morning ascent and afternoon descent on the WFS [Hela, 1955; Heil, 1986; Walsh et al., 2002; Kerfoot et al., 2004] as the *Trichodesmium* colonies (Figure 13). On the mid and outer WFS, these initial small red tides may thus intercept amino acids and ammonium, intended for transfer between the incompatible photosynthetic and nitrogen-fixing loci of the *Trichodesmium* trichomes [Carpenter et al., 1992].

[82] No red tides were observed on the WFS during September 2002, but a weekly time series of the stocks of *K. brevis* was obtained during August–December 1999, along the same cross-shelf transect off Sarasota, FL (Figure 14b) as the SIPPER observations (Figure 13). This earlier red tide exhibits initial subsurface maxima of the shade-adapted cells of *Karenia* [Shanley and Vargo, 1993] at the 30-m isobath during September 1999 (Figure 14a). Moreover, off eastern Japan, above the same bottom depths of 21–36 m on the shelf, *K. mikimotoi* displays the same diel vertical pattern of morning ascent and afternoon descent at speeds of up to 2.2 m hr^{-1} [Koizumi et al., 1996] as found for *K. brevis* [Heil, 1986; Walsh et al., 2001; Kerfoot et al., 2004] and *Trichodesmium* (Figure 13) on the WFS.

[83] Concurrent excretion of DON by *Trichodesmium*, at a rate of $\sim 50\%$ of their nitrogen-fixation [Glibert and Bronk, 1994], is consistent with a $\sim 50\%$ respiration loss of carbon during gross photosynthesis [Carpenter and Roenneberg, 1995]. This DON could then serve as the initial nitrogen source in offshore breeding waters for the subsequent noxious red-tides found later at the coast (Figure 14a). But, as the population size of the small red tide of *K. brevis* increases, its daily nitrogen demands can not be met by such phytoplankton excretion, instead requiring sacrifice of first diazotroph, and thence of fish, biomass.

3.6. Lysis of DON Stocks

[84] During early September 1999, before onset of the October red tide, no *K. brevis* were found within surface

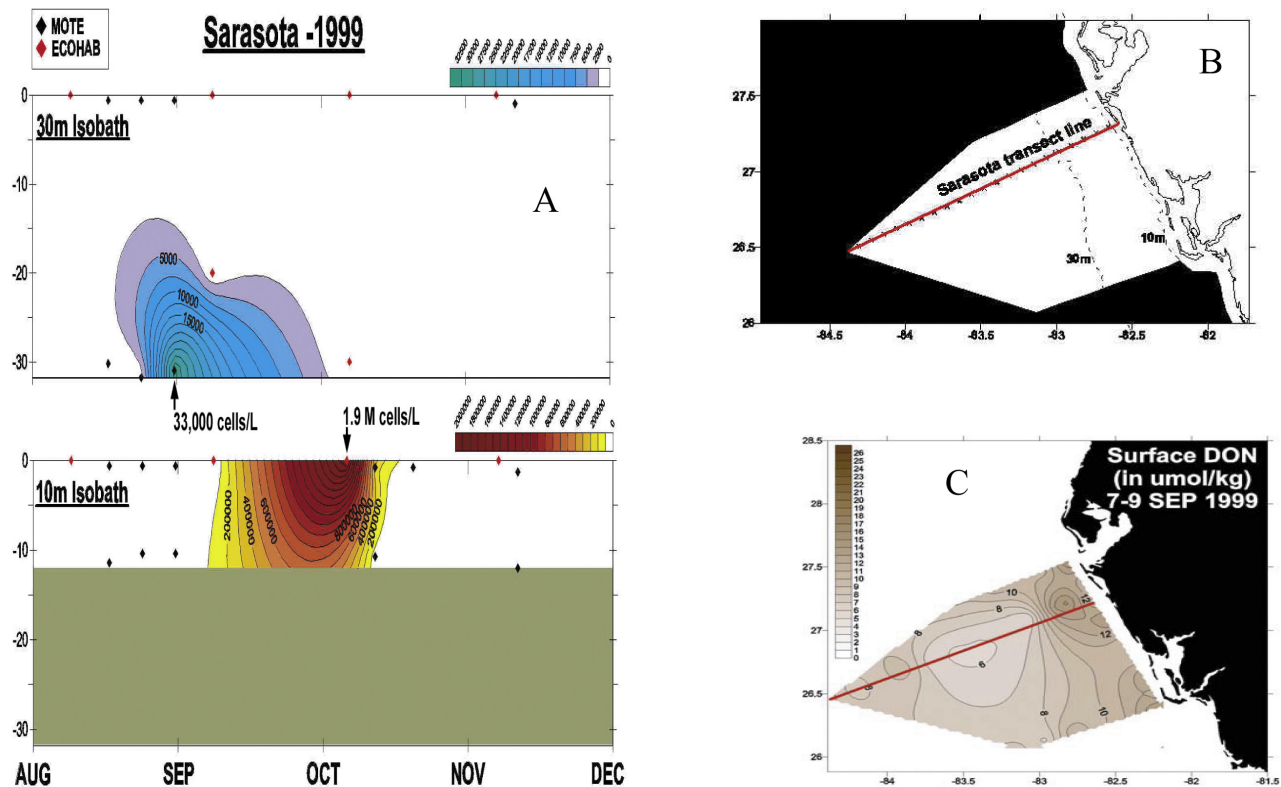


Figure 14. The (a) weekly distributions of *Karenia brevis* above the 30-m and 10-m isobaths during August–December 1999 of (b) the Sarasota, FL transect in relation to (c) surface DON stocks (umol kg^{-1}) during September 1999, when the nitrate stocks were then $<0.3 \text{ umol NO}_3 \text{ kg}^{-1}$ over the water column. The sampling interval was ~ 7 days (www.floridamarine.org), but only the occasions when *K. brevis* were present ($>1000 \text{ cells l}^{-1}$) are shown in Figure 14a.

waters above the 10-m isobath of the Sarasota transect (Figure 14a). In contrast, near bottom populations of $\sim 2 \times 10^4 \text{ cells l}^{-1}$, or $\sim 0.2 \text{ ug chl l}^{-1}$, of *K. brevis* were observed on the 30-m isobath in September 1999 (Figure 14a). Here, surface populations were then also negligible. Such sub-surface, ubiquitous [Geesey and Tester, 1993] background populations of *K. brevis* at midshelf [Tester and Steidinger, 1997] would have traveled $\sim 40 \text{ km}$ inshore (Figure 14b) during September 1999, with a net growth rate of $\sim 0.13 \text{ day}^{-1}$, to accumulate $1.9 \times 10^6 \text{ cells l}^{-1}$ at the 10-m isobath of the WFS (Figure 14a) within a month, or so.

[85] The WFS and Texas stocks of *K. brevis* do indeed have a net growth rate of as much as $\sim 0.25 \text{ day}^{-1}$ [Van Dolah and Leighfield, 1999; Loret et al., 2002], and N-isotope studies suggested that they used DON of *Trichodesmium* origin off Florida during 1999–2001 [Mulholland et al., 2004, 2006; Havens et al., 2004]. The mean monthly near-bottom currents at our moored ADCP array on the 30-m isobath of the Sarasota transect (Figure 14b) were also inshore (NNE) at $\sim 1.5 \text{ km day}^{-1}$ (45 km month^{-1}) during September 1999. Finally, assuming a chlorophyll content of $1 \times 10^{-5} \text{ ug chl cell}^{-1}$ for *K. brevis*, a PC/Chl weight ratio of 50/1, and a PC/PN molar ratio of 6.6, such a population increment of $19.8 \text{ ug chl l}^{-1}$, or $12.5 \text{ umol PN l}^{-1}$, during 1999 (Figure 13) implies a minimal dissolved nitrogen demand of $\sim 12.5 \text{ umol DIN} + \text{DON kg}^{-1}$. This is a conservative

estimate, since it assumes no grazing, excretion, settling, or lysis losses of the toxic dinoflagellate during their accumulation of PN in September 1999.

[86] During September–October 1999, the nitrate stocks were $<0.3 \text{ umol NO}_3 \text{ kg}^{-1}$ over the water column above the 10-m and 30-m isobaths of the Sarasota transect, such that “new nitrogen” was then a negligible DIN source for such growth of *K. brevis*. Instead, decaying diazotrophs fueled the 1999 red tide. We assume the same *Trichodesmium* colony size of $\sim 3 \times 10^4 \text{ cells}$ [Carpenter, 1983] and a chlorophyll content of $1.2 \times 10^{-6} \text{ ug chl cell}^{-1}$ [Borstad, 1982], with a PC/Chl weight ratio of 220/1 [Carpenter, 1983], and a PC/PN molar ratio of 6.1 [McCarthy and Carpenter, 1979] for Florida diazotroph populations, like those off Texas (Figure 3). An observed population decrement of $\sim 10 \text{ Trichodesmium colonies l}^{-1}$ along the 10-m isobath of the WFS between August (Figure 12e) and September (Figure 12f) 1999 thus represents a biomass loss for these diazotroph populations of $10.9 \text{ umol PN kg}^{-1}$.

[87] Since these diazotrophs are poorly grazed [Guo and Tester, 1994], the most likely form of their population loss in 1999 is cell lysis to yield the equivalent amount of $\sim 10.9 \text{ umol DON kg}^{-1}$. Note that this same amount of surface DON was observed along the coast (Figure 14c) during September 1999. Most of this DON is labile, since it did not covary with salinity [Lenes et al., 2001]. A similar amount of surface DON (Figure 14c) was also found the

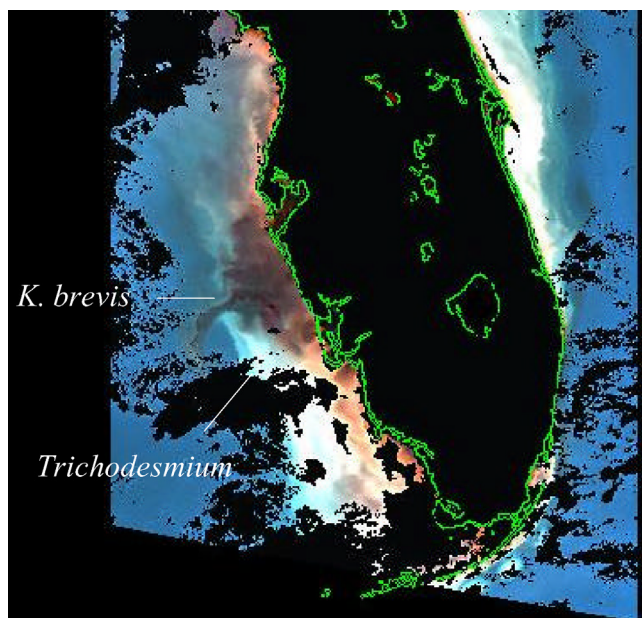


Figure 15. A SeaWiFS satellite estimate of red tides and diazotrophs within the eastern Gulf of Mexico during 17 September 2001. Based upon a backscatter algorithm, the reddish-black color is a red tide of *Karenia brevis* and the pale blue color is co-occurring nitrogen fixers at depth, i.e. *Trichodesmium* within offshore waters. The yellow-white regions depict suspended sediments and bottom reflectance effects within the south central region of the West Florida shelf.

previous year, within the same region of the WFS, during September 1998 (Figure 8b).

[88] A similar cell lysis of diazotroph populations to fuel initial red tides of *K. brevis* off Texas is inferred from the satellite imagery of this region in July–September 2000 (Figure 3). Note that along the coast, south of Galveston, the backscatter per unit chlorophyll on the Texas shelf is ~ 10 -fold greater on 17 August 2000 (Figure 3d), than on 28 July 2000 (Figure 3c), suggesting a population increment of the Texas diazotrophs. In contrast, by 29 September 2000, the backscatter is ten-fold less on most of the south Texas shelf (Figure 3b), then indicating a population loss of the diazotrophs, i.e. cell lysis, since they are poorly grazed.

[89] Within Florida coastal waters, *K. brevis* responds to the demise of the *Trichodesmium* populations (Figure 12), induced by either predation, or “convenient” autocatalysis of the latter [Berman-Frank *et al.*, 2004]. During 1999, large *K. brevis* populations of $\sim 2 \times 10^6$ cells l^{-1} , or ~ 20 μg chl l^{-1} of red tide, were then found within near shore surface waters above the 10 m isobath (Figure 14), between Tampa Bay and Charlotte Harbor, FL. In the following year, another red tide of $> 1 \times 10^6$ cells l^{-1} of *K. brevis* was observed off Charlotte Harbor, with a mean molar DIN/PO₄ ratio of ~ 0.5 and a PN/PP ratio of ~ 46 during 2000 [Vargo *et al.*, 2004].

[90] This DIN/PO₄ ratio on the WFS during 2000 implies initial N-limitation of the nutrient supply, if nitrate and ammonium are the major inorganic forms available to the phytoplankton community, i.e. the usual diatom base of

coastal food webs, or the microflagellate base of oceanic food webs. *Trichodesmium*, of course, uses N₂, which is unavailable to both diatoms and microflagellates. The PN/PP ratio instead indicates final P-limitation of the phytoplankton assimilation of dissolved materials into cellular forms of nitrogen, PN, and phosphorus, PP. Under phosphorus-limitation, moreover, *Trichodesmium* does undergo cell death [Berman-Frank *et al.*, 2004].

[91] Alternatively, *K. brevis* may instead be allelopathic [Freeburg *et al.*, 1979], killing other plants - as does the cognate species *G. nagasakiense*. The latter is also known as *K. mikimotoi* [Gentien, 1998], which is observed on the Texas [Steidinger *et al.*, 1998b; Villareal *et al.*, 2001] and Florida shelves. In response to either case of allelopathy [Freeburg *et al.*, 1979] and/or prescient timing [Berman-Frank *et al.*, 2004], at least four *Karenia* spp. [Heil *et al.*, 2006] are co-located with dying populations of *Trichodesmium* on the inner shelf. During the 2005 red tide on the inner WFS, *K. brevis*, *K. mikimotoi*, *K. papilionacea*, and *K. stelliformis* were all observed, with *K. brevis* exhibiting the broadest ecological niche [Heil *et al.*, 2006].

[92] On the outer shelf, the mutual vertical migration patterns, in which the diazotroph may release nitrogen to other parts of the colony to avoid ill effects of photosynthesis [Berman-Frank *et al.*, 2001], provide the potential for co-location as well. During both initiation and maintenance of red tides, *Karenia* is evidently the benefactor of diazotroph evolutionary adaptations to deal with nitrogen fixation, photosynthesis, and nutrient stress, if the two phytoplankton populations remain in the same water mass at depth and along the coast.

[93] Indeed, coastal upwelling on each side of the Gulf of Mexico introduces both nutrients and a combination of aggregated, Sun-adapted diazotrophs and dark-adapted red tides to an euphotic zone, shaded initially by CDOM and thence by red tides. Recall that just CDOM removed 85% of the incident blue light within the upper 10 m of the near shore WFS water column during 1998 [Walsh *et al.*, 2003]. At a near-surface stock of 50–100 mg chl m^{-3} [Carder and Steward, 1985] and a specific attenuation of 0.035 m^2 (mg chl) $^{-1}$ for *K. brevis* [Walsh *et al.*, 2003], however, just light attenuation by the red tide, ignoring additional attenuation by CDOM and water, would lead to a self-shaded euphotic zone of only 1.3–2.6 m thickness.

3.7. Onshore Transport of Seed Populations

[94] Both *K. brevis* and *Trichodesmium* migrate vertically each day at a speed of ~ 1 m hr^{-1} [Kromkamp and Walsby, 1992; Walsh *et al.*, 2002], to seek optimal light conditions during mutualistic aggregations of self-shading, phosphate-mining, and nutrient exchange. Of the two, *Karenia* is the most shade-adapted, with a light saturation intensity of ~ 65 μE m^{-2} sec^{-1} , compared to either ~ 300 μE m^{-2} sec^{-1} for *Trichodesmium*, or a noon surface incident radiation of ~ 1100 μE m^{-2} sec^{-1} above the WFS [Walsh *et al.*, 2001; Darrow *et al.*, 2003].

[95] Like the Florida clone of *K. brevis* isolated by W. B. Wilson in 1953 from a field population off St. Petersburg, laboratory studies [Magana and Villareal, 2003] of *K. brevis* isolated from the 1999 red tide off Brownsville, TX yield similar maximum growth rates of 0.2–0.4 divisions day^{-1} , compared to 0.2–0.4 divisions day^{-1} for

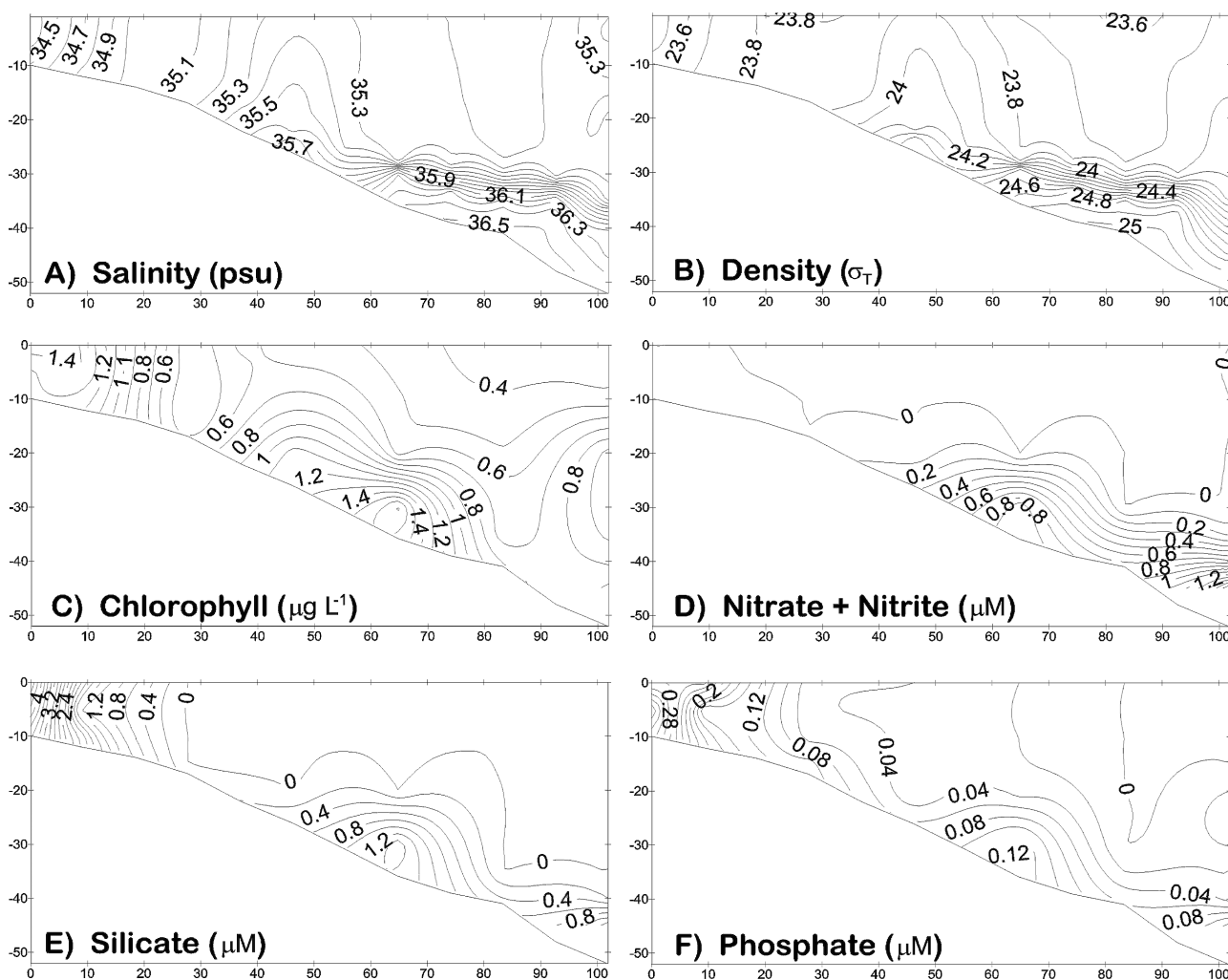


Figure 16. The cross-shelf distributions of (a) salinity, (b) density, and (c) chlorophyll in relation to stocks of (d) nitrate and nitrite, (e) silicate, and (f) phosphate, between the coast and the 50-m isobath, off Fort Myers, FL during the ECOHAB section of 9 November 1998.

Florida isolates [Steidinger, 1983]. Their saturation light intensities are $67 \mu\text{mol m}^{-2} \text{sec}^{-1}$ off Texas, compared to $65 \mu\text{mol m}^{-2} \text{sec}^{-1}$ off Florida [Shanley and Vargo, 1993].

[96] Under high light intensities at the sea surface, *K. brevis* photo-adapts, reducing the amount per cell of photosynthetic pigments, carotenoids [Higham et al., 2004], and thylakoid lipids [Evans and Leblond, 2004], allowing them to persist within surface waters and eventually to be detected [Cannizzaro et al., 2004] by satellites (Figures 3 and 15). Other dinoflagellates also produce mycosporine-like amino acids as potential blockers of UV damaging radiation [Yentsch and Yentsch, 1982; Negri et al., 1992]. Until photo-adaptation and self-shading by large red tides are operative, the CDOM within near shore waters of terrestrial origin in the WFS [Jolliff et al., 2003] alleviates light inhibition of the small red tides, since the presence of CDOM in prior models [Walsh et al., 2003] allowed *K. brevis* to out-compete both diatoms and microflagellates.

[97] On the middle and outer shelves of smaller CDOM sunscreen, however, small populations of *Karenia brevis* must instead move to the bottom of the euphotic zone (Figure 14a) to seek low light intensities, where recent

imports of slope water diazotrophs (Figure 12) are found at depth each day (Figure 13) in pools of deep-sea phosphate (Figure 16f), upwelled previously onto the outer shelf. During the fall transition, a series of upwelling and downwelling events occur each year on the WFS [Yang and Weisberg, 1999; Weisberg et al., 2000; Weisberg and He, 2003], such that, at times, the bottom of the euphotic zone at midshelf coincides with near-bottom, shoreward moving Ekman layers.

[98] For example, a cross-shelf transect of salinity (Figure 16a) and density (Figure 16b) depicts upwelling during 9 November 1998 at the 25-m isobath, on the seaward side of a near-bottom convergence front off Fort Myers, FL. Similar density features were also seen in the Sarasota and Tampa transects of the ECOHAB program to the north (Figure 6). Such upwelling is consistent with earlier wind-induced September–October 1998 offshore flows at the surface.

[99] These flows were detected by the CODE near-surface drifter, set farther south, off Shark River (region (3) of Figure 5), during August 1998 (Figure 17b). Under downwelling-favorable winds from the south during sum-

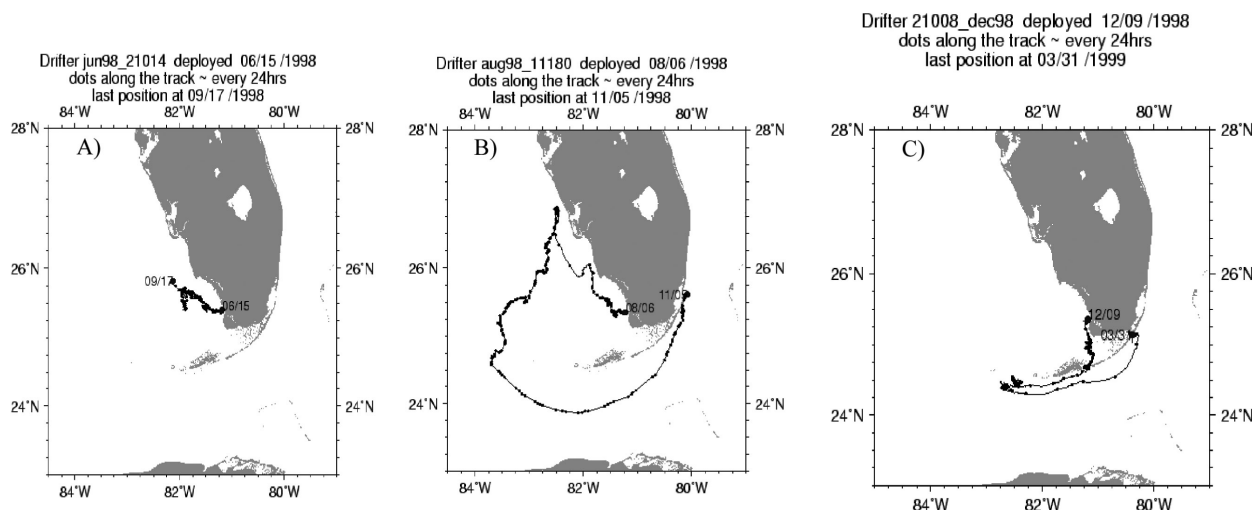


Figure 17. The daily trajectories during June–December 1998 of near-surface CODE drifters, set off Shark River Slough during (a) June, (b) August, and (c) December on the West Florida shelf.

mer, the drifters set in the same place during both June and August 1998 first move northwest along the coast (Figures 17a and 17b). Upon seasonal reversal of the wind forcing to upwelling-favorable ones from the north [Yang and Weisberg, 1999], these two drifters and the third set in December 1998 (Figure 17c) then move offshore to the southwest during fall.

[100] This upwelling circulation pattern is fully three-dimensional on the WFS, as indicated by our concurrent observations of water motion at 4 moored arrays along the Sarasota and Fort Myers transects (Figure 18). In response to upwelling-favorable winds during 4–7 November 1998, sea level at St. Petersburg drops by 6 November 1998. The temperature then declines and the salinity increases on the 25-m isobath (Figure 18), with the onshore advection of the colder and more saline (Figure 16a) offshore waters.

[101] The observed surface flows move seaward, with Ekman veering at depth (Figure 18). The maximal upwelling rate of $\sim 4 \text{ m day}^{-1}$ (Figure 19) during 5 October–13 November 1998, focused by the bathymetry to the north of Tampa Bay [Weisberg *et al.*, 2000], is simulated by our USF adaptation [Weisberg and He, 2003] of the Princeton Ocean Model (POM) [Blumberg and Mellor, 1987]. Note that the simulated drifter's offshore trajectory of the POM, when at the surface (see Figure 19), follows the observed ones of the CODE drifter (Figure 17), as it also turns offshore to the southwest at the same location near Venice, FL during September–October 1998.

[102] Onshore flows within the bottom Ekman layer would move landward the near-bottom seed populations of phytoplankton, contributing to a sum of $\sim 1.6 \text{ ug chl l}^{-1}$ at the 30-m isobath on 9 November 1998 (Figure 16c). These near-bottom phytoplankton inocula (Figure 16c) represent at least two components: *K. brevis* and *Trichodesmium* (Figures 13 and 14). As observed in September 1999 (Figure 14a), an initial stock of at least $\sim 3.3 \times 10^4 \text{ cells l}^{-1}$, or $0.3 \text{ ug chl l}^{-1}$, of *K. brevis* is present above the 30-m isobath in November 1998, since it was then found inshore as well [Vargo *et al.*, 2004]. Indeed,

subsurface populations of red tide were also found on the 30-m isobath of the WFS during November 2000 and 2001 [Milroy *et al.*, 2006].

[103] The second component of near-bottom phytoplankton during November 1998 is a postinoculum phase of $\sim 36 \text{ colonies l}^{-1}$, or $1.3 \text{ ug chl l}^{-1}$ of *Trichodesmium* populations, based upon the above conversion factors. For example, the surface stock of *Trichodesmium* is $\sim 18 \text{ colonies l}^{-1}$ in this region during August 1999 (Figure 10e), the same as that observed in Texas near-surface slope waters during July 2000 (Figure 3).

[104] Off Barbados, these diazotrophs exhibit a persistent subsurface maximum during July–October, with 3.2-fold larger amounts of *Trichodesmium* found at a depth of 16 m than at the surface [Borstad, 1978]. Recall that depth profiles of continuous particle counters [Sutton *et al.*, 2001; Remsen *et al.*, 2004] confirm subsurface maxima of *Trichodesmium* populations on the WFS during September 2002 (Figure 13). Further note that the near-bottom silica maxima (Figure 16e) remains unutilized on the outer shelf during November 1998, where the subsurface chlorophyll maximum prevails (Figure 16c), ruling out diatoms as a major floral component.

[105] Such subsurface maxima of phosphate-seeking, light-adapted diazotrophs and shade-adapted, initial red tides are at the bottom of the euphotic zone on the 30-m isobath during 1998 (Figure 16c), in the absence of photo-acclimatization and/or CDOM. Here, they are each entrained within upwelled waters of the bottom Ekman layer (Figures 16a and 16b), as they move onshore (Figure 18) towards phosphorus-rich (Figure 16f) and CDOM-rich [Walsh *et al.*, 2003] coastal regions of the WFS. There, the migratory *Trichodesmium* and *K. brevis* also use organic forms of phosphorus (Figure 8), since they both have the ability to make alkaline phosphatase [Yentsch *et al.*, 1972; Vargo and Howard-Shamblott, 1990].

[106] Once all sources of dissolved phosphorus are exhausted on the WFS, however, particulate forms of fish phosphorus must then be utilized by *K. brevis* [Walsh *et al.*,

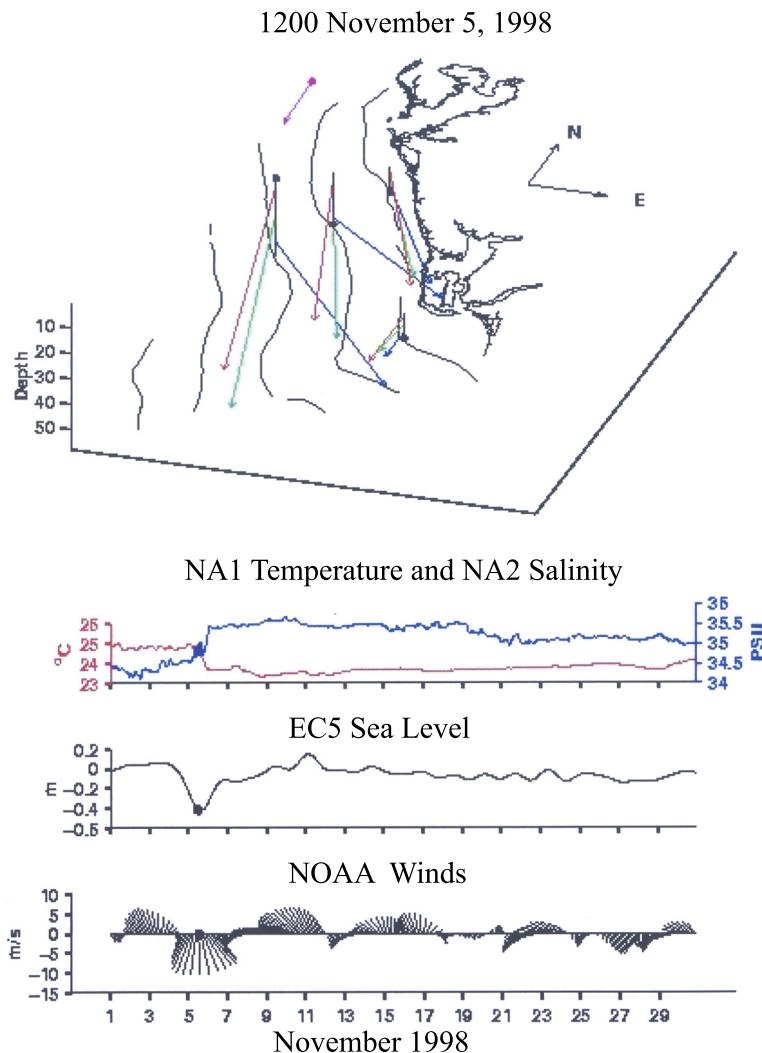


Figure 18. The three-dimensional current structure at noon on 5 November 1998 at the ECOHAB/HyCODE moored arrays, in relation to daily records of wind forcing at the NOAA offshore buoy, temperature and salinity at the 25-m isobath of the Sarasota, FL transect, and sea level at St. Petersburg, FL, during November 1998. The red, green, and blue colored vectors denote near-surface, middepth, and near-bottom flows.

2006] - does the same sequence of causal events occur within Texas waters? Indeed, small red tides first form on the Texas shelf, in response to the same set of physical and chemical factors. For example, two holey-sock drifters were set at a nominal depth of ~ 6 m on the Louisiana-Texas shelves during 1992–1993 [Howard and DiMarco, 1998]. These LATEX drifters exhibit the expected circulation pattern in relation to the surface salinity fields (Figure 20) and seasonal wind forcing of the Louisiana-Texas shelves.

[107] One drifter was set on the inner Louisiana shelf above the ~ 20 -m isobath during 9 November 1992 (the red solid triangle of Figure 20). Seasonal winds from the northeast then prevailed, and this near shore drifter moved southwest at speeds of ~ 20 cm sec^{-1} along the landward side of a salinity front. This is a downwelling pattern at the

coast, with onshore cross-shelf flows at the surface, and offshore flows in the bottom Ekman layer.

[108] Another holey-sock drifter was launched above the ~ 50 -m isobath on the outer Texas shelf during 2 May 1993 (the green solid triangle of Figure 20). It instead moved northeast at speeds of as much as ~ 50 cm sec^{-1} along the seaward side of the front. Seasonal upwelling-favorable winds - as recorded at the Corpus Christi airport - had commenced from the southeast during April and persisted through most of October 1993.

[109] These upwelled waters would have added the ^{226}Ra tag of nearshore Texas waters (the solid square of Figure 7) to the midshelf water column (the open square of Figure 7). At the same time, offshore transport of the upwelled, near bottom remineralized nutrients (Figures 10c, 10d, and 10f) would have occurred within surface plumes (Figures 9b, 9c,

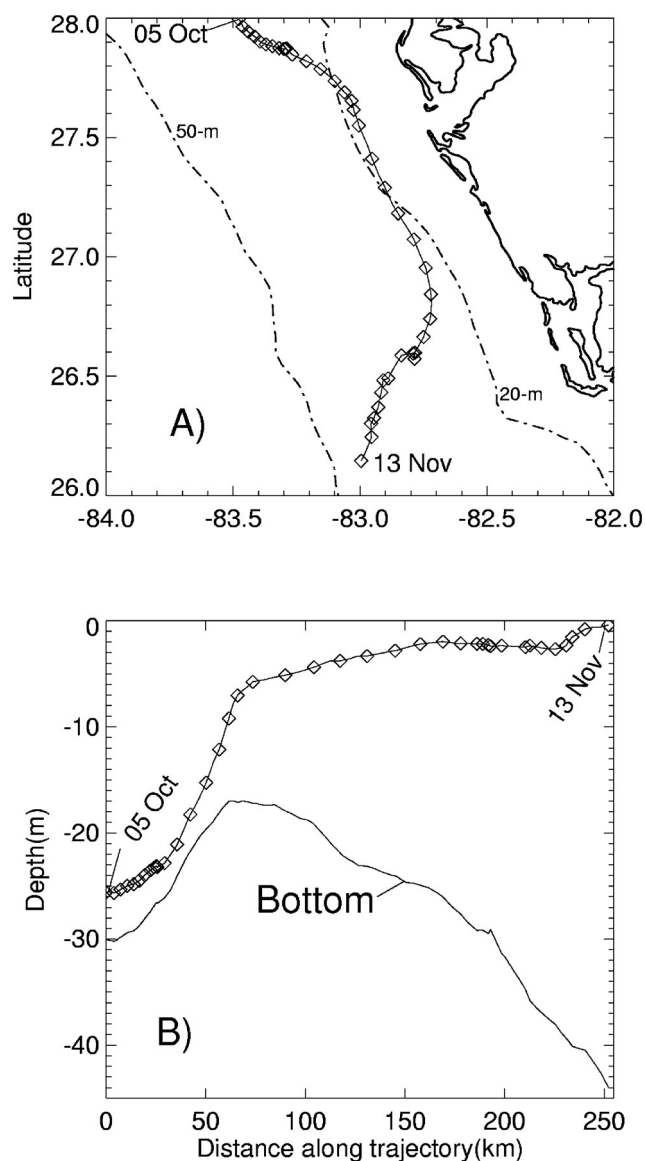


Figure 19. The daily three-dimensional trajectory () of a simulated near-bottom water parcel during 5 October–13 November 1998, with respect to (a) its location and (b) depth during transit.

and 9e) of greater salinity (Figure 20) and colder temperature (Figure 9a).

[110] A set of six cross-shelf sections (Figure 7) between the coast and the 50-m isobath, from off Corpus Christi, TX to Cameron, LA during July–August 1993 in the LATEX program captures this upwelling response [Jochens and Nowlin, 1999]. The strong salinity fronts, reflecting hydrographic evidence of upwelling, are mainly located across the two most eastward sections, off Port Arthur and Cameron. The density isopleths have an upward tilt on the seaward side of the inferred near-bottom convergence front at the 30-m isobath off Cameron (Figure 21e), as similarly observed off the West Florida shelf (Figure 16b).

[111] Across the same Louisiana salinity front of 34.5–35.5 psu (Figure 21b), as also found on the WFS (Figure 16a), near-bottom pools of $0.3\text{--}0.4\ \mu\text{mol NH}_4\ \text{kg}^{-1}$

(Figure 21k), $0.5\text{--}1.0\ \mu\text{mol NO}_3\ \text{kg}^{-1}$ (Figure 21h), and $0.1\text{--}0.2\ \mu\text{mol PO}_4\ \text{kg}^{-1}$ (not shown), i.e. DIN/PO₄ ratios of 5–6, are upwelled to depths of 10–20 m, above the 30-m isobath off Cameron in 1993. Like the WFS (Figure 16f), more phosphorus is found on the landward side of the Louisiana front than on the seaward side.

[112] During the previous and next years, in the same place, hydrographic evidence of upwelling is again seen off the western Louisiana coast (Figures 21d and 21f). The freshwater influxes to the Texas-Louisiana shelves during summer of 1993 are about two-fold those of 1992 and 1994 [Etter *et al.*, 2004]. During July–August 1992, near-bottom pools of $0.3\text{--}0.4\ \mu\text{mol NH}_4\ \text{kg}^{-1}$ now broach the surface above the 30-m isobath off Cameron (Figure 21m). The initial conditions here of May 1992 indicate that $\sim 0.2\ \mu\text{mol PO}_4\ \text{kg}^{-1}$ and $0.5\ \mu\text{mol NH}_4\ \text{kg}^{-1}$ then broached the surface above the 25-m isobath as well. Based on pigment composition and phytoplankton cell counts during the LATEX cruise of May 1992 [Neuhard, 1994; Bontempi, 1995], precursor diazotrophs were most abundant farther offshore above the 45–50 m isobaths in May 1992. Moreover, *Karenia brevis* was then rare.

3.8. Phytoplankton Response to Allochthonous Nutrient Supplies of the WFS

[113] Other near-surface drifters were also set during May–July 1998 on the outer northwestern WFS, north of Tampa Bay [Fan *et al.*, 2004]. They turned offshore in the same region, inshore of the 50-m isobath off Venice, like the drifter set off Shark River in August 1998 (Figure 17b). Their trajectories were also accurately simulated by another version of the POM [Fan *et al.*, 2004]. We thus use this circulation model (Figure 19) to drive one of plankton dynamics. The coupled model explores the fate of nutrients, supplied both by Florida estuaries and the offshore Loop Current. After analysis of the impacts of allochthonous

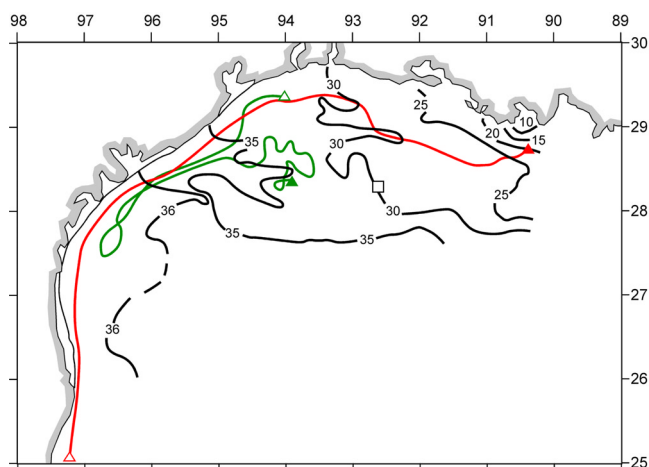


Figure 20. The near-surface distribution of salinity during the LATEX survey of 26 July–8 August 1993 in relation to the daily trajectories of holey-sock drifters [Howard and DiMarco, 1998] set at nominal depth of ~ 6 m on the inner shelf in November 1992 (red solid and open triangles) and on the outer shelf in May 1993 (green solid and open triangles). The same surface salinity of ~ 29.68 was found on the outer shelf (open square) in July 1975 [Reid, 1984].

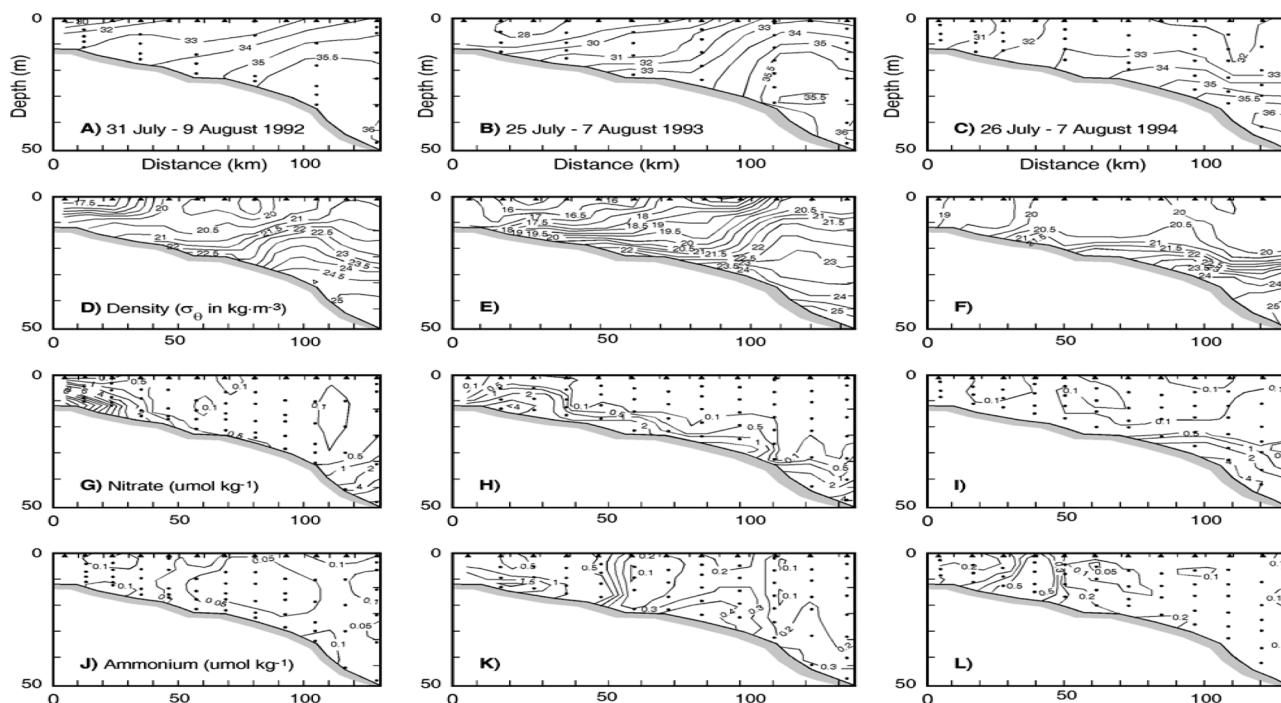


Figure 21. The cross-shelf distributions of (a–c) salinity, (d–f) density, (g–i) nitrate, and (j–l) ammonium between the coast and the 50-m isobath, off Cameron, LA during the LATEX surveys of July–August 1992, 1993, and 1994.

estuarine and deep-sea nutrient supplies of phosphorus to the WFS for generation of smaller red tides, we then consider the autochthonous sources of recycled nutrients from dead fish for maintenance of the larger red tides.

[114] We simulate the initial interaction of physical forcing and biochemical processes of nutrient transfer among phytoplankton by releasing daily amounts of inorganic nitrogen and phosphorus, as well as DOC, CDOM, and suspended solids to the surface layer of the model at its land boundary (Table 2). The biological model is driven by a physical circulation model that mimics correctly (Figure 19) the near-surface trajectories of the CODE drifters (Figure 17) and offshore flows at our current meters (Figure 18). The coupled biophysical model receives the influxes of nutrients from 30 estuaries between the Mississippi River and the Florida Keys.

[115] Such estuarine nutrient inputs are based upon seasonal freshwater discharge rates and mean concentrations of nitrate, ammonium, and phosphate (Table 2) at zero salinity of each estuary (see Appendix A). We also add nutrients of deep-sea origin of $25.1 \text{ NO}_3 \text{ kg}^{-1}$, $1.5 \text{ NH}_4 \text{ kg}^{-1}$ and $1.7 \text{ PO}_4 \text{ kg}^{-1}$, i.e. a DIN/PO₄ ratio of 15.6, at depths of $\geq 300 \text{ m}$ on the shelf-break boundary of the WFS, estimated from NEGOM data (Figure 6). Although the model's spatial grid extended over the shelf, slope, and basin regions of the eastern Gulf of Mexico, we show here only the results from the WFS domain for March and August 1998.

3.8.1. Spring Case of the Coupled Model

[116] The spring results of the model, with both estuarine and deep-sea allochthonous supplies of nutrients, mimic the seasonal appearance of the “Green River” [Gilbes *et al.*, 1996, 2002] as a chlorophyll plume. It extends south from Cape San Blas, both at the surface and at middepth

(Figures 22a and 22b). A similar pattern appears in SeaWiFS imagery for late March 1998 (Figure 22c), when no in situ chlorophyll validation data are available. This feature of a plankton source for subsequent recycled nutrients is an important factor of red tide initiation on the Louisiana-Texas shelves as well (Figures 10 and 21).

[117] A prior use of just the physical model [He and Weisberg, 2002] described the evolution of this hydrographic feature as a consequence: of (1) upwelled water near Cape San Blas, leading to a cold tongue of 19°C water south along the 30-m isobath (Figure 22d), and (2) eastward advection of low salinity water from the northern rivers. The surface result is a low salinity tongue of $<35.3 \text{ psu}$, seaward of the cold tongue (Figure 22e). Baroclinic factors add a positive feedback to southeastward flow at midshelf. These effects arise independent of the remote Loop Current forcing [He and Weisberg, 2002]. The upwelling of colder, greater salinity water leads to a divergence front in the model of higher density water mass at the surface, with temperature of $<20.0^\circ\text{C}$, salinity of $>36.0 \text{ psu}$, and density of $>25.5 \sigma_t$, extending southwards at midshelf as the yellow-red colored region of Figure 22f, with surface waters of lower density on either side.

[118] Our coupling of an ecological model to the physical one indicates that much of the spring phytoplankton biomass is a consequence of the seasonally recurring upwelled nutrient supply, focused along Cape San Blas. It is not a result of just estuarine nutrient and CDOM supplies. We find, of course, that the Mississippi River, with much greater inflows than those of the Apalachicola and Suwannee Rivers, has a much greater quantitative, but similar qualitative impact on nutrient recycling within the northwestern Gulf of Mexico (Figures 9 and 10).

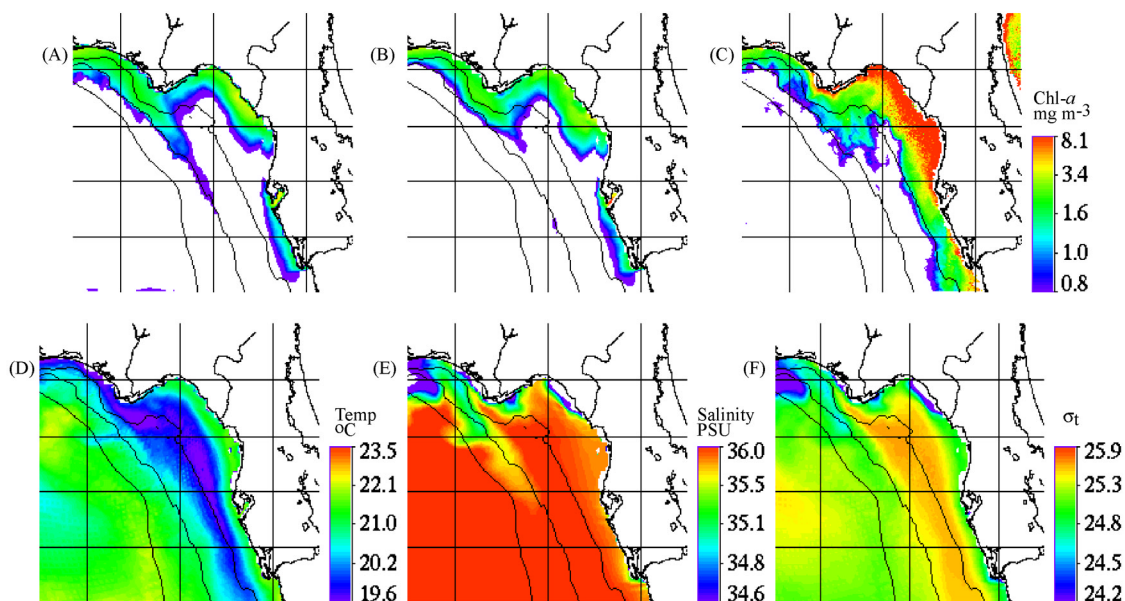


Figure 22. Simulated chlorophyll stocks at (a) surface and (b) middepth in relation to (c) composite SeaWiFS imagery and surface (d) temperature, (e) salinity, and (f) density fields of the circulation model during March 1998. The color codes of Figures 22a, 22b, and 22c are the same.

[119] The residual, unbleached CDOM of terrestrial origin adds to the satellite's color signal, seaward of the midshelf chlorophyll maximum within surface waters of the model. Note that we allow photolytic losses of the model's CDOM, whose land influxes are a constant fraction of the DOC boundary conditions (Table 2). However, the DON of CDOM origin has minimal nutritional value to the phytoplankton of either our model, or in the "real world" [Jolliff *et al.*, 2003].

[120] In terms of phosphorus budgets, the model's opposing physical factors of water circulation for nutrient supply is more important than light attenuation of incident radiation by CDOM and lithogenic suspended debris, such that net biological removal of surface phosphate stocks occurs. Over most of the northwestern inner WFS, the simulated surface phosphate is reduced to $<0.1 \text{ } \mu\text{mol PO}_4 \text{ kg}^{-1}$ during March 1998 (Figure 23a). Exceptions of higher phosphate stocks are simulated at the mouths of the Suwannee River, Tampa Bay, and Charlotte Harbor (Figure 23a).

[121] In contrast to some of the August results (Figures 24 and 25), the depth-averaged DIN/PO₄ ratios of the model's coastal water column in March remain <16 , only between Tampa Bay and Apalachee Bay (Figure 23b). Note the surface feature of simulated March DIN/PO₄ ratios of >16 over most of the northwestern WFS (Figure 23b). It is dominated by the DIN/PO₄ loading ratio of 80.0 from the Apalachicola River, not of 9.9 from the Suwannee River (Table 2).

3.8.2. Summer Cases of the Coupled Model

[122] During late August, sea surface temperatures are typically $>25^\circ\text{C}$ throughout the Gulf of Mexico [Müller-Karger *et al.*, 1991]. The second set of results from the coupled model mimics this thermal pattern during August 1998 (Figure 24d), when the southern part of the WFS warms faster than the northern region. This thermal structure has important ramifications for the distribution of

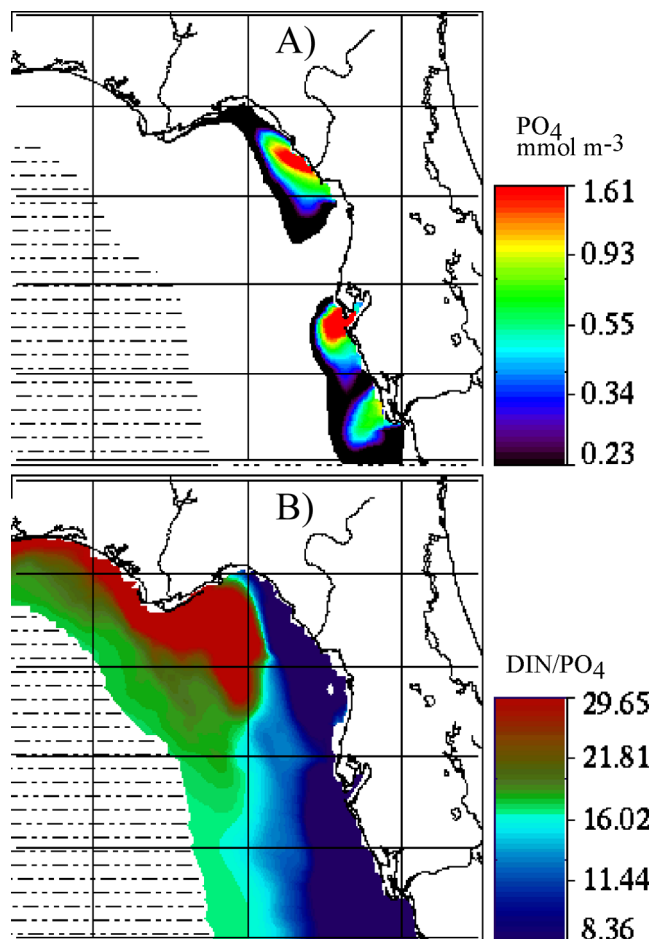


Figure 23. Simulated surface (a) phosphate stocks and (b) molar DIN/PO₄ ratios during March 1998.

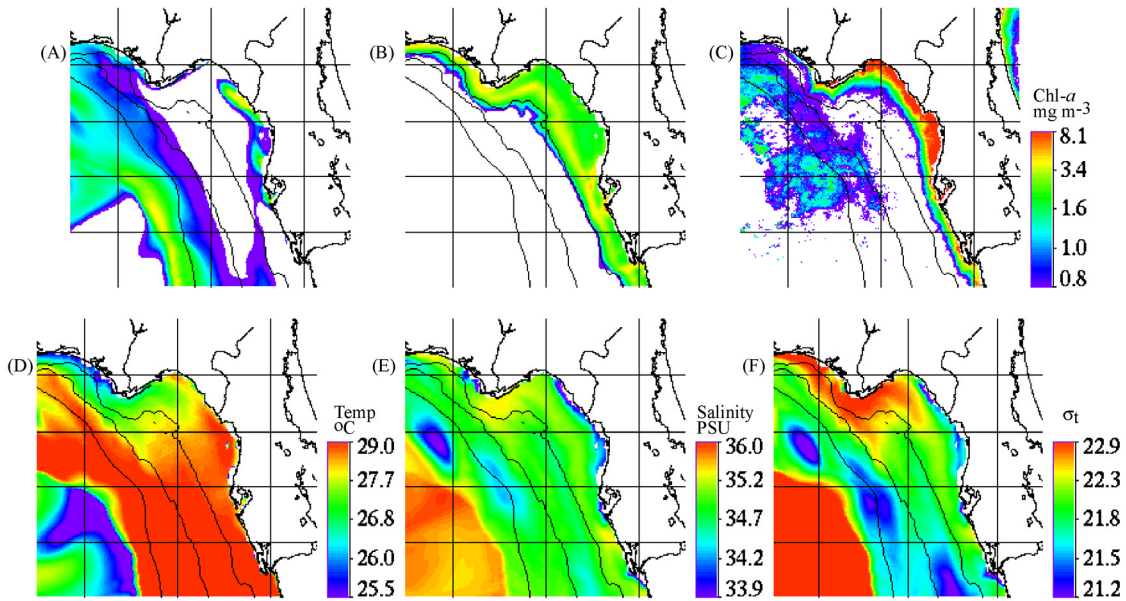


Figure 24. Simulated chlorophyll stocks at (a) surface and (b) middepth in relation to (c) composite SeaWiFS imagery and surface (d) temperature, (e) salinity, and (f) density fields of the circulation model during August 1998 upwelling and outwelling sources of nutrients.

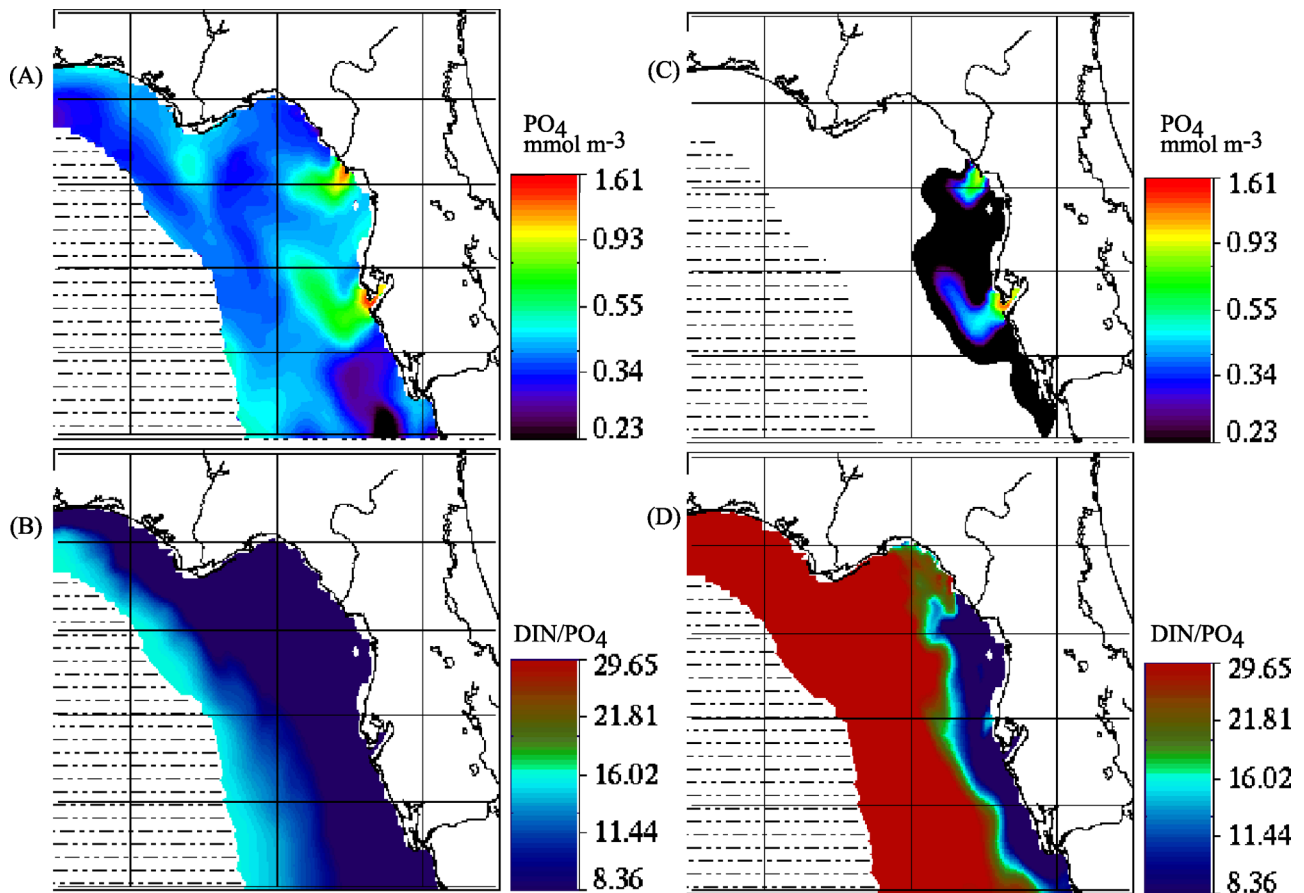


Figure 25. Simulated surface phosphate stocks and molar DIN/PO₄ ratios during August 1998, in response to (a and b) upwelling and outwelling sources, and (c and d) only estuarine supplies.

freshwater, as well as the associated estuarine and deep-sea nutrient inputs along the coast.

[123] In March–April, the coupled model’s river plumes only impact the shelf-wide salinity distribution (Figure 22e) by entrainment within the POM’s parabolic flows. The surface layers then respond to wind stress, but remain frictionally coupled to bottom boundaries. The river plume distributions are largely constrained by Taylor-Proudman Theorem, and thus are unlikely to cross isobaths. Upwelling fronts (Figure 22f) provide additional lateral boundaries at the surface.

[124] After the onset of strong thermal stratification by August, however, responses of the model’s surface layer to buoyancy and wind forcings become frictionally decoupled from the bottom boundary layers. The freshwater influxes thus spread laterally throughout the warm surface layer (Figure 24d) during August 1998. The model’s surface salinity is now <35 psu over large portions of the late summertime shelf (Figure 24e).

[125] Given this physical habitat, the first scenario of the summer model’s two nutrient sources of both estuarine and deep-sea origin yields as much as 3 $\mu\text{g chl l}^{-1}$ within coastal surface waters to the north of Tampa Bay (Figure 24a). But, in the same region, the satellite estimate of phytoplankton biomass in August 1998 (Figure 24c) indicates higher chlorophyll stocks of >10 $\mu\text{g chl l}^{-1}$. Moreover, where are the model’s blooms of 20–30 $\mu\text{g chl l}^{-1}$ of red tides observed in the WFS during 1998–2001 [Vargo *et al.*, 2004]?

[126] Furthermore, as a consequence of the model’s processes of allochthonous supply and algal utilization of nutrients, the simulated surface phosphate field left behind unutilized in the first case (Figure 25a) matches the validation data of August 1998 (Figure 26a). Both the simulated and observed phosphorus fields indicate that plumes of >0.5 $\mu\text{mol PO}_4 \text{ kg}^{-1}$ and low DIN/PO₄ ratios (Figure 25b) emanating from Tampa Bay, have low TDP/TDN (Figure 5) and DIN/PO₄ (Table 2) ratios, fed by the Alafia and Hillsborough Rivers.

[127] Without the deep sea supply of phosphate in the second summer case, the model results (Figure 25c) no longer match the observations (Figure 26a). Yet, the mismatch of the simulated phytoplankton field and match of the inorganic nutrient fields in the first case of the model indicate that an additional internal phosphorus source is still required to match the observed phytoplankton stocks on the WFS.

[128] Our present model recycles phosphorus, but only from particulate phytoplankton debris to dissolved forms. It regenerates phosphorus within the water column faster than nitrogen recycling, as is often observed in aquatic systems [Grill and Richards, 1964; Myers and Iverson, 1981]. Thus, by August 1998 in the first case of both estuarine and deep-sea sources, the model’s surface nutrient fields indicate a nitrogen limited system of a low DIN/PO₄ ratio (Figure 25b) along the landward side of the upwelling front (Figure 24f), favorable for diazotrophs to fuel small red tides. But, what about nutrient sources for large red tides?

3.9. Autochthonous Nutrient Supplies of Dead Fish

[129] At small red tide levels of $\sim 1 \times 10^5$ cells l^{-1} of *K. brevis*, or a biomass of ~ 1 $\mu\text{g chl l}^{-1}$, fish and manatee

kills begin within Florida coastal waters [Landsberg, 2002]. The nutrient sources to fuel larger blooms of ≥ 10 $\mu\text{g chl l}^{-1}$ of these ichthyotoxic dinoflagellates remain an enigma. A combination of initial deep-sea phosphorus loading, secondary estuarine phosphorus loading, and concomitant nitrogen-fixation by *Trichodesmium* can only support the small red tides of our model. Budgets of the organic nitrogen and phosphorus contents of dead fish, co-occurring with *K. brevis* and *Trichodesmium* at convergence fronts during both 1946–47 [Gunter *et al.*, 1948] and 2001 demonstrate a positive feedback mechanism of decomposing fish, whose organic nutrient supplies promote large red tides.

[130] During the 2001 red tide on the WFS (Figure 15), only about half of the phosphorus demand of a mature red tide of 20 $\mu\text{g chl l}^{-1}$ could have been met by estuarine supplies. We compute a maximum river supply of ~ 1.3 $\mu\text{mol PO}_4 \text{ kg}^{-1}$ from the unutilized silicate, the SiO₄/PO₄ ratio in the Peace River [Fraser and Wilcox, 1981], and the observed phosphate stocks of ~ 0.1 $\mu\text{mol PO}_4 \text{ kg}^{-1}$ during August 2001.

[131] A now familiar sequence of events led at first to formation of a small red tide during 2001 on the WFS. During 1–3 July 2001, for example, the dissolved iron stocks on the outer WFS were ~ 0.7 nmol Fe kg^{-1} (Figure 11). Phosphate was then undetectable on the inner shelf, but not on the outer shelf. Weekly sampling of the WFS by a network of volunteer fisherman, between Tampa Bay and Key West, found no populations of *K. brevis* during the preceding months of March–June 2001.

[132] Unutilized offshore silicate stocks, however, suggested prior upwelling of slope waters, with seed populations of *K. brevis* [Milroy *et al.*, 2006] and *T. erythraeum* then found on the 30-m isobath in September 2001, as in 2002 (Figure 13). During the preceding July 2001, a maximum of only 1 colony l^{-1} , or $\sim 1 \times 10^4$ cells l^{-1} , of *T. erythraeum* had been observed offshore during combined ECOHAB/DOTGOM surveys of the WFS.

[133] A month later, however, during 1–4 August 2001, another Saharan dust event led to measurements of >1.1 nmol Fe kg^{-1} on the outer WFS (Figure 11). By 12–23 August 2001, moreover, >10 colonies l^{-1} , or $>1 \times 10^5$ cells l^{-1} of *T. erythraeum* were found (B. Landing, personal communication) within surface waters of the outer shelf on the Fort Myers transect.

[134] Thus far, it was the same plot of a familiar story, but the red tide “thickened”. On 23 August 2001, a cumulative red tide of $>4 \times 10^6$ cells l^{-1} , or >40 $\mu\text{g chl l}^{-1}$ of *K. brevis*, as well as dead fish were sampled by aircraft and ship off Port Charlotte, FL. A few months later, this large red tide was still seen by satellite on 15 October 2001 (Figure 15), using an algorithm that separated *K. brevis* from *Trichodesmium*, based upon relative backscatter [Cannizzaro *et al.*, 2004]. This red tide represented a positive feedback of supplemental nutrition from dead fish.

[135] When the WFS 2001 red tide reached population levels of >20 $\mu\text{g chl l}^{-1}$ (Figure 15), it and the precursor diazotrophs had then already stripped most of the original deep-sea phosphate and local estuarine phosphate stocks. Indeed, a PN/chl ratio ratio of 0.4 $\mu\text{mol/ug}$ for shade-adapted populations of *K. brevis* [Shanley and Vargo,

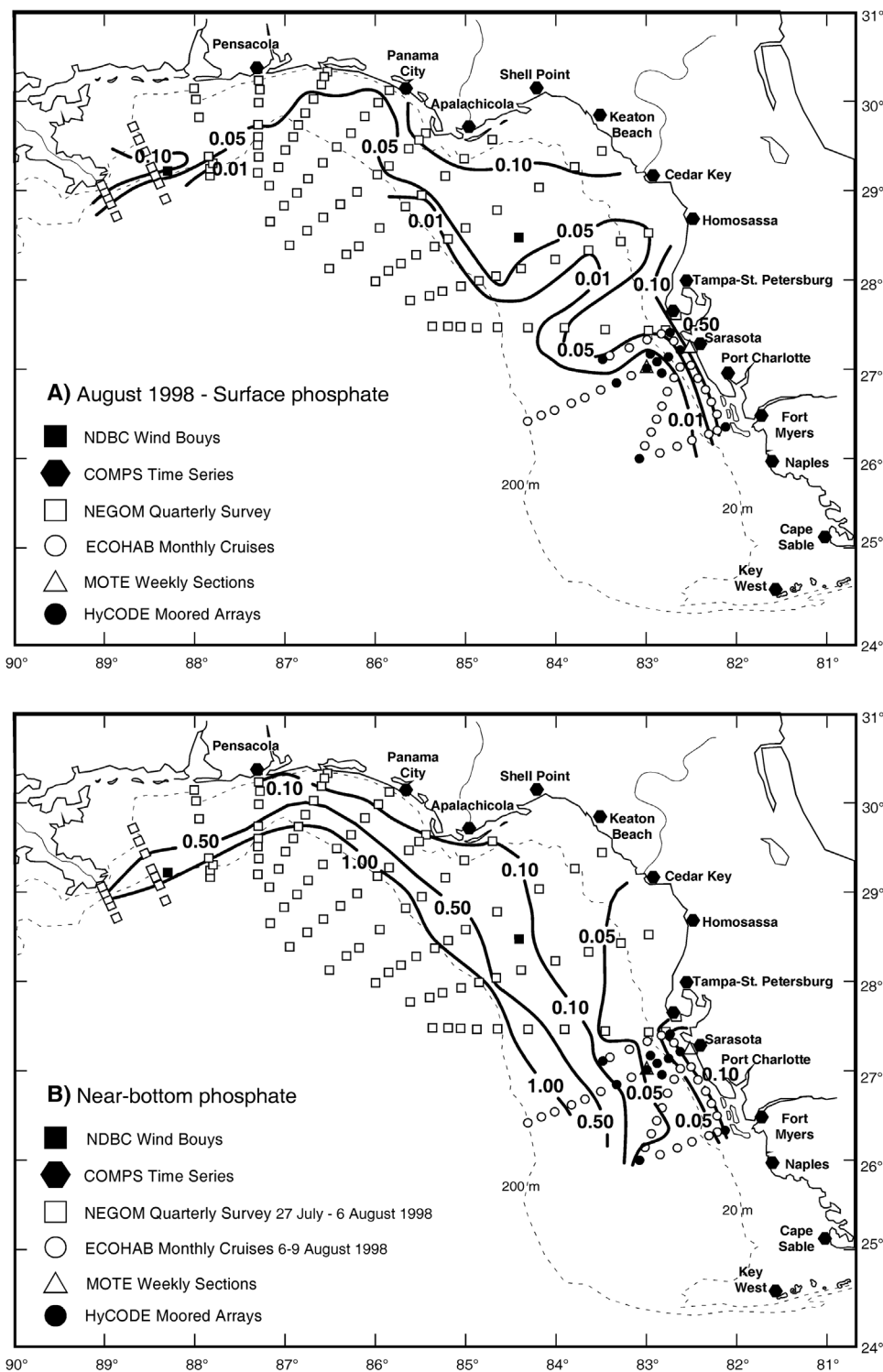


Figure 26. A composite of (a) near-surface and (b) near-bottom phosphate stocks on the West Florida shelf during NEGOM and ECOHAB surveys of 27 July–9 August 1998.

1993], and a Redfield PN/PP ratio of 16, suggest that at least $2.0 \mu\text{mol P kg}^{-1}$ of dissolved phosphate and/or dissolved organic phosphorus are required to yield such dinoflagellate stocks of $\sim 80 \mu\text{g chl l}^{-1}$ [Carder and Steward, 1985]. Dead fish provide the incremental nutrients [Wilson and Collier, 1955] for formation of a larger red tide here and within Texas waters.

[136] During 23 August 2001, an airplane survey found a drift line of dead fish of $\sim 5\text{--}10 \text{ m}$ width, above the $\sim 10\text{-m}$ isobath off Port Charlotte, FL. Dead fish were again noted during October 2001 off Tampa, FL on the DOTGOM cruise, when the large red tide persisted. Recall that dead fish were also associated with stocks of $1 \times 10^7 \text{ cells l}^{-1}$, or

100 $\mu\text{g chl l}^{-1}$, of *K. brevis* during November–December 1954, north of Fort Myers [Hela, 1955].

[137] Furthermore, during November 1946 to August 1947, earlier airplane photographs depicted similar drift lines of dead fish along the West coast of Florida [Gunter et al., 1948]. With a spacing of ~ 1 individual m^{-2} within the 1946–47 drift lines [Gunter et al., 1948], the dead fish were coincident with populations of *Trichodesmium*, and of *K. brevis*. Using estimates of a mean fish wet weight (ww) of 90 g, a dry weight (dw) of 25% ww, a nitrogen content of $\sim 10\%$ dw, and a phosphorus content of 0.7% dw [Walsh et al., 2006], we derive a potential fish supply of 160 mmol N m^{-2} and 5 mmol P m^{-2} .

[138] Within the upper 10 meters of the WFS water column, vertical mixing would yield a fish source of recycled dissolved nutrients of 16 $\mu\text{mol N kg}^{-1}$ and 0.5 $\mu\text{mol P kg}^{-1}$ beneath the fall fish drift lines in either 1946, 1954, or during 2001. This represents a continuing positive feedback process during the maturation of red tides. At the start of the DOTGOM study of the persistent red tide in October 2001 (Figure 15), for example, 6.0 $\mu\text{mol NH}_4 \text{ kg}^{-1}$ and 0.35 $\mu\text{mol TDP kg}^{-1}$ were indeed measured close to dead fish. These recycled nutrients were then found within surface waters above the 10-m isobath off Tampa Bay, where the *K. brevis* stock was $3.0 \times 10^5 \text{ cells l}^{-1}$, i.e. at initial ichthyotoxic levels of $\sim 3 \text{ ug chl l}^{-1}$.

[139] Off Texas, large red tides are found after fish kills, not before [Villareal et al., 2001]. At background levels, initial stocks of *K. brevis* are usually most abundant on the landward side of the coastal salinity front off Port Arthur, TX. Here, initial populations of $\sim 20 \text{ cells l}^{-1}$, i.e. $\sim 0.0002 \text{ ug chl l}^{-1}$, were found in July during onset of the 1999 red tide (Figure 2a). A few months later during October–November 1999, when $\sim 0.5 \text{ ug chl l}^{-1}$ were then found here at a near shore salinity of ~ 32 psu, the toxic dinoflagellate levels had increased 100-fold to $2.5 \times 10^3 \text{ cells l}^{-1}$. The red tide then amounted to $\sim 5\%$ of the phytoplankton biomass.

[140] During the intervening time period at an alongshore drift of 20 cm sec^{-1} – as depicted (Figure 20) by the previous inner shelf LATEX drogue during November 1992 [Howard and DiMarco, 1998], or $\sim 20 \text{ km day}^{-1}$, it would take about 25 days for an initial July stock of $\sim 20 \text{ cells l}^{-1}$ of *K. brevis* to be transported $\sim 500 \text{ km}$ alongshore, from off Port Arthur to near Brownsville, TX. Off Brownsville, greater red tide amounts of $>1 \times 10^6 \text{ cells l}^{-1}$, or $>10 \text{ ug chl l}^{-1}$ of the ichthyotoxic phytoplankton, were instead found after a fish kill in October 1999, when *K. brevis* was the dominant phytoplankton. Then strong winds from the northeast would have induced southwestward flow with onshore transport [Villareal et al., 2001] at the surface, and downwelling at the coast. How often do red tides and dead fish drift south along the Texas coast, and north along the WFS (Figure 4)?

3.10. Alongshore Propagation of Red Tides

[141] Like previous red tides in 1998 [Vargo et al., 2001], the 2001 HAB started off southwest Florida in late August [Vargo et al., 2004]. Moreover, the first wave of *K. brevis* had moved northwards along the coast by September 2001 (Figure 15), despite the upwelling-favorable winds which predominated during fall – as in other years. During the

1953 red tide, another northward propagation of *K. brevis* was observed during August–October 1953, from off Venice, FL to St. Petersburg [Feinstein et al., 1955]. Similarly, in June–July 1947, an earlier red tide of *K. brevis* first occurred off Venice and Fort Myers; it was within Tampa Bay and off northern beaches by August 1947 [Gunter et al., 1948; Davis, 1948]. Yet, these time sequences of red tides during summer-fall 1947, 1953, 1998, and 2001 are consistent with instead a downwelling circulation pattern of northward water motion on the landward side of near-bottom convergence fronts.

[142] The same northward fall movement of Florida red tides is observed, moreover, in our plot of the red tide [Dragovich et al., 1961; Dragovich, 1963] during late October 1957 (Figure 4b). At ichthyotoxic levels of $>3 \text{ ug chl l}^{-1}$, this 1957 red tide moves northeast towards Tampa, FL, past the mouth of the Caloosahatchee River at Fort Myers by early November 1957. This red tide occurred before eutrophication of Lake Okeechobee and the Caloosahatchee River, after 1965 (Figure 2b). Note that during most of November 1957, no further red tide was observed off Naples, FL (Figure 4b), until wind reversals from the northeast lead to southeastward advection of the red tide by December 1957.

[143] The red tide off Naples during October 1957 (Figure 4b) represents the second phase of the co-joining of offshore seeds of *K. brevis* and *Trichodesmium* with estuarine supplies of phosphorus in steps 6–7 of our hypothesis, like the plankton communities observed there in September 2001 (Figure 15). At the pier off Naples on 25 July 1957, the NO_3/PO_4 ratio of near shore surface waters was <2.0 [Dragovich, 1963], similar to the DIN/PO_4 ratio of 2.2 observed off Port Arthur, TX during August 2000 [Villareal and Magana, 2001] at the onset of that red tide (Figure 4a). Recall that the first phase of nitrogen transfer between diazotrophs and dinoflagellates is driven by deep-sea supplies of phosphorus on the outer shelf (Figures 16 and 26).

[144] The September 1957 red tide found to the north of Tampa Bay (Figure 4b) represents a prior wave of net northward advection of the red tide – as simulated by the path of our model's low N/P ratios during August 1998 (Figure 25b). Based upon these shipboard snapshots, satellite images, and simulated Florida red tides during 1947, 1953, 1957, and 1998–2001, one might consider the southern WFS as a “conveyor belt” of red tide fabrication. It is modulated by a seasonal series of wind-related injections and subsequent dispersions of offshore seed populations of *Trichodesmium* and *K. brevis*. Each set of downwelling and subsequent upwelling events has the potential to form waves of red tides, propagating forward from the southern epicenters, like a coastally trapped physical wave of the coastal boundary layer. Because of the asymmetry in response of water motion to downwelling- and upwelling-favorable winds on the WFS [Weisberg et al., 2001], the same amount of wind stress leads to rectification of a greater movement north than south during the fall. Thus, red tides exhibit a net up coast movement (Figure 4b) during the “upwelling” season [Yang and Weisberg, 1999].

[145] The Texas red tides begin in early August off Port Arthur, TX, as in 2000 and move southwest (Figure 4a), like the previous trajectories of the 1986 [Buskey et al., 1996]

and 1999 red tides. Another red tide moved south along the Texas coast by November 1990, since one was then observed off Brownsville [Buskey et al., 1996]. Extending southwards, with coincident dead fish ~ 200 km along the coast of Tamaulipas, Mexico, an earlier red tide during 1955 amounted to as much as 2×10^7 cells l^{-1} (~ 200 μg chl l^{-1}) of *K. brevis* at 50 km south of the Rio Grande [Wilson and Ray, 1956].

[146] In the western Gulf, the source of P-enriched pools of nutrients is near-bottom recycled phosphate at low N/P ratios (Figures 10c and 10e), after spring fallout of diatoms on the Louisiana shelf (Figure 2a). In the eastern Gulf, the estuarine phosphate stocks on the WFS (Figure 8) of low N/P ratios are instead mainly of fossil origin from the Miocene deposits (Figure 6). Both coastal nutrient regimes prime nitrogen fixers and thence consequent red tides in these two regions of the Gulf of Mexico (designated by arrows of Figure 5). Since $\sim 53\%$ of the influx of the Mississippi River flows southwest along the Texas coast [Dinnel and Wiseman, 1986; Etter et al., 2004], however, we expected the low N/P ratios of recycled nutrients on the shelf at the Texas-Louisiana border to reflect anthropogenic transients of both iron and nutrient supplies.

3.11. Anthropogenic Transients

[147] The Sahara Desert supplies about half of the global supply of aeolian dust to the oceans [Goudie and Middleton, 2001; Jickells et al., 2005], impacting coastal seas off Europe, Africa, North and South America, as described by Darwin [1839]. Since 1900, rainfall over West Africa has declined $\sim 20\%$ per decade, with moisture of the soils there less during the last century, than over the preceding millennium [Hulme, 1991; Vose et al., 1992; Hulme et al., 1994; Eischeid et al., 1991]. The major factor effecting the frequency of dust storms within such arid regions is rainfall [Gillette, 1981].

[148] A reduction in rainfall leads to an increase of dust storms, and subsequently an increment of downstream iron fertilization of *Trichodesmium* populations. Dust storm frequency in the Saharan Desert indeed appears to have increased since 1950 [Prospero and Nees, 1986; Jickells et al., 2005]. Furthermore, as a result of drought and expansion of the Sahel after 1970, for example, the annual mean amount of mineral aerosols of Saharan origin observed at Barbados has recently increased 3-fold, from $3.9 \mu g m^{-3}$ during 1965–69 to $11.0 \mu g m^{-3}$ in 1970–92 [Prospero, 1996].

[149] Over the same century, the anthropogenic nutrient loading of rivers, adjacent to western boundary currents has also increased, with a ten-fold increment of global phosphorus influxes since the Industrial Revolution [Walsh, 1988]. Locally, for example, the nitrate content of the Mississippi River doubled by 1957 (Figure 2a), compared to that of 1905 [Turner and Rabelais, 1994], providing the first documented fish kills by *K. brevis* in south Texas waters during 1955 [Wilson and Ray, 1956]. Furthermore, the DIN content of the Mississippi River at New Orleans was only $\sim 16 \mu mol NO_3 + NH_4 kg^{-1}$ in 1935 [Riley, 1937], compared to $\sim 21 \mu mol DIN kg^{-1}$ far downstream, at the same salinity of ~ 12 parts per thousand, off Port Arthur during July 1999 [Villareal et al., 2001].

[150] With another doubling of the Mississippi River supply of nutrients [Turner and Rabelais, 1994] by 1976 (Figure 2a), a fish kill of ~ 10 million dead fish then occurred over a wider area, from Galveston to the Rio Grande [Buzan et al., 1998]. By 1986, the nutrient loading of the Mississippi River had doubled yet again. Then, the extensive red tide of *K. brevis* started on 27 August 1986 off Galveston Island and led to ~ 22 million dead fish over the same downstream coastal region [Trebatoski, 1988]. Subsequently, a red tide of 3×10^7 cells l^{-1} ($\sim 300 \mu g$ chl l^{-1} of *K. brevis*) was sampled within Corpus Christi Bay on 16 October 1986 [Trebatoski, 1988].

[151] Monitored by a set of aircraft overflights and in situ observations, this red tide followed the same alongshore trajectory during 1986 [Buskey et al., 1996] as those of the ones in 1999 and 2000 (Figure 4a). By 3 November 1986, the red tide was then found on beaches off Tampico, Mexico; and it persisted in the Bay of Campeche until January 1987. Like the later red tide during 2000, oyster harvesting was prohibited, vertebrate mortality amounted to more than 7.5 million fish [Trebatoski, 1988], and both Texas and Mexican beaches were closed as a result of aerosol toxins during 1986–1987.

[152] The Texas red tides originated in the recycled nutrient portion of the Louisiana river plumes off Port Arthur during 1986, 1999, and 2000. Increased nutrient loading and diatom inputs to the benthos off Louisiana (Figure 2a) evidently led to both larger red tides and perhaps more frequent ones on the downstream Texas shelf, than those seen ~ 400 years earlier [Cabeza de Vaca, 1871]. The premodern impact of *K. brevis* was observed in 1528–1534 on Galveston Island, which was much closer to our proposed epicenter (Figure 5), than Brownsville. Larger blooms of greater spatial extent of *Trichodesmium* and *K. brevis* would have followed the increased supplies of these P-enriched recycled nutrients. Thus, over time they would have been noticed more often by coastal observers (Figure 2a).

[153] Other Texas red tides followed in 1990 [Buskey et al., 1996], and thence more frequently during 1996, 1997, 1999 [Denton and Contreras, 2004], 2000, 2001 and 2002 [Biegalski and Villareal, 2005]. Indeed, the longest seasonal persistence of a *K. brevis* bloom was observed in Corpus Christi and Nueces Bays during January–April 2002, with millions of dead menhaden even found in open waters off the Gulf beaches of the Padre Island National Seashore (<http://www.tpwd.state.tx.us/fish/recreat/tideup.htm>). These Texas red tides of anthropogenic origin now appear to be annual events, like those of fossil origin off Florida.

[154] In contrast, the P-loading of the Caloosahatchee River (Figure 2b) had doubled after 1975, as well, in response to fertilization of its drainage basin and that of Lake Okeechobee. Yet, the annual frequency of red tides off southwest Florida did not increase. Given the aeolian iron supplies of Saharan dust to the Gulf of Mexico, inferred during 1528–1534 [Cabeza de Vaca, 1871] and observed before 1832 [Darwin, 1839], and the fossil supplies of Miocene phosphorus (Figure 6), it is not surprising that red tides are annual events within the eastern Gulf of Mexico.

[155] After the well-publicized events of the red tides during 1946–47 [Gunter et al., 1948], when *K. brevis* was

first identified as the cause of Florida red tides [Davis, 1948], their annual occurrences (Figure 2b) were dutifully reported by the media, interested citizens, and scientists as yearly events during the next 50 years [Kusek et al., 1999]. Dead fish, for example, were subsequently documented by local newspapers in 1949, 1952, 1953, 1954 [Feinstein et al., 1955], and 1959, with an increased number of “red tide” articles published in the *St. Petersburg Times*: from three in 1953 to thirty-six by 1957 [Kusek et al., 1999].

[156] Before the 1949 large red tide [Kusek et al., 1999], moreover, a precursor bloom of *Trichodesmium* washed ashore during April 1949 within Sarasota Bay. “The accumulated decomposing organic matter created such a nuisance that it was necessary for the city of Sarasota to haul it away in trucks” [Graham et al., 1954]. Increased sampling and observations of red tides and diazotrophs seem to dominate the 150-year record off Florida, rather than an increase in red tides, since agricultural application of phosphorus during the 1960s had evidently little impact on their occurrence each year.

[157] Mining did not really exacerbate the natural runoff process from southern rivers, as well. “Enrichment of the Gulf waters with phosphorus by way of river drainage from phosphate mines in the interior was early suspected as a contributing cause of the red tide, but the importance of this contamination was later minimized . . . as historical records of occurrences of noxious red water along the Florida west coast came to light.” [Graham et al., 1954]. We make the same conclusion with respect to the consequences of farming in south central Florida.

[158] The paucity of nitrate on the WFS also led to the early hypothesis that “*G. breve* . . . red tide organisms might be able to utilize atmospheric nitrogen as some of the blue-green algae are capable of doing” [Lasker and Smith, 1954]. Continuous phosphorus loading from fossil sources of west central Florida (Figure 6) does yield a low DIN/PO₄ ratio of <16 that prevents dominance of diatoms and instead favors the precursor diazotrophs and thence toxic red tides, as they both harvest phosphorus on the outer and inner WFS. This region is thus one chemical milieu favorable to initiation of red tides within the southeastern Gulf of Mexico (Figure 5).

[159] But, it is not the only region of phosphorus-rich initial chemical conditions. Nutrient recycling [Grill and Richards, 1964] by the benthos of initial estuarine-fed diatom blooms at N/P ratios of >16 eventually leads to other regions of low DIN/PO₄ ratios [Darrow et al., 2003] within the northwestern Gulf of Mexico. The discharges of both the Suwannee and Apalachicola Rivers are ten-fold less than that of the Mississippi River [Gilbes et al., 1996], however, such that red tides are still rare within the Big Bend region of Florida.

[160] In contrast, the recycled nutrients of Mississippi River origin on the east Texas shelf, with a low N/P ratio (Figure 9d) similar to that of the northern WFS [Darrow et al., 2003], lead to co-occurring *Trichodesmium* and *K. brevis* blooms, as far away as the Texas shelf (Figures 3 and 4a). Moreover, the discharge of the Amazon River is again ten-fold larger than the effluxes of the Mississippi River. Accordingly, the high P-content of the recycled Amazon River plume off Barbados is responsible for the onset there of iron-sated *Trichodesmium* blooms [Lenes et al., 2005].

[161] Thus, we find that the origin of toxic dinoflagellate blooms within the western Gulf is related to differential recycling of diatom debris [Grill and Richards, 1964] into regenerated P-rich nutrients, beneath the plumes of the Mississippi and Atchafalaya Rivers on the Louisiana-Texas shelves. These larger rivers have also been subjected to increased anthropogenic nutrient loading (Figure 2a), such that the same processes that led to red tides off Galveston Island during 1528–1534 prevail today, but with a wider dispersal of the initial conditions leading to ecological succession of red tides of *K. brevis*. Are there other coastal regions, where the fish-killing niche of *K. brevis* and cognate species has expanded? Given that our hypothesis appears to work for both sides of the Gulf of Mexico, how well does it apply to other fish kills, observed both recently and over the last century, downstream of other arid regions (Table 1)?

3.12. Global Ramifications

[162] Thus far, we have presented information on the Gulf of Mexico that suggests the Saharan dust loading has persisted since at least 1528–1534, when shellfish harvest was suspended seasonally on Texas beaches [Cabeza de Vaca, 1871], like ancient deposits of African dust in southern France [Bucher and Lucas, 1984]. The increased frequency of red tides in the western Gulf thus reflects increments of phosphorus, not of iron. Does a similar conclusion apply to the other red tide regions (Table 1)?

[163] At most low latitudes, sub-tropical rainfall is now ~10% less since 1970, as part of a long-term trend begun in the 1950s [Bradley et al., 1987]. In some arid lands, such as West Africa and northern Chile, precipitation has declined ~20% per decade since 1900 [Hulme, 1991; Vose et al., 1992; Hulme et al., 1994; Eischeid et al., 1991]. Consequently, the moisture conditions of the Sahara, Saudi Arabian, Gobi, Simpson, Great Western, Kalahari, Atacama, and Patagonian Deserts have been substantially drier over the last century than during the preceding millenium.

[164] Since one of the major factors effecting the frequency of dust storms, and thus the associated aerosol export of trace metals, is soil moisture [Gillette, 1981], one might expect the frequency of downstream, dust-stimulated *Trichodesmium* blooms and associated red tides of *Karenia* to have also increased over the last 100 years. Indeed, within just the last ten years, previously cryptic species of *Karenia* have led to fish kills off Hong Kong, New Zealand, Tasmania, South Africa, Kuwait, Tunisia, Greece, Ireland, France, Denmark, Norway, Chile, and Argentina (Table 1). All of these shelves are influenced by deserts on the landward side of the shelf, and most by western boundary currents on the seaward side. Moreover, like the WFS, red tides have persisted off the east coast of Japan for more than a century, as well.

3.12.1. Japanese and Chinese Red Tides

[165] Japan is located downstream of dust storms from the Gobi Desert [Duce and Tindale, 1991; Young et al., 1991], first noted in 1150 B.C. as “dust rain” by Chinese observers [Sheng et al., 1981]. Furthermore, *Trichodesmium* is a ubiquitous component of the phytoplankton within Japanese and Chinese shelf seas [Carpenter, 1983; Minagawa and Wada, 1986], particularly within the warm waters of the Kuroshio Current [Nagasawa and Marumo,

1967; Marumo and Nagasawa, 1976]. Thus, it is not surprising that *Gymnodinium nagasakiense*, or *K. mikimotoi*, was responsible during 1893, 1910, 1926, 1933–34, 1979–80, 1982, 1985, and 1994 for suspended shellfish harvests and fish kills both off Toba at the mouth of Ise Bay (region **B** of Figure 1) and within the Bongo Channel on the eastern side of Honshu Island, Japan [Landsberg, 2002], adjacent to the ready source of *Trichodesmium* within the Kuroshio Current.

[166] Recall that the upstream source of *Trichodesmium* populations on the Brazil and Venezuela shelves, as well as those on the outer Florida and Texas shelves [Walsh, 1996; Walsh and Steidinger, 2001], are waters of the warm western boundary current, flowing northeast into the Caribbean Sea and Gulf of Mexico as the Guiana and Loop Currents [Margalef, 1965; Caley and Grice, 1966]. Similarly, the Kuroshio Current seeds the outer eastern Japanese shelf and the East China Sea with these diazotrophs [Marumo and Asaoka, 1974a]. The toxic dinoflagellate response of *K. mikimotoi* to anthropogenic nutrient loading within Hong Kong environs may also be analogous to the recent blooms of *K. brevis* within Texas waters, after respective increased nutrient loadings of the Mississippi River and of Chinese fish farms.

[167] Over the last decade, the nutrient loadings of Chinese and Korean rivers have indeed doubled, but at an N/P molar ratio of 111/1. Thus, P-limitation prevails over most of the East China Sea shelf, except where: (1) subsurface Kuroshio waters upwell nutrients at the Redfield ratio along the shelf-break [Chen and Wang, 1999] - as in our present model of the WFS; and (2) organic matter accumulates, with regeneration of P-rich nutrients. Accordingly, the recycling of phosphorus from precursor diatom blooms - as observed within shallow Hong Kong coastal waters (region **D** of Figure 1) before the massive red tide during 1998 [Yang and Hodgkiss, 2001] - set the stage for initial diazotroph and toxic dinoflagellate blooms. However, the major nutrient source for the Chinese red tides is the supplemental nutrient supply of fish biomass introduced by humans in the form of fish farms, rather than by eutrophication of adjacent rivers. During 1988, 90% of the cultured fish at ~1,500 farms around Hong Kong died, amounted to a loss of ~\$32 million from red tides of *K. mikimotoi/digitata* that were first observed here in 1971 [Dickman, 2001; Yang and Hodgkiss, 2001].

[168] The Chinese red tides are thought to start like the Japanese ones under the same weather patterns [Yang and Hodgkiss, 2001], conducive for frontal aggregations [Kishi and Ikeda, 1986; Yanagi et al., 1995], described here for the Florida and Texas shelves, i.e. “after strong wind” for onset of Ekman transport of the offshore populations of dinoflagellates and diazotrophs and “some rain” for supply of estuarine nutrients and CDOM. Future isotope studies should verify nitrogen transfer between these Asian functional groups of phytoplankton, which we maintain is a persistent phenomenon for the origin of red tides on both sides of the Gulf of Mexico, recently documented by direct isotope transfer studies between field populations of diazotrophs and dinoflagellates in the WFS [Mulholland et al., 2004, 2006].

3.12.2. Australian and New Zealand Red Tides

[169] Finally, as the rates of desertification increase globally, so should the anthropogenic inducements of nitrogen fixation and subsequent toxic red tides, but only within the downstream areas subject to both iron fertilization and phosphorus loading. Within another western boundary current - that of the East Australian Current, for example, small populations of $<1 \text{ ug chl l}^{-1}$ of *Trichodesmium* may modulate seasonal succession of phytoplankton on the Great Barrier Reef, favoring dinoflagellate growth there as well [Revelante and Gilmartin, 1982; Revelante et al., 1982], but not *Karenia* blooms (Table 1). The small diazotroph biomass there exhibits little nitrogen-fixation on the Reef [Furnas and Mitchell, 1986, 1996], while phosphate stocks [Crosbie and Furnas, 2001] are two orders of magnitude less than those of the WFS.

[170] Without a dust supply of iron (Figure 1), the riverine stocks of dissolved iron of $\sim 38 \text{ nmol Fe kg}^{-1}$ on the inner East Australian shelf [Jones et al., 1986] are similar to those on the WFS at the mouth of Florida Bay [Caccia and Millero, 2003]. They were reduced to $\sim 7 \text{ nmol Fe kg}^{-1}$ at the 25-m isobath of the Great Barrier Reef in 1977 [Jones et al., 1986]. A potential yield of $\sim 6.2 \text{ ug chl l}^{-1}$ of *Trichodesmium* from an apparent iron deficit of $31 \text{ nmol Fe kg}^{-1}$ on the Great Barrier Reef and a Chl/Fe (ng/nmol) ratio of 200 for this diazotroph [Walsh et al., 2001] is ten-fold larger, however, than the concurrent stocks of $0.5 \text{ ug chl l}^{-1}$ of all phytoplankton found across the Reef during 1977 [Revelante and Gilmartin, 1982].

[171] A particulate phosphorus/chlorophyll ratio (umol/ug) of 0.08 for *Trichodesmium* [Walsh et al., 2001] indicates that balanced growth of such a potential accumulation of $\sim 6.2 \text{ ug chl l}^{-1}$ of diazotrophs on the Reef would also demand $\sim 0.50 \text{ umol PO}_4 \text{ kg}^{-1}$. Yet, a mean stock of only $0.20\text{--}0.02 \text{ umol PO}_4 \text{ kg}^{-1}$ has been repeatedly observed there during 1976–1977 [Revelante and Gilmartin, 1982], 1983–87 [Furnas and Mitchell, 1996], and 1994–97 [Crosbie and Furnas, 2001]. The smaller phosphate stocks reflect the increased sensitivity of the phosphate analyses over time. We thus conclude that phosphorus limitation prevails on the East Australian shelf, with the riverine dissolved iron supply to the Reef phytoplankton community mainly dispersed by mixing, rather than utilized by phosphorus-starved diazotrophs, despite prior assumptions of eutrophication in this region [Bell, 1992].

[172] Indeed, we shall next find that an order of magnitude larger phytoplankton stock of $\sim 4.9 \text{ ug chl l}^{-1}$ occurs on the eastern New Zealand shelf [Rhodes et al., 1993], compared to that of $0.5 \text{ ug chl l}^{-1}$ on the Great Barrier Reef [Revelante and Gilmartin, 1982], bathed by the same shelf-break supply of nutrients from the Coral Sea [Andrews and Gentian, 1982]. Given the same upwelled phosphate supply of $\sim 0.60 \text{ umol PO}_4 \text{ kg}^{-1}$ [Furnas and Mitchell, 1996] to the East Australian and North New Zealand shelves, from the continuous western boundary current [Tomczak and Godfrey, 1994], the ten-fold difference of phytoplankton yield implies that the presence of extensive coral reefs on the Australian shelf represents an additional sink of phosphorus, not found in the Hauraki Gulf of New Zealand. For example, smaller reef systems at Eniwetok Atoll are surrounded by ambient stocks of $\sim 0.2 \text{ umol PO}_4 \text{ kg}^{-1}$ [Pilson and Betzer, 1973], not the

0.02 $\mu\text{mol PO}_4 \text{ kg}^{-1}$ of the Great Barrier Reef [Furnas and Mitchell, 1996].

[173] A yield of $\sim 4.9 \text{ ug chl l}^{-1}$ on the inner New Zealand shelf during 1992 [Rhodes et al., 1993], from a potential phosphate supply of $\sim 0.60 \text{ umol PO}_4 \text{ kg}^{-1}$ at the shelf-break, suggests balanced growth of the phytoplankton community, with little iron-limitation as well. The Great Barrier Reef, i.e. region **Z** of Figure 1, is not downstream of wind-transported dust from the Great Western and Simpson Deserts, whereas both Tasmania and the north Island of New Zealand are downwind (Figure 1). Seasonal plumes of dust haze have been observed by ships at sea during fall and winter, as they exit the southeast Australian mainland towards Tasmania, and thence disperse to the east over the north island of New Zealand [Prospero, 1981].

[174] Over the last 40 years, there have been persistent declines of rainfall to eastern Australia, with a 15% reduction of precipitation to the Simpson Desert environs from 1965 to 1985 [Nicholls et al., 1996]. Consequently, previously cryptic species of *Karenia* have been observed off both Tasmania and Western Australia, as well as off New Zealand (Table 1). In contrast to the Great Barrier Reef environs, moreover, within the last decade fish kills and NSP symptoms of adjacent human populations have also been more frequent within the warm waters of the subtropical East Auckland Current, drifting south along the east coast of the north island of New Zealand, as an extension of the East Australian Current [Tomczak and Godfrey, 1994].

[175] Along the beaches of the Hauraki Gulf to the east of Auckland, New Zealand, 180 cases of NSP during 1992–1993 [Rhodes et al., 1993] were eventually attributed to *K. mikimotoi* [Haywood et al., 2004]. Here, the chlorophyll stocks are ten-fold those of the Great Barrier Reef. Later, massive fish kills and deaths of other marine fauna and flora, as well as respiratory irritation of humans, were observed within Wellington Harbor, in response to blooms of *K. brevisulcata* during 1998. A small red tide of *Gyrodinium aureolum* had been observed earlier in a fish farm off the South Island of New Zealand during 1987 [Boustead et al., 1987].

[176] The latest New Zealand red tides of *K. brevisulcata* and *K. mikimotoi* led to mass deaths of eels and fish within Hauraki Gulf during October 2002 [Rhodes et al., 2004]. Yet, a half century earlier no observations of *Gymnodinium brevis*, *Gyrodinium aureolum*, or *Karenia mikimotoi*, were made during monthly surveys of the same region during 1957–58 [Cassie, 1960], where *Trichodesmium* was not rare within the warmer waters off the east coast of the north island of New Zealand [Cassie, 1961]. As the rate of desertification increases globally, we expect the rate of nitrogen fixation to increase within downstream areas as well, but with larger blooms of associated red tides (Figure 1) in areas subject to phosphorus additions at either the phytoplankton bottom, or the fish top of the coastal food web.

[177] We conclude that regions **A** and **B** off West Florida and Japan (Figure 1) now represent background coastal regions of relatively unaccelerated supplies of nutrients from land and the shelf-break exchange from western boundary currents. Here, red tides of *Karenia brevis* of more than 100 year persistence are in response to long-term aeolian supplies of iron from the Sahara and Gobi Deserts.

Instead, regions **C** off Texas and **D** off Hong Kong reflect more recent red tides over the last decade, under the same dust loadings, but accelerated nutrient supplies in the form of fertilization of both terrestrial and marine farms. Region **Z** off northeast Australia represents our second null case of no red tides, in the absence of both iron and phosphorus supplies for these phytoplankton, whereas region **E** off northern New Zealand instead reflects an accelerated supply of dust loading and no algal reef competitors for the same phosphorus supply from the Coral Sea.

[178] The Leeuwin Current off western Australia is an unusual eastern boundary that seasonally flows poleward at varying rates, in response to varying alongshore pressure gradients [Tomczak and Godfrey, 1994]. Like remote sensing of red tides off Texas (Figure 3), CZCS imagery has also suggested blooms of *Trichodesmium* off the northwest coast of Australia [Capone et al., 1997], where dust from the Great Western desert (Figure 1) would alleviate iron-limitation of both *Trichodesmium* here and of downstream populations advected south towards Cape Leeuwin. Indeed, the later observations of the *Challenger* Expedition during 1872–1876 - “we met with this alga in greatest abundance in the Arafura Sea between Torres Straits and the Aru Island . . . And at length the whole sea, far and wide, was discolored with it” [Mosely, 1879] confirm those sightings of *Trichodesmium* made ~ 40 years earlier by Darwin off Cape Leeuwin.

4. Discussion

[179] The Loop Current supplies both near-bottom phosphorus stocks and *Trichodesmium* seed populations for use of atmospheric iron and dinitrogen gas by diazotrophs and thence transfer to dinoflagellates on the outer shelves of the Gulf of Mexico. However, strong upwelling of these deep-sea supplies of inorganic nutrients favors diatom blooms on the WFS [Walsh et al., 2003]. Weak upwelling instead sets the stage for initial accumulation of diazotroph and dinoflagellate stocks there on the outer shelf, since they vertically migrate together into bottom Ekman layers, unlike the diatoms, to both assimilate phosphorus and avoid high light. Upon onset of seasonal upwelling, they are entrained within subsequent onshore transport to coastal waters. Here, low N/P ratios of ambient inorganic nutrients favor the Sun-adapted diazotrophs, and high CDOM the associated shade-adapted dinoflagellates, not the faster-growing diatoms. After initial deep-sea and atmospheric supplies of inorganic nutrients, recycled organic forms, from dead diazotrophs and fish, supplement the additional estuarine supplies of nitrogen, phosphorus, and iron for *Karenia* spp. Thus, the maintenance and ultimate impacts of nondiatomaceous phytoplankton on fish and mammals are instead determined by the factors effecting recycled nutrient conditions on the inner shelves of these and other coastal regions, downstream of aeolian iron supplies.

[180] With respect to other western boundary currents, *Trichodesmium* is also observed within the Gulf Stream at 35°N off the east coast of the United States [Dunstan and Hosford, 1977], as well as off Ireland [Farran, 1932], where *K. mikimotoi* was first found during 1971–1976 [Ballentine and Smith, 1973; Helm et al., 1974; Ottway et al., 1979]. Before then, *Gymnodinium aureolum* was first seen off

Norway in 1966 [Braarud and Heimdal, 1970]. Saharan dust penetrates (Figure 1) both Irish [Tullet, 1984] and Scandinavian [Franzen et al., 1995] skies, with an increase in frequency of Saharan dust events over England and Ireland, since 1968 [Goudie and Middleton, 2001]. Rare observations of African dust falls between 1903 and 1968 became almost monthly events during spring, summer, and fall of 1991 and 1992, when red tides of *K. mikimotoi* had already spread to French, Danish, and Norwegian waters, as well [Landsberg, 2002].

[181] *Trichodesmium* was first described from four blooms in the Red Sea during 1823, with speculation that the name of this sea was derived from the color of these organisms [Ehrenberg, 1830]. Extensive blooms of *Trichodesmium* were also noted in the Red Sea during 1843 [Montagne, 1844], as well, such that in writing later about their observations aboard the *Beagle* [Darwin, 1839] and the *Challenger* [Mosely, 1879], early naturalists were familiar with this phytoplankton. It is thus not surprising that large rates of nitrogen fixation by this cyanophyte and blooms of toxic *Karenia sp.* were found a century later within the adjacent Arabian Sea [Dugdale et al., 1964], and in the Persian Gulf [Heil et al., 2001].

[182] Farther south within the Indian Ocean, *Trichodesmium* is also found within the warm waters of the Agulhas Current [Taylor, 1966], a western boundary current drifting south along the eastern coast of South Africa, where rainfall decreased by ~20% from 1965 to 1985 [Nicholls et al., 1996]. Downstream of the Kalahari Desert (Figure 1), toxic red tides of *K. bicuneiformis* and *K. cristata* were first observed during 2003 in Gordon's Bay and Walker Bay (Table 1), east of Cape Town and adjacent to the Agulhas Current. Neither *Trichodesmium* [Carpenter, 1983], nor *Karenia spp.* are found within the Benguela Current, however, the cold, upwelling eastern boundary current flowing north along the west coast of South Africa.

[183] By contrast, in response to a flow reversal of the Humboldt Current off the west coast of South America and another anthropogenic nutrient supply of the supplemental form of dead fish, an enormous red tide of ~150 ug chl l⁻¹ of ichthyotoxic *Karenia spp.* was observed within salmon farms off the Chiloe Archipelago (44°S, 75°W) of southern Chile during March–April 1999 [Clement et al., 2001; Carreto et al., 2001]. Like the Hong Kong red tide in 1998, the Chilean one also dispersed over a larger area, extending along the coast from 42°S to 54°S during 1999, i.e. downstream of the coastal Atacama Desert around Antofogasta, Chile at 24°S (Figure 1).

[184] Here, rainfall in northern Chile decreased by ~50% from 1965 to 1985 [Nicholls et al., 1996]. The local rainfall during both 1998 and 1999 in southern Chile was lower than normal [Clement et al., 2001] as well, following the longer-term trend. Moreover, the surface temperature of seawater in the Chiloe Archipelago during March 1999 was 1.5°C warmer than usual [Clement et al., 2001], suggesting southward advection of subtropical water.

[185] El Nino during the preceding year of 1998 was the strongest event over the last century [Chavez et al., 1999], with warm sea surface temperature anomalies of >5.0°C found at 100°W, averaged over 2°N to 2°S (www.pmel.noaa.gov/tao). As the equatorial Kelvin waves propagate eastward across the Pacific Ocean during such major events,

poleward transports of tropical indicator species, i.e. red and pelagic crabs, *Pleuroncodes planipes* and *Euphyllax dovii*, occur within the eastern boundary currents off North and South America, as in El Nino of 1972 [Walsh, 1978]. During El Nino of 1982–83, populations of the shrimp, *Penaeus occidentalis*, propagated south from Equador to Peru, as well [Barber and Chavez, 1983].

[186] Similarly, background populations of *Trichodesmium* are found over 2°N to 2°S along 165°W [Marumo and Asaoka, 1974b]. We speculate that these diazotrophs may have been advected southwards during 1998 along the Peru-Chile coasts of local dust influxes (Figure 1) to pass DON and ammonium to small initial red tides of *Karenia*. At times, the nontoxic dinoflagellate *Gymnodinium splendens* is a dominant of the phytoplankton community off the Peru coast, amounting to as much as 25 ug chl l⁻¹, derived from upwelled nutrients [Walsh, 1996]. Thus, we further speculate that if the salmon farms were not already present as a supplemental food supply for *Karenia spp.* in the Chiloe Archipelago, their red tide during 1999 might have much less, i.e. 7–10 fold smaller. Furthermore, since the major El Ninos of 1972 and 1998 are rare events off Peru and Chile, we presume that such future toxic red tides of *Karenia spp.* at 43°S within the Humboldt Current off western South America will also continue to be unusual.

[187] This may no longer be the case for the same latitude off eastern South America, however, where another western boundary current flows south as the Brazil Current. Here, populations of *K. mikimotoi*, also known as *Gyrodinium aureolum*, have been found both during 1981 off Brazil at ~32°S [Rosa and Buselato, 1981] and in 1999 off Argentina at ~39°S [Negri et al., 1992]. Off Mar del Plata [Carreto et al., 1986], and at 43°S within the Golfo Nuevo of Patagonia, the NO₃/PO₄ ratios of the shallow water column above the 10–40 m isobaths of the Argentine shelf are also 2.0–4.6, after the spring and fall blooms of diatoms [Negri et al., 1992; Gayoso, 2001], like the nutrient stocks on the inner Texas and Florida shelves.

[188] Furthermore, similar *Trichodesmium* blooms have washed ashore at 35°S on Uruguayan beaches [Mendez and Medina, 2004], like those found off St. Petersburg Beach and Sarasota, FL. Other “vast swarms” of *Trichodesmium* were observed at 40°S, 45°W, between Montevideo and South Georgia Island [Hart, 1934], reflecting southward transport in western boundary currents along Argentina. Finally, plumes of dust haze have been observed by ships at sea during each season of the year, as they exit the southeast Argentine mainland towards South Georgia [Prospero, 1981], and the rainfall decreased by ~30% in the western Patagonian Desert from 1965 to 1985 [Nicholls et al., 1996].

[189] However, since the warm Brazil Current separates from the Argentine shelf, “somewhere between 33 and 38°S, forming an intense front with the cold water of the Malvinas Current, a northward extension of the Circumpolar Current” [Tomczak and Godfrey, 1994], a focal point of nitrogen exchange between *Trichodesmium* and *Karenia* may lie far offshore, away from most human observers. As yet, moreover, only a few cases of anemic shellfish poisoning [Negri et al., 2004] and diarrhetic shellfish poisoning [Gayoso et al., 2004] have been reported within

shelf waters off Patagonia, not NSP from *Karenia spp.* Time will tell!

Appendix A

[190] Our coupled model consists of 23 state variables: temperature, salinity, u , v , w , K_z , spectral light, CDOM, dissolved organic carbon, dissolved organic nitrogen, dissolved organic phosphorus, nitrate (+nitrite), ammonium, phosphate, phytoplankton (POC, PON, POP, chlorophyll), heterotrophic bacteria, large and small particulate detritus of biotic origin, as well as lithogenic suspended sediments. The model has three components of (1) circulation, (2) bio-optical, and (3) ecological processes. The third one is forced by outputs of the first two submodels [Jolliff, 2004].

[191] Flow, thermal, and buoyancy fields are computed by the USF application of the Princeton Ocean Model (POM), which solves the primitive equations of motion [Blumberg and Mellor, 1987] over a horizontal grid of 2–6 km and a vertical sigma coordinate of 21 layers. The coupled model is forced by NCEP reanalysis winds, air pressure, net surface heat fluxes, river inflows, and offshore pressure gradients of the Loop Current. It ignores tides, however.

[192] The internal light field, as well as the water-leaving radiances, are computed from the bio-optical submodel's inherent optical properties (IOP's). They are a function of some of the absorption and backscatter properties of sea water and of the state variables of the ecological model, i.e. phytoplankton biomass, heterotrophic bacteria, colored dissolved organic matter, particulate detritus, and inorganic suspended sediments [Jolliff, 2004].

[193] Food web closure is exerted by imposing an empirical estimate of grazing pressures on the phytoplankton community of the northern Gulf of Mexico [Fahnenstiel et al., 1995]. However, silica limitation of diatoms [Dortch and Whitley, 1992] is ignored, as well as iron limitation of precursor diazotrophs. Since dust loading of iron has prevailed in the Gulf of Mexico, since before 1830 [Darwin, 1839] - and presumably before 1530 [Cabeza de Vaca, 1871], we focus instead on phosphorus-limitation in the WFS, as suggested from our analyses of both Texas waters and the Great Barrier Reef. The phytoplankton state variable thus represents a composite community, with mean properties of diatoms, coccolithophores, diazotrophs, and red tides (Table 3).

[194] As before [Walsh et al., 2003; Jolliff et al., 2003], the state equations of the ecological and bio-optical submodels are solved over the curvilinear horizontal grid and vertical sigma coordinate system of the POM [He and Weisberg, 2002, 2003; Weisberg and He, 2003]. During the March and August 1998 cases of this model, the POM results are read in once every simulation day and then interpolated over 240 time steps to solve for advection and vertical turbulent mixing of the ecological and bio-optical constituents every 6 minutes. Since our use of the POM had been published, here we focus on the ecological interactions. Similarly, the bio-optical formulation of the IOPs has been described [Jolliff, 2004], such that we restrict discussion here to our present assumptions of the simulated nutrient-plankton interactions, whose results are displayed in Figures 22–25.

[195] We start with the boundary conditions, because, of course, they ultimately determine the solutions of the state equations over the model grid. Estimates of daily freshwater discharge are made from United States Geological Survey (USGS) discharge data (<http://waterdata.usgs.gov/nwis>) and the South Florida Water Management District's (SFWMD) annual reports for 1998–2000 (<http://www.sfwmd.gov/org/ema/everglades/previous.html>). Values of flow were selected, based upon the following criteria: (1) gauging station readings were not obscured by tidal forces, and (2) the gauging station contributed to the cumulative freshwater discharge for a given watershed, but its contribution was not duplicated by a discharge gauge located farther downstream. Thus, we used a network of 70 discharge gauging stations to estimate total daily freshwater inflows to the northeastern Gulf of Mexico.

[196] Our numerical analyses consider two contrasting periods of regional freshwater bimodal discharges during March and August 1998, in response to mainly spring rainfall in the north and summer precipitation in the south. Given estimates of freshwater influxes, DOC and associated CDOM loadings, the most important factors are then the inorganic nutrient contents (Table 2). They constitute the boundary conditions for 30 river systems, impinging the WFS, from the Mississippi River delta to the Florida Keys.

[197] Average concentrations (Table 2) for the freshwater end-member of (1) the colored dissolved organic carbon (CDOC) component of CDOM, (2) the nitrate + nitrite, (3) ammonium, (4) phosphate stocks, and (5) the suspended sediments (SS) are multiplied by the daily flow-rate to establish an estuarine loading for the upper five m of the water column at appropriate coastal boundary grid cells. The CDOC concentrations are estimated with a combination of CDOM absorption and DOC measurements for rivers of the model's domain [Stovall-Leonard, 2003], as well as literature values [Clark et al., 2002; Miller et al., 2002; Zepp and Schlotzhauer, 1981]. The CDOC of terrestrial origin is assumed to be largely refractory to biological degradation as it moves through the estuaries [Mantoura and Woodward, 1983]. The inorganic nutrient and SS end-member concentrations are obtained from the USGS-NWIS and the SFWMD-DBHYDRO databases. In particular, our choice for the nitrogen and phosphorus contents at the heads of two of these contrasting estuaries, i.e. those of the Caloosahatchee and Apalachicola Rivers, reflects our initial analysis of the consequences of mining and farming activities over the last 25–50 years within their drainage basins.

[198] The Altamaha River drains similar Georgia soils as those surrounding the basin of the Apalachicola River. The former exhibits some impacts of agriculture by 1975, when, the nitrate content of the Altamaha River had doubled to $\sim 16 \text{ umol NO}_3 \text{ kg}^{-1}$, from that of $\sim 8 \text{ umol NO}_3 \text{ kg}^{-1}$ in 1955 [Walsh et al., 1981]. In 1975, the nutrient content of the Apalachicola River at Chattahoochee was similarly $16.7 \text{ umol NO}_3 \text{ kg}^{-1}$, with more recent estimates of $23.2 \text{ umol NO}_3 \text{ kg}^{-1}$ (Table 2). Furthermore, the nitrogen content of another northern Florida river - the Cipola River, which is a tributary of the Apalachicola River - had doubled between 1958 and 1975 [Dickson, 2001].

[199] In our model, we instead use a larger estimate of nutrient loading from this northern river of $23.2 \text{ umol NO}_3 \text{ kg}^{-1}$, not 8 or $16 \text{ umol NO}_3 \text{ kg}^{-1}$ (Table 2). It thus

emphasizes any consequences of northern anthropogenic nutrient loading. Furthermore, the outflow of the Apalachicola River (Figure 5) is larger than the sum of all other Florida rivers between Capes San Blas and Romano [Nordlie, 1990]. Yet, we shall find that the southern fossil source of phosphorus still predominates in our model as the trigger for iron-sated diazotroph initiation of red tides on the WSF.

[200] In our numerical analyses, we allow for modulation of the fossil sources by possible effects of human additions of nutrients to both southern and northern estuaries, entering the WFS (Table 2). But to not over-emphasize the role of the southern estuaries in our model, we assume a boundary condition for the Caloosahatchee River of $4.3 \text{ umol PO}_4 \text{ kg}^{-1}$ (Table 2). It is not that of $\sim 6.0 \text{ umol PO}_4 \text{ kg}^{-1}$ found in 1982 (Figure 2a). But it exceeds the mean amount of $\sim 1.5 \text{ umol PO}_4 \text{ kg}^{-1}$ estimated and observed along the southern edge of the WFS during 1947–1954 and 2001.

[201] The NEGOM cruises [Jochens and Nowlin, 1999] provide deep-water (>300 m depth) measurements of inorganic nutrients over the continental slope of the WFS and the deep Gulf of Mexico. These data are averaged over all cruises, from spring 1998 to summer 2000, to construct composite means for the deep Gulf of Mexico of $25.1 \text{ um NO}_3 \text{ kg}^{-1}$, $1.5 \text{ um NH}_4 \text{ kg}^{-1}$, and $1.7 \text{ um PO}_4 \text{ kg}^{-1}$, i.e. a DIN/PO₄ ratio of 15.6. These values are inserted as time-invariant boundary conditions below a depth of 300 m in the coupled model. This approach allows the deep-water nutrient fields to evolve over the continental slope and shelf with the simulated temperature fields, such that the position and slope of the 18°C isotherm are generally consistent with those of the nitricline.

[202] The composite phytoplankton biomass in terms of carbon, PC, as well as those of PN, PP, and chlorophyll via appropriate ratios (Table 3) is computed from

$$\frac{\partial P}{\partial t} = \text{Tr}(P) - \frac{\partial}{\partial z}(wP) + (g - \epsilon - \eta)P \quad (\text{A1})$$

where all $\text{Tr}(\dots)$ terms represent physical advective and diffusive transport of the nutrient and plankton variables, i.e. A = nitrate, ammonium, phosphate, DOC, DON, DOP, CDOM, bacteria, and phytoplankton, described as

$$\text{Tr}(A) = - \left[\frac{\partial}{\partial x}(uA) + \frac{\partial}{\partial y}(vA) + \frac{\partial}{\partial z}(wA) \right] + \frac{\partial}{\partial z} \left(K_h \frac{\partial A}{\partial z} \right) \quad (\text{A2})$$

with u , v , w and K_z supplied at each grid point of the coupled model from the POM, after correction for the additional settling velocities of the plankton.

[203] The net carbon-based growth rate of the phytoplankton community is computed from the gross realized growth rate, g , minus the basal respiration rate, ϵ , and the grazing rate, η in equation (A1). Here, g is the minimum carbon-equivalent of the light-regulated, g_l , nitrogen-regulated, g_n , and phosphorus-regulated, g_p , uptake rates of phytoplankton computed over the water column at each time step of the numerical integration. Firstly, the light limited growth rate, g_l , is a partial function of the apparent quantum yield of photosynthesis and the temperature-adjusted maximal assimilation rate, derived from two submodels of spectral-dependent (λ) light fields.

[204] Incident irradiance is computed with both a clear sky submodel [Gregg and Carder, 1990] for the visible range of light over 350–700 nm and the GCSOLAR UV submodel [Zepp and Cline, 1977] over the lower spectral range of 295–350 nm. They yield direct and diffuse irradiances just below the sea surface, with respective $\Delta\lambda$ of 10 nm and 20 nm. The first submodel is also adjusted to account for cloud cover, using NCEP (National Center for Environmental Prediction) regional cloud fractions over 8 regions of the Gulf of Mexico. The direct component of irradiance is reduced by 15% to 85% as linear function of the cloud cover.

[205] Just below the sea surface, the planar irradiance, $E_d(0, \lambda)$ is then estimated from the diffuse attenuation of the downwelling irradiance, $K_d(\lambda)$, with a single-scatter approximation of

$$K_d(\sigma, \lambda) = [a_t(\sigma, \lambda) + bb_t(\sigma, \lambda)]u_d^{-1} \quad (\text{A3})$$

The average cosine of downwelling irradiance, u_d , is estimated from the solar zenith angle, after accounting for light refraction through the air/sea interface. Attenuation of the spectral light of 300–700 nm over each vertical sigma coordinate level (σ) follows the Beer-Lambert law of

$$E_d(\sigma, \lambda) = E_d(\sigma - 1, \lambda) * \exp[-K_d(\sigma, \lambda) dz] \quad (\text{A4})$$

[206] The total quantity of photons absorbed by the phytoplankton is used to calculate their light limitation and photo-inhibition terms. Absorption by CDOM is also used to estimate photochemical yields [Jolliff et al., 2003]. Photons removed from the upwelling radiance stream are also estimated from the irradiance reflectance [$R = E_u/E_d$] for each sigma coordinate level [Mobley, 1994] by

$$R(\sigma, \lambda) = K_d(\sigma, \lambda) - a_t(\sigma, \lambda)u_d^{-1}/K_u(\sigma, \lambda) - a_t(\sigma, \lambda)u_u^{-1} \quad (\text{A5})$$

where the average cosine of upwelling irradiance, u_u , is constant at 0.39 [Kirk, 1994].

[207] The absorbed photon flux density of photosynthetically usable radiation (PUR) over 350–700 nm absorbed within each sigma level of the POM is obtained from

$$\rho_{\text{PUR}} = \int_{350\text{nm}}^{700\text{nm}} [E_d(\sigma - 1, \lambda) - E_d(\sigma, \lambda)] fa_{\phi\text{PS}} d\lambda \quad (\text{A6})$$

where the fraction of light absorbed by phytoplankton pigments is given by

$$fa_{\phi\text{PS}} = a_{\phi\text{PS}}/a_t + bb_t \quad (\text{A7})$$

with the spectral and sigma coordinate notation dropped for simplicity.

[208] Only photons absorbed are available to do photochemical work, such that in the enzymatically mediated photochemical process of photosynthesis, this simple relationship is expressed by the apparent quantum yield of

$$\Phi_c = \text{moles organic carbon produced/moles photons absorbed} \quad (\text{A8})$$

The maximum rate of photon absorption by phytoplankton biomass is then computed as the maximal rate of growth by the phytoplankton biomass and the inverse of the apparent quantum yield as

$$\rho_{\text{mPUR}} = g_{\text{max}} P(\Phi_c)^{-1} \quad (\text{A9})$$

[209] It follows from these relationships that absorbed photon fluxes below this threshold would limit phytoplankton photosynthesis, while larger fluxes may inhibit their growth. However, a strictly linear reduction of their maximal growth rate did not replicate the usual hyperbolic relation of micro-algal growth (or photosynthesis) rate and irradiance. Since photosynthesis is an enzymatically mediated photochemical process, the kinetics of such metabolic activities is best mimicked by Michaelis-Menten type functions.

[210] Accordingly, we calculate the TPCY (theoretical photosynthesis carbon yield) as the product of the absorbed photon flux density and the quantum yield of photosynthesis. In our model, if the ratio of TPCY to the temperature-adjusted maximal assimilation rate ($g_{\text{max T}}$) is <1 , we obtain the light-limited growth rate from

$$g_l = \text{TPCY}/g_{\text{max T}} P[\text{MM}_l + \text{TPCY}/g_{\text{max T}} P]^{-1} \quad (\text{A10})$$

where MM_l is the Michaelis-Menten half saturation constant for photon flux of ~ 0.072 [Rubio et al., 2003].

[211] Since little is known about the environmental factors that trigger photo-adaptation of *K. brevis* [Evens and Leblond, 2004], little explicit modification of light-regulated photosynthesis was attempted. If the ratio of TPCY to the temperature-adjusted maximal assimilation rate ($g_{\text{max T}}$) was >4 , the photo-inhibition simply resulted in

$$g_l = \left[1.0 + [E_d(\sigma, \text{PAR})]^{1/2} \right]^{-1} \quad (\text{A11})$$

where PAR is the integrated irradiance over 350–700 nm.

[212] Finally, the light-regulated growth of the phytoplankton community is also a function of the POM's temperature field as

$$g_l = f[\Phi_c, g_{\text{max}}(T)] \quad (\text{A12})$$

[213] Nitrogen limitation of phytoplankton growth is given by

$$g_N = g_{\text{max}} \left[\frac{NO_3}{k_{NO_3} + NO_3}, \frac{NH_4}{k_{NH_4} + NH_4} \right] \quad (\text{A13})$$

where nitrate uptake is also inhibited in the presence of ammonium.

[214] Similarly, phosphorus limitation is expressed by

$$g_P = g_{\text{max}} \left[\frac{PO_4}{k_{PO_4} + PO_4} \right] \quad (\text{A14})$$

[215] In terms of temperature effects on phytoplankton metabolism, both their growth, respiration, ϵ and grazing, η ,

rates of equation (A1) are impacted by POM's temperature fields. Since zooplankton data were scarce, however, the grazing losses are also a simple function [Ivlev, 1955] of their biomass expressed by

$$\eta = \eta_{\text{max}} [1 - e^{-I}] \quad (\text{A15})$$

where η_{max} is the temperature-adjusted grazing rate and I is the Ivlev parameter of $0.05 \text{ m}^3 \text{ mmol C}^{-1}$. The specific grazing rates on phytoplankton within the northern Gulf of Mexico ranged from 0.1 to 2.0 day^{-1} [Fahnenstiel et al., 1995], which we apply to respective phytoplankton stocks of 0.1 and $>8.0 \text{ ug chl}^{-1}$.

[216] The respective bulk DOC stocks within Charlotte Harbor and Apalachicola River are 25.3 and 3.6 mg C l^{-1} (Table 2). The smaller carbon substrate and the larger TDN/TDP ratio of the latter suggested that the organic matter is more refractory in the Apalachicola River, than in Charlotte Harbor. Since bacteria compete against the phytoplankton in utilization of both phosphate and ammonium within the Gulf of Mexico [Pakulski et al., 2000], they may use PO_4 rather than DOP in this northern river. Such heterotrophic activity would exacerbate the P-limitation of the phytoplankton on the northern WFS [Myers and Iverson, 1981].

[217] Bacterial secondary production is also an order of magnitude higher within a red tide on the WFS than in surrounding waters [Heil et al., 2004]. The heterotrophs may thus be competing against *K. brevis* for utilization of the DON of *Trichodesmium* origin. Indeed, since bacteria compete against the phytoplankton in utilization of both phosphate and ammonium in the Gulf of Mexico [Pakulski et al., 2000], they are included as a second explicit plankton state variable in the form of

$$\frac{\partial B}{\partial t} = \text{Tr}(B) + (g - \epsilon - \eta)B \quad (\text{A16})$$

where they have no settling velocity as a consequence of their small size. Like the autotrophic rates of the phytoplankton, the heterotrophic processes of the bacteria are impacted by POM's temperature fields. Their net growth rate is also a minimal function of the available carbon, nitrogen, or phosphorus.

[218] To calculate the assimilation of nitrogen required for balanced bacterial growth in our model, a ratio is constructed of the maximum amount of inorganic nutrients that could potentially be assimilated by them and the amount of NH_4 supplement required, if dissolved organic nitrogen (DON) were insufficient to meet their balanced growth needs. If DON uptake is sufficient [Fasham et al., 1990] to meet bacterial growth at a molar C/N ratio of 5:1, however, ammonium is not used by the bacteria of our model.

[219] A similar calculation is performed for the potential inorganic phosphorus supplement, since DOM tends towards a low phosphorus content, with a large molar C/P ratio of 250. Instead, bacteria have a smaller molar C/P ratio of 53 (Table 3). The net result of these calculations is that in our model, the bacteria compete with the phytoplankton for phosphate, when labile DOC is abundant. This result is consistent with the observations that DOC-rich aquatic

systems tend towards P-limitation [Kirchman, 1994]. The state equations for nitrate, ammonium, phosphate are similar to those of the previous model of the WFS [Walsh et al., 2003].

[220] **Acknowledgments.** This analysis was funded by grants: NA16OP2787 to J.J.W., R.H.W., and K.A.S. from the National Oceanic and Atmospheric Administration as part of the MERHAB program; N00014-99-1-0212 to J.J.W., N00014-96-1-5024 to K.A.F. and J.J.W., N00014-98-1-0158 to R.H.W., N00014-02-1-02661 and N00014-99-1-5020 in support of Tom Hopkins and A.R., from the Office of Naval Research as part of the HyCODE and FSLE programs; NAG5-11254 to F.M.K., NNG04GG04G to F.M.K. and J.J.W., and R-ESSF/03-0000-0039 to J.M.L. from the National Aeronautics and Space Administration; OCE 0095970 to C.A.H. from the National Science Foundation as part of the DOTGOM project; 14-35-0001-30509 and 1435-01-97-CT-30851 to A.E.J. from the Minerals Management Service for the LATEX and NEGOM studies; and USACOE W912HZ-05-C-0040 to J.J.W., C.A.H., R.H.W., K.A.F., K.L.C., and F.M.K. from the Army Corps of Engineers. The State of Florida provided support to C.R.T., K.A.S., and G.J.K. for the Coastal Production and ECOHAB projects, as well as salary support of J.J.W., G.A.V., K.A.F., R.H.W., F.M.K., and C.A.H.. Finally, J.J.W. would like to thank the University of South Florida for a sabbatical leave to undertake such a synthesis. This is ECOHAB contribution 173.

References

- Amon, R. M., and R. Benner (1996), Photochemical and microbial consumption of dissolved organic carbon and dissolved oxygen in the Amazon River system, *Geochim. Cosmochim. Acta*, **60**, 1783–1792.
- Andrews, J. P., and P. Gentian (1982), Upwelling as a source of nutrients for Great Barrier Reef ecosystems: A solution to Darwin's question, *Mar. Ecol. Prog. Ser.*, **8**, 257–269.
- Baden, D. G., and T. J. Mende (1979), Amino acid utilization by *Gymnodinium breve*, *Phytochemistry*, **18**, 247–251.
- Baird, D., E. Jarolim, D. Laine, B. Laine, E. Peterson, and N. E. Schlecht (2003), *Frommer's Texas*, 2nd ed., 211 pp., Hungry Minds, New York.
- Ballentine, D., and F. M. Smith (1973), Observations on blooms of the dinoflagellate *Gyrodinium aureolum* Hulbert in the river Conwy and its occurrence along the north Wales coast, *Br. Phycol. J.*, **8**, 233–238.
- Barber, R. T., and F. P. Chavez (1983), Biological consequences of El Niño, *Science*, **222**, 1203–1210.
- Bates, J. D. (1963), Heavy mineral reconnaissance Florida west coast, *Econ. Geol.*, **58**, 1237–1245.
- Bell, P. R. (1992), Eutrophication and coral reefs—Some examples in the Great Barrier Reef lagoon, *Water Res.*, **26**, 553–568.
- Benner, R., J. D. Pakulski, M. McCarthy, J. I. Hedges, and P. G. Hatcher (1992), Bulk chemical characteristics of dissolved organic matter in the ocean, *Science*, **255**, 1561–1564.
- Berman-Frank, I., P. Lundgren, Y.-B. Chen, H. Kupper, Z. Kolber, B. Bergman, and P. G. Falkowski (2001), Segregation of nitrogen fixation and oxygenic photosynthesis in the marine cyanobacterium *Trichodesmium*, *Science*, **294**, 1534–1537.
- Berman-Frank, I., K. D. Bidle, L. Haramity, and P. G. Falkowski (2004), The demise of the marine cyanobacterium *Trichodesmium* spp., via an autocatalyzed cell death pathway, *Limnol. Oceanogr.*, **49**, 997–1005.
- Biegalski, S. R., and T. A. Villareal (2005), Correlations between atmospheric aerosol trace element concentrations and red tide at Port Aransas, Texas, on the Gulf of Mexico, *J. Radioanal. Nucl. Chem.*, **263**, 767–772.
- Birdsall, B. C. (1979), Eastern Gulf of Mexico continental shelf phosphorite deposits, Ph.D. dissertation, Univ. of South Fla., Tampa.
- Blumberg, A. F., and G. L. Mellor (1987), A description of a three dimensional coastal ocean circulation model, in *Three-Dimensional Coastal Ocean Models, Coastal Estuarine Ser.*, vol. 4, edited by N. S. Heaps, pp. 208–233, AGU, Washington, D. C.
- Bontempi, P. S. (1995), Phytoplankton distributions and species composition across the Texas-Louisiana continental shelf during two flow regimes of the Mississippi River, M. S. thesis, Tex. A & M Univ., College Station.
- Borstad, G. A. (1978), Some aspects of the occurrence and biology of *Trichodesmium* (Cyanophyta) in the western tropical Atlantic near Barbados, West Indies, Ph.D. thesis, McGill Univ., Montreal.
- Borstad, G. A. (1982), The influence of the meandering Guiana Current on the surface conditions near Barbados—Temporal variations of *Trichodesmium* (Cyanophyta) and other plankton, *J. Mar. Res.*, **40**, 435–452.
- Boustead, N. C., F. H. Chang, and H. J. McAllum (1987), Plankton blooms and salmon farming, *Aquacult. Inf. Leaf.*, **1**, 2–3.
- Braarud, X., and X. Heimdal (1970), Brown water on the Norwegian coast in autumn in 1966, *Nytt. Mag. Botany*, **17**, 91–97.
- Bradley, R. S., H. F. Diaz, J. K. Eischeid, P. D. Jones, P. M. Kelly, and C. M. Goodess (1987), Precipitation fluctuations over Northern Hemisphere land areas since the mid-19th century, *Science*, **237**, 171–175.
- Brand, L. E. (2002), The transport of terrestrial nutrients to south Florida coastal waters, in *The Everglades, Florida Bay, and Coral Reefs of the Florida Keys: An Ecosystem Source Book*, pp. 361–413, CRC Press, Boca Raton, Fla.
- Bryceson, I., and P. Fay (1981), Nitrogen fixation in *Oscillatoria (Trichodesmium) erythraea* in relation to bundle formation and trichome differentiation, *Mar. Biol.*, **61**, 159–166.
- Bucher, A., and G. Lucas (1984), Sedimentation eolienne intercontinentale, poussières sahariennes et géologie, *Bull. Cent. Rech. Explor. Prod. Elf Aquitaine*, **8**, 151–165.
- Buskey, E. J., J. Stewart, J. Peterson, and C. Collumb (1996), Current status and historical trends of brown tide and red tide phytoplankton blooms in the Corpus Christi Bay National Estuary Program study area, *Rep. CCBNEP-07*, 174 pp., Tex. Nat. Resour. Conserv. Comm., Austin.
- Buzan, D., W. G. Denton, J. Mambretti, K. Rice, and K. Quinez (1998), Fish kills in the northwestern Gulf of Mexico, 26 April–27 June 1994, *NOAA Tech. Rep. NMFS*, **143**, 27–32.
- Cabeza de Vaca, A. N. (1871), *Le Relacion*, translated by T. B. Smith, Bradford Club, New York.
- Caccia, V. G., and F. J. Millero (2003), The distribution and seasonal variation of dissolved trace metals in Florida Bay and adjacent waters, *Aquat. Geochem.*, **9**, 114–144.
- Calef, G. W., and G. D. Grice (1966), Relationship between the blue-green alga *Trichodesmium thiebautii* and the copepod *Macrosetella gracilis* in the plankton off northeastern South America, *Ecology*, **47**, 855–856.
- Cannizzaro, J. P., K. L. Carder, F. R. Chen, J. J. Walsh, Z. Lee, and C. Heil (2004), A novel optical classification technique for detection of red tides in the Gulf of Mexico, in *Harmful Algae 2002*, edited by K. A. Steidinger et al., pp. 282–434, Fla. Fish and Wildlife Comm., St. Petersburg.
- Capone, D. G., M. D. Ferrier, and E. J. Carpenter (1994), Amino acid cycling in colonies of the planktonic marine cyanobacterium *Trichodesmium thiebautii*, *Appl. Environ. Microbiol.*, **60**, 3989–3995.
- Capone, D. G., J. P. Zehr, H. W. Paerl, B. Bergman, and E. J. Carpeneter (1997), *Trichodesmium*, a globally significant marine cyanobacterium, *Science*, **276**, 1221–1229.
- Carder, K. L., and R. G. Steward (1985), A remote-sensing reflectance model of a red-tide dinoflagellate off west Florida, *Limnol. Oceanogr.*, **30**, 286–298.
- Carpenter, E. J. (1983), Nitrogen fixation by marine *Oscillatoria (Trichodesmium)* in the world's oceans, in *Nitrogen in the Marine Environment*, edited by E. J. Carpenter and D. G. Capone, pp. 65–103, Elsevier, New York.
- Carpenter, E. J., and T. Roenneberg (1995), The marine planktonic cyanobacterium *Trichodesmium* spp.: Photosynthetic rate measurements in the SW Atlantic Ocean, *Mar. Ecol. Prog. Ser.*, **118**, 267–273.
- Carpenter, E. J., B. Bergman, R. Dawson, P. J. Siddiqui, E. Soderback, and D. G. Capone (1992), Glutamine synthetase and nitrogen cycling in colonies of the marine diazotrophic cyanobacteria *Trichodesmium* spp., *Appl. Environ. Microbiol.*, **58**, 3122–3129.
- Carreto, J. I., M. L. Lasta, R. M. Negri, and P. D. Glorioso (1986), Toxic red tide in the Argentine Sea: Phytoplankton distribution and survival of the toxic dinoflagellate *Gonyaulax excavata* in frontal area, *J. Plankton Res.*, **8**, 15–18.
- Carreto, J. I., M. Seguel, N. G. Montoya, A. Clement, and M. O. Carignan (2001), Pigment profile of the ichthyotoxic dinoflagellate *Gymnodinium* sp. from a massive bloom in southern Chile, *J. Plankton Res.*, **23**, 1171–1175.
- Cassie, V. (1960), Seasonal changes in diatoms and dinoflagellates off the east coast of New Zealand during 1957 and 1958, *N. Z. J. Sci.*, **3**, 137–172.
- Cassie, V. (1961), Marine phytoplankton in New Zealand waters, *Botany Mar.*, **2**, 1–55.
- Chavez, F. P., P. G. Srutton, G. E. Firederich, R. A. Feely, G. C. Feldman, D. C. Foley, and M. J. McPhaden (1999), Biological and chemical response of the equatorial Pacific Ocean to the 1997–98 El Niño, *Science*, **286**, 2126–2131.
- Chen, C.-T. A., and S.-L. Wang (1999), Carbon, alkalinity and nutrient budgets on the East China Sea continental shelf, *J. Geophys. Res.*, **104**, 20,675–20,686.
- Chew, F. (1953), Results of hydrographic and chemical investigations in the region of the “red tide” bloom on the west coast of Florida in November 1952, *Bull. Mar. Sci. Gulf Carrib.*, **2**, 610–625.
- Clark, C. D., J. Jimenez-Morias, J. Jones, E. Zanardi-Lombardo, C. A. Moore, and R. D. Zika (2002), A time-resolved fluorescence study of dissolved organic matter in a riverine to marine transition zone, *Mar. Chem.*, **78**, 121–135.

- Clement, A., M. Seguel, G. Arzul, L. Guzman, and C. Alarcon (2001), Widespread outbreak of a haemolytic, ichthyotoxic *Gymnodinium* sp. in southern Chile, in *Proceedings of the IX International Symposium on Harmful Algal Blooms, Feb 7–11, 2000, Hobart, Australia*, edited by G. M. Hallegraeff et al., pp. 66–69.
- Crosbie, N. D., and M. J. Furnas (2001), Abundance, distribution and flow cytometric characterization of picophytoplankton populations in central (17°S) and southern (20°S) shelf waters of the Great Barrier Reef, *J. Plankton Res.*, **23**, 809–828.
- Cunningham, K. J., D. F. McNeil, L. A. Guertin, P. F. Ciesielski, T. M. Scott, and L. de Verteuil (1990), New tertiary stratigraphy for the Florida Keys and southern peninsula of Florida, *Geol. Soc. Am. Bull.*, **110**, 231–258.
- Dagg, M. J. (1995), Copepod grazing and the fate of phytoplankton in the northern Gulf of Mexico, *Cont. Shelf Res.*, **15**, 1303–1318.
- Darrow, B. P., J. J. Walsh, G. A. Vargo, R. T. Masserini, K. A. Fanning, and J.-Z. Zhang (2003), A simulation study of the growth of benthic microalgae following the decline of a surface phytoplankton bloom, *Cont. Shelf Res.*, **23**, 1265–1283.
- Darwin, C. (1839), *The Voyage of the Beagle*, Cambridge Univ. Press, New York.
- Darwin, C. (1846), An account of fine dust which often falls on vessels in the Atlantic Ocean, *Q. J. Geol. Soc. London*, **2**, 26–30.
- Davis, C. C. (1948), *Gymnodinium brevis* sp. nov., a cause of discolored water and animal mortality in the Gulf of Mexico, *Botany Gaz.*, **109**, 358–360.
- del Giorgio, P. A., and J. J. Cole (2000), Bacterial energetics and growth efficiency, in *Microbial Ecology of the Oceans*, edited by D. L. Kirchman, pp. 289–325, John Wiley, Hoboken, N. J.
- Denton, W., and C. Contreras (2004), The red tide (*Karenia brevis*) bloom of 2000, *Water Qual. Tech. Ser. WQTS-2004-01*, Tex. Parks and Wildlife Dept., Austin.
- Derr, M. (1998), *Some Kind of Paradise: A Chronicle of Man and the Land in Florida*, Univ. Press of Fla., Gainesville.
- Devassy, V. P., P. M. Bhattathiri, and S. Z. Qasim (1978), *Trichodesmium* phenomena, *Ind. J. Mar. Sci.*, **7**, 168–186.
- Dickman, M. D. (2001), Hong Kong's worst red tide induced fish kill (March–April 1998), in *Proceedings of the IX International Symposium on Harmful Algal Blooms, Feb 7–11, 2000, Hobart, Australia*, edited by G. M. Hallegraeff et al., pp. 58–61.
- Dickson, L. K. (2001), Red tide bloom dynamics with respect to rainfall and river flow, *Tech. Rep. 795*, Mote Mar. Lab., Saratoga, Fla.
- Dinnel, S. P., and W. J. Wiseman (1986), Fresh water on the Louisiana and Texas shelf, *Cont. Shelf Res.*, **6**, 765–784.
- Doering, P. H., and R. H. Chamberlain (1999), Water quality and the source of freshwater discharge to the Caloosahatchee Estuary, FL, *Water Res. Bull.*, **35**, 793–806.
- Donahy, P. L., and T. R. Osborn (1997), Toward a theory of biological-physical control of harmful algal bloom dynamics and impacts, *Limnol. Oceanogr.*, **42**, 1283–1296.
- Dortch, Q., and T. E. Whitledge (1992), Does nitrogen or silicon limit phytoplankton production in the Mississippi River plume and nearby regions?, *Cont. Shelf Res.*, **12**, 1293–1309.
- Doucette, G. J., and P. J. Harrison (1991), Aspects of iron and nitrogen nutrition of the red tide dinoflagellate *Gymnodinium sanguineum*. I. Effects of iron depletion and nitrogen source on biochemical composition, *Mar. Biol.*, **110**, 165–171.
- Dragovich, A. (1963), Hydrology and plankton of coastal waters at Naples, Florida, *J. Fla. Acad. Sci.*, **26**, 22–47.
- Dragovich, A., J. H. Funicane, and B. Z. May (1961), Counts of red tide organisms, *Gymnodinium breve*, and associated oceanographic data from Florida west coast, 1957–59, *Spec. Sci. Rep. Fish. 369*, U. S. Fish and Wildlife Serv.
- Dragovich, A., J. A. Kelly, and H. G. Goodell (1968), Hydrological and biological characteristics of Florida's west coast tributaries, *Fish. Bull.*, **66**, 463–477.
- Duce, R. A., and N. W. Tindale (1991), Atmospheric transport of iron and its deposition in the ocean, *Limnol. Oceanogr.*, **36**, 1715–1726.
- Ducklow, H. (2000), Bacterial and biomass production in the oceans, in *Microbial Ecology of the Sea*, edited by D. L. Kirchman, pp. 85–120, John Wiley, Hoboken, N. J.
- Dugdale, R. C., J. J. Goering, and J. H. Ryther (1964), High nitrogen fixation rates in the Sargasso Sea and the Arabian Sea, *Limnol. Oceanogr.*, **9**, 507–510.
- Dunstan, W. M., and J. Hosford (1977), The distribution of planktonic blue-green algae related to the hydrography of the Georgian Bight, *Bull. Mar. Sci.*, **27**, 624–629.
- Ehrenberg, C. G. (1830), Neue beobachtungen uber blauartige erbscheinungen in Aegypten, Arabien, and Siberien nebst einer uebersicht und kritik der fruher bekannten, *Ann. Phys. Chem.*, **18**, 477–514.
- Eischeid, J. K., H. F. Diaz, R. S. Bradley, and P. D. Jones (1991), A comprehensive precipitation data set for global land areas, Rep. ER-69017T-H1, U. S. Dept. of Energy, Washington, D. C.
- Ertel, J. R., J. I. Hedges, A. H. Devol, J. E. Richey, and M. Ribeiro (1986), Dissolved humic substances in the Amazon river system, *Limnol. Oceanogr.*, **31**, 739–754.
- Etter, P. C., M. K. Howard, and J. D. Cochran (2004), Heat and freshwater budgets of the Texas-Louisiana shelf, *J. Geophys. Res.*, **109**, C02024, doi:10.1029/2003JC001820.
- Evans, G., and L. Jones (2001), Economic impact of the 2000 red tide on Galveston county, Texas: A case study, *Rep. 666226*, Austin, Tex.
- Evens, T. J., and J. D. Leblond (2004), Photophysiology of the Florida red tide *Karenia brevis*: Modifications in the thylakoid lipid composition in response to environmental conditions, in *Harmful Algae 2002*, edited by K. A. Steidinger et al., pp. 414–416, Fla. Fish and Wildlife Comm., St. Petersburg.
- Fahnenstiel, G. L., M. J. McCormick, G. A. Lang, D. G. Redalje, S. E. Lohrenz, M. Markowitz, B. Wagoner, and H. J. Carrick (1995), Taxon-specific growth and loss rates for dominant phytoplankton populations from the northern Gulf of Mexico, *Mar. Ecol. Prog. Ser.*, **117**, 229–239.
- Fan, S., L.-Y. Oey, and P. Hamilton (2004), Assimilation of drifter and satellite data in a model of the northeastern Gulf of Mexico, *Cont. Shelf Res.*, **24**, 1001–1014.
- Fanning, K. A., J. A. Breland, and R. H. Byrne (1982), Radium-226 and radon-222 in the coastal waters of West Florida shelf: High concentrations and atmospheric degassing, *Science*, **215**, 667–670.
- Farran, G. P. (1932), The occurrence of *Trichodesmium thiebautii* off the south coast of Ireland, *Rapp. P.V. Reun. Cons. Int. Explor. Mer.*, **77**, 60–64.
- Fasham, M. J. R., H. W. Ducklow, and S. M. McKelvie (1990), A nitrogen based model of plankton dynamics in the oceanic mixed layer, *J. Mar. Res.*, **48**, 591–639.
- Feinstein, A. (1956), Correlations of various ambient phenomena with red tide outbreaks on the West Florida shelf, *Bull. Mar. Sci.*, **6**, 209–232.
- Feinstein, A., A. R. Ceurvels, R. F. Hutton, and E. Snoek (1955), Red tide outbreaks off the Florida west coast, *Tech. Rep. ML 9491*, Univ. of Miami, Fla.
- Flaig, E. G., and K. E. Havens (1995), Historical trends in Lake Okeechobee ecosystem. I. Land use and nutrient loading, *Arch. Hydrobiol. Suppl. Mongr. Beitr.*, **107**, 1–24.
- Franks, P. J. (1997), Models of harmful algal blooms, *Limnol. Oceanogr.*, **42**, 1273–1282.
- Franzen, L. J., M. Hjelmroos, P. Kallberg, A. Rapp, J. O. Mattsson, and E. Brorstrom-Lunden (1995), The Saharan dust episode of south and central Europe, and northern Scandinavia, March 1991, *Weather*, **50**, 313–318.
- Fraser, T. H., and W. H. Wilcox (1981), Enrichment of a subtropical estuary with nitrogen, phosphorus, and silica, in *Estuaries and Nutrients*, edited by B. J. Watson and L. E. Cronin, pp. 481–498, Humana Press, Totowa, N. J.
- Freeburg, L. R., A. Marshall, and M. Heyl (1979), Interrelationships of *Gymnodinium breve* (Florida red tide) within the phytoplankton community, in *Toxic Dinoflagellate Blooms*, edited by L. T. Taylor and H. H. Seliger, pp. 139–144, Elsevier, New York.
- Furnas, M. J., and A. W. Mitchell (1986), Phytoplankton dynamics in the central Great Barrier Reef. I. Seasonal changes in biomass and community structure and their relation to intrusive activity, *Cont. Shelf Res.*, **6**, 363–384.
- Furnas, M. J., and A. W. Mitchell (1996), Nutrient inputs into the central Great Barrier Reef (Australia) from subsurface intrusions of Coral Sea waters: A two-dimensional displacement model, *Cont. Shelf Res.*, **16**, 1127–1148.
- Gayoso, A. M. (2001), Observations on *Alexandrium tamarense* (Lebour) Balech and other dinoflagellate populations in Golfo Nuevo, Patagonia (Argentina), *J. Plankton Res.*, **23**, 463–468.
- Gayoso, A. M., V. K. Fulco, and C. I. Muglia (2004), Distribution of *Prorocentrum lima* epiphytic on macroalgae in Patagonian Gulfs (Argentina), in *Harmful Algae 2002*, edited by K. A. Steidinger et al., pp. 338–340, Fla. Fish and Wildlife Comm., St. Petersburg.
- Geesey, M., and P. A. Tester (1993), *Gymnodinium breve*: Ubiquitous in Gulf of Mexico waters? in *Toxic Phytoplankton Blooms in the Sea*, edited by T. J. Smayda and Y. Shimizu, pp. 251–255, Elsevier, New York.
- Geider, R. J. (1992), Respiration: Taxation without representation? in *Primary Productivity and Biogeochemical Cycles in the Sea*, edited by P. G. Falkowski and A. D. Woodhead, pp. 333–360, Springer, New York.
- Gentien, P. (1998), Bloom dynamics and ecophysiology of the *Gymnodinium mikimotoi* species complex, in *Physiological Ecology of Harmful Algal Blooms*, edited by D. M. Anderson, A. D. Cembella, and G. M. Hallegraeff, pp. 156–173, Springer, New York.
- Gilbes, F., C. R. Tomas, J. J. Walsh, and F. E. Muller-Karger (1996), An episodic chlorophyll plume on the West Florida shelf, *Cont. Shelf Res.*, **16**, 1201–1224.

- Gilbes, F., F. E. Muller-Karger, and C. E. Del Castillo (2002), New evidence for the West Florida shelf plume, *Cont. Shelf Res.*, 22, 2479–2496.
- Gillette, D. A. (1981), Production of dust that may be carried great distances, *Geol. Soc. Am. Spec. Pap.*, 186, 11–26.
- Glazier, W. C. (1880), On the destruction of fish by polluted waters in the Gulf of Mexico, *Proc. U.S. Nat. Mus.*, 4, 126–127.
- Glibert, P. M., and D. A. Bronk (1994), Release of dissolved organic nitrogen by marine diazotrophic cyanobacteria, *Trichodesmium* spp., *Appl. Environ. Microbiol.*, 60, 3996–4000.
- Goudie, A. S., and N. J. Middleton (2001), Saharan dust storms: Nature and consequences, *Earth Sci. Rev.*, 56, 179–201.
- Graham, H. W., J. M. Amison, and K. T. Marvin (1954), Phosphorus content of waters along the west coast of Florida, *Spec. Sci. Rep.* 122, U. S. Fish and Wildlife Serv.
- Gregg, W., and K. L. Carder (1990), A simple spectral solar irradiance model for cloudless maritime atmospheres, *Limnol. Oceanogr.*, 35, 1657–1675.
- Grill, X., and F. A. Richards (1964), Nutrient regeneration from phytoplankton decomposing in seawater, *J. Mar. Res.*, 22, 51–69.
- Gunter, G. (1952), The importance of catastrophic mortalities for marine fisheries along the Texas coast, *J. Wildlife Manage.*, 16, 63–69.
- Gunter, G., and G. E. Hall (1965), A chemical investigation of the Caloosahatchee River of Florida, *Gulf Res. Rep.*, 21, 1–71.
- Gunter, G., R. H. Williams, C. C. Davis, and F. G. Smith (1948), Catastrophic mass mortality of marine animals and coincident phytoplankton bloom on the west coast of Florida, November 1946 to August 1947, *Ecol. Monogr.*, 18, 309–324.
- Guo, C., and P. A. Tester (1994), Toxic effect of the bloom-forming *Trichodesmium* sp. (Cyanophyta) to the copepod *Acartia tonsa*, *Nat. Toxins*, 2, 222–227.
- Hammet, K. M. (1988), Land use, water use, stream flow, and water-quality characteristics of the Charlotte Harbor inflow area, Florida, *U. S. Geol. Surv. Open File Rep.*, 87–472, 104 pp.
- Hart, T. J. (1934), On the phytoplankton of the southwest Atlantic and the Bellingshausen Sea, *Discovery Rep.*, 8, 3–268.
- Havens, K. E., N. G. Aumen, R. T. James, and V. H. Smith (1996), Rapid ecological changes in a large subtropical lake undergoing cultural eutrophication, *Ambio*, 25, 150–155.
- Havens, J., C. A. Heil, D. Hollander, G. A. Vargo, D. Ault, S. Murasko, and J. J. Walsh (2004), Isotopic constraints on nutrient sources supporting the 2001 *Karenia brevis* bloom, in *Harmful Algae 2002*, edited by K. A. Steidinger et al., pp. 32–34, Fla. Fish and Wildlife Comm., St. Petersburg.
- Haywood, A. J., K. A. Steidinger, E. W. Truby, P. R. Bergquist, P. L. Bergquist, J. Adamson, and L. MacKenzie (2004), Comparative morphology and molecular phylogenetic analysis of three new species of the genus *Karenia* (DINOPHYCEAE) from New Zealand, *J. Phycol.*, 40, 165–179.
- He, R., and R. H. Weisberg (2002), West Florida Shelf circulation and temperature budget for the 1999 spring transition, *Cont. Shelf Res.*, 22, 719–748.
- He, R., and R. H. Weisberg (2003), West Florida Shelf circulation and temperature budget for the 1998 fall transition, *Cont. Shelf Res.*, 23, 777–800.
- Heil, C. A. (1986), Vertical migration of *Ptychodiscus brevis*, M. S. thesis, 118 pp., Univ. of South Fla., Tampa.
- Heil, C. A., P. M. Glibert, M. A. Al-Sarawi, M. Faaj, M. Behbehani, and M. Husain (2001), First record of a fish-killing *Gymnodinium* sp. bloom in Kuwait Bay, Arabian Sea: Chronology and potential causes, *Mar. Ecol. Prog. Ser.*, 214, 15–23.
- Heil, C. A., M. R. Mulholland, D. A. Bronk, P. Bernhardt, and J. M. O'Neil (2004), Bacterial and size fractionated primary production within a *Karenia brevis* bloom on the West Florida shelf, in *Harmful Algae 2002*, edited by K. A. Steidinger et al., pp. 38–40, Fla. Fish and Wildlife Comm., St. Petersburg.
- Heil, C. A., et al. (2006), The multi-species nature of the 2005 *Karenia* bloom: Implications for management and monitoring in Florida, paper presented at the XII International HAB Conference, Copenhagen, Sept.
- Hela, I. (1955), Ecological observations on a locally limited red tide bloom, *Bull. Mar. Sci. Gulf Caribb.*, 5, 269–291.
- Helm, M. M., B. T. Hepper, B. E. Spencer, and P. R. Walne (1974), Lugworm mortalities and a bloom of *Gyrodinium aureolum* Hulbert in the eastern Irish Sea, autumn 1971, *J. Mar. Biol. Assoc. U.K.*, 54, 857–869.
- Herzfeld, M., and D. Hamilton (2000), *The CWR Computational Aquatic Ecosystem Dynamics Model, CAEDYM, Science Manual*, 83 pp., Cent. for Water Res. Univ. West. Aust., Nedlands.
- Higham, C. J., G. J. Kirkpatrick, B. A. Pederson, and B. A. Berg (2004), Photopigment content of three *Karenia brevis* clones in response to varying light levels, in *Harmful Algae 2002*, edited by K. A. Steidinger et al., pp. 417–419, Fla. Fish and Wildlife Comm., St. Petersburg.
- Holm, N. P., and D. E. Armstrong (1981), Role of nutrient limitation and competition in controlling the populations of *Asterionella formosa* and *Microcystis aeruginosa* in semicontinuous culture, *Limnol. Oceanogr.*, 26, 622–634.
- Hopkinson, C. S., B. Fry, and A. L. Nolin (1997), Stoichiometry of dissolved organic matter dynamics on the continental shelf of the north-eastern U.S.A., *Cont. Shelf Res.*, 17, 473–489.
- Hopkinson, J., J. J. Vallino, and A. Nolin (2002), Decomposition of dissolved organic matter from the continental margin, *Deep Sea Res.*, 49, 4461–4478.
- Howard, M. K., and S. F. DiMarco (1998), LATEX shelf data report: Drifters and miscellaneous instruments, *Tech. Rep. 96-6-T*, Dept. of Oceanogr. Tex. A&M Univ., College Station.
- Hulme, M. (1991), An intercomparison of model and observed global precipitation climatologies, *Geophys. Res. Lett.*, 18, 1715–1718.
- Hulme, M., Z.-C. Zhao, and T. Jiang (1994), Recent and future climate change in East Asia, *Int. J. Climatol.*, 14, 637–658.
- Ingersoll, E. (1881), On the fish mortality in the Gulf of Mexico, *Proc. U.S. Nat. Mus.*, 4, 74–76.
- Ivlev, V. S. (1955), *Experimental Ecology of the Feeding of Fishes*, 302 pp., Pischpromizdat, Moscow.
- Janson, S., E. J. Carpenter, and B. Bergman (1994), Compartmentalisation of nitrogenase in a non-heterocystous cyanobacterium: *Trichodesmium contotrum*, *FEMS Microbiol. Lett.*, 118, 9–14.
- Jickells, T. D., et al. (2005), Global iron connections between desert dust, ocean biogeochemistry, and climate, *Science*, 308, 67–71.
- Jochens, A. E., and W. D. Nowlin (1999), Northeastern Gulf of Mexico chemical hydrography and hydrography study: Annual report: Year 2, *Study MMS 99-0054*, OCS, New Orleans, La.
- Jochens, A. E., D. A. Wiesenburg, L. E. Sahl, C. N. Lyons, and D. A. DeFreitas (1998), LATEX shelf data report: Hydrography, April 1992 through November 1994, *Tech. Rep. 96-6-T*, Dept. of Oceanogr. Tex. A&M Univ., College Station.
- Johnson, S. H. (1881), Notes on the mortality among fishes of the Gulf of Mexico, *Proc. U.S. Nat. Mus.*, 4, 205.
- Jolliff, J. K. (2004), The relative influence of coastal effluent and deep water masses on surface optical signals and margin productivity in the northeastern Gulf of Mexico: A three-dimensional simulation analysis, Ph.D. dissertation, Univ. of South Florida, Tampa.
- Jolliff, J. K., et al. (2003), Dispersal of the Suwannee River plume over the West Florida shelf: Simulation and observation of the optical and biochemical consequences of a flushing event, *Geophys. Res. Lett.*, 30(13), 1709, doi:10.1029/2003GL016964.
- Jones, G. B., F. G. Thomas, and C. Burdon-Jones (1986), Influence of *Trichodesmium* blooms on cadmium and iron speciation in Great Barrier Reef lagoon waters, *Estuarine Coastal Shelf Sci.*, 23, 387–401.
- Karl, D. M., R. Letelier, D. V. Hebel, D. F. Bird, and C. D. Winn (1992), *Trichodesmium* blooms and new nitrogen in the North Pacific Gyre, in *Marine Pelagic Cyanobacteria: Trichodesmium and Other Diazotrophs*, edited by E. J. Carpenter, D. G. Capone, and J. G. Reuter, pp. 219–238, Springer, New York.
- Kemp, P., S. Lee, and J. LaRoche (1993), Estimating the growth rate of slowly growing marine bacteria from RNA content, *Appl. Environ. Microbiol.*, 59, 2594–2601.
- Kerfoot, J., G. Kirkpatrick, S. Lohrenz, K. Mahoney, M. Molene, and O. Schofield (2004), Vertical migration of a *Karenia brevis* bloom: Implications for remote sensing of harmful algal blooms, in *Harmful Algae 2002*, edited by K. A. Steidinger et al., pp. 279–281, Fla. Fish and Wildlife Comm., St. Petersburg.
- Ketchum, B. H., and J. Keen (1948), Unusual phosphorus concentrations in the Florida “red tide” sea water, *J. Mar. Res.*, 7, 17–21.
- King, J. E. (1950), A preliminary report on the plankton of the west coast of Florida, *Q. J. Fla. Acad. Sci.*, 12, 109–137.
- Kirchman, D. L. (1994), The uptake of inorganic nutrients by heterotrophic bacteria, *Microbial Ecol.*, 284, 255–271.
- Kirchman, D. L. (2000), Uptake and regeneration of inorganic nutrients by marine heterotrophic bacteria, in *Microbial Ecology of the Oceans*, edited by D. L. Kirchman, pp. 261–289, John Wiley, Hoboken, N. J.
- Kirk, J. T. (1994), *Light and Photosynthesis in Aquatic Ecosystems*, 509 pp., Cambridge Univ. Press, New York.
- Kishi, M., and S. Ikeda (1986), Population dynamics of “red tide” organisms in eutrophicated coastal waters—Numerical experiment of phytoplankton bloom in the east Seto Inland Sea, *Jpn. Ecol. Modell.*, 31, 145–174.
- Klausmeier, C. A., E. Litchman, T. Daufresne, and S. A. Levin (2004), Optimal nitrogen-to-phosphorus stoichiometry of phytoplankton, *Nature*, 429, 171–174.
- Koizumi, Y., T. Uchida, and T. Honjo (1996), Diurnal vertical migration of *Gymnodinium mikimotoi* during a red tide in Hoketsu Bay, Japan, *J. Plankton Res.*, 18, 289–294.

- Kromkamp, J., and A. E. Walsby (1992), Buoyancy regulation and vertical migration of *Trichodesmium*: A computer model prediction, in *Marine Pelagic Cyanobacteria: Trichodesmium and Other Diazotrophs*, edited by E. J. Carpenter, D. A. Capone, and J. G. Rueter, pp. 239–248, Springer, New York.
- Kusek, K. M., G. A. Vargo, and K. A. Steidinger (1999), *Gymnodinium breve*—A scientific and journalistic analysis, *Contrib. Mar. Sci.*, *34*, 1–229.
- Landsberg, J. H. (2002), The effects of harmful algal blooms on aquatic organisms, *Rev. Fish. Sci.*, *10*, 113–390.
- Lasker, R., and F. G. Smith (1954), Red tide in Gulf of Mexico: Its origin, waters, and marine life, *Fish. Bull.*, *89*, 173–176.
- Laws, E. A. (1991), Photosynthetic quotients, new production and net community production in the open ocean, *Deep Sea Res., Part A*, *38*, 143–167.
- Lenes, J. M., et al. (2001), Iron fertilization and the *Trichodesmium* response on the West Florida shelf, *Limnol. Oceanogr.*, *46*, 1261–1277.
- Lenes, J. M., J. J. Walsh, D. B. Otis, and K. L. Carder (2005), Iron fertilization of *Trichodesmium* off the west coast of Barbados: A one-dimensional numerical model, *Deep Sea Res.*, *52*, 1021–1041.
- Livingston, R. J. (1984), The ecology of the Apalachicola Bay system: An estuarine profile, *Rep. FWS/OBS-82/05*, U. S. Fish and Wildlife Serv.
- Loret, P., T. Tengs, T. A. Villareal, H. Singler, B. Richardson, P. McGuire, S. Morton, M. Busman, and L. Campbell (2002), No difference found in ribosomal DNA sequences from physiologically diverse clones of *Karenia brevis* (Dinophyceae) from the Gulf of Mexico, *J. Plankton Res.*, *24*, 735–739.
- Luca, A., C. M. Duarte, S. Agusti, and M. Sondergaard (2003), Nutrient (N, P and Si) and carbon partitioning in the stratified NW Mediterranean, *J. Sea Res.*, *49*, 157–170.
- Lund, E. J. (1936), Some facts relating to the occurrences of dead and dying fish on the Texas coast during June, July, and August 1935, in *Annual Report of the Texas Game, Fish, and Oyster Commission (1934–35)*, pp. 47–50, Austin.
- Luo, T., K. Kramer, D. Goldgof, L. Hall, S. Samson, A. Remsen, and T. Hopkins (2004), Recognizing plankton images from the Shadow Image Particle Profiling Evaluation Recorder, *IEEE Trans. Syst. Man Cybernetics, Part B*, *34*, 1753–1762.
- Luo, T., K. Kramer, D. Goldgof, L. Hall, S. Samson, A. Remsen, and T. Hopkins (2005), Active learning to recognize multiple types of plankton, *J. Mach. Learning Res.*, *6*, 589–613.
- Magana, H. A., and T. A. Villareal (2003), The effect of environmental factors on the growth rate of *Karenia brevis* (Davis) G. Hansen and Moestrup, final report, Tex. Parks and Wildlife Dept., Austin.
- Mantoura, R., and E. Woodward (1983), Conservative behavior of riverine organic carbon in the Severn estuary, *Geochim. Cosmochim. Acta*, *47*, 1293–1309.
- Margalef, R. (1965), Composicion y distribucion del fitoplancton, *Mem. Soc. Cienc. Natl. La Salle*, *25*, 11–40.
- Marumo, R., and O. Asaoka (1974a), *Trichodesmium* in the east China Sea. I. Distribution of *Trichodesmium thiebautii* Gomont during 1961–1967, *J. Oceanogr. Soc. Jpn.*, *30*, 48–53.
- Marumo, R., and O. Asaoka (1974b), Distribution of pelagic bluegreen algae in the North Pacific Ocean, *J. Oceanogr. Soc. Jpn.*, *30*, 77–85.
- Marumo, R., and S. Nagasawa (1976), Seasonal variation of the standing crop of a pelagic blue-green alga *Trichodesmium* in the Kuroshio water, *Bull. Plankton Soc. Jpn.*, *23*, 19–25.
- Masserini, R. T., and K. A. Fanning (2000), A sensor package for the simultaneous determination of nanomolar concentrations of nitrite, nitrate, and ammonia in seawater by fluorescence detection, *Mar. Chem.*, *68*, 323–333.
- McCarthy, J. J., and E. J. Carpenter (1979), *Oscillatoria* (*Trichodesmium*) *thiebautii* (Cyanophyta) in the central North Atlantic Ocean, *J. Phycol.*, *15*, 75–82.
- McPherson, B. F., R. T. Montgomery, and E. E. Emmons (1990), Phytoplankton productivity and biomass in the Charlotte Harbor estuarine system, Florida, *Water Res. Bull.*, *26*, 787–800.
- Meigs, P. (1953), World distribution of arid and semi-arid climates, in *Review of Research on Arid Zone Hydrology*, pp. 203–210, UNESCO, Paris.
- Mendez, S. M., and D. Medina (2004), Twenty-three years of red tide monitoring at fixed stations along the coast of Uruguay, in *Harmful Algae 2002*, edited by K. A. Steidinger et al., pp. 341–343, Fla. Fish and Wildlife Comm., St. Petersburg.
- Miller, W. L., M. A. Moran, W. M. Sheldon, R. G. Zepp, and S. Opsahl (2002), Determination of apparent quantum yield spectra for the formation of biologically labile photoproducts, *Limnol. Oceanogr.*, *47*, 343–352.
- Mills, M. M., C. Ridame, M. Davey, J. LaRoche, and R. J. Geider (2004), Iron and phosphorus co-limit nitrogen fixation in the eastern tropical North Atlantic, *Nature*, *429*, 292–294.
- Milroy, S. P., D. A. Dieterle, R. He, G. J. Kirkpatrick, K. M. Lester, K. A. Steidinger, G. A. Vargo, J. J. Walsh, and R. H. Weisberg (2006), A three-dimensional biophysical model of *Karenia brevis* dynamics on the West Florida shelf: A preliminary look at physical transport and zooplankton grazing controls, *Cont. Shelf Res.*, in press.
- Minagawa, M., and E. Wada (1986), Nitrogen isotope ratios of red tide organisms in the East China Sea: A characterization of biological nitrogen fixation, *Mar. Chem.*, *19*, 245–259.
- Mobley, C. D. (1994), *Light and Water*, 595 pp., Elsevier, New York.
- Montagne, C. (1844), Memoire sur la phenomene de la coloration des eaux de la mer rogue, *Ann. Sci. Nat. Botany Biol. Veg.*, *2*, 332–362.
- Moore, W. S. (1967), Amazon and Mississippi River concentrations of uranium, thorium, and radium isotopes, *Earth Planet. Sci. Lett.*, *2*, 231–234.
- Mosely, H. N. (1879), *Notes by a Naturalist on the "Challenger"*, Macmillan, New York.
- Mulholland, M. R., C. A. Heil, D. A. Bronk, J. M. O'Neil, and P. W. Bernhardt (2004), Does nitrogen regeneration from the N₂ fixing cyanobacteria *Trichodesmium* spp. fuel *Karenia* blooms in the Gulf of Mexico? in *Harmful Algae 2002*, edited by K. A. Steidinger et al., pp. 47–49, Fla. Fish and Wildlife Comm., St. Petersburg.
- Mulholland, M. R., P. W. Bernhardt, C. A. Heil, D. A. Bronk, and J. M. O'Neil (2006), Nitrogen fixation and release of fixed nitrogen by *Trichodesmium* spp. in the Gulf of Mexico, *Limnol. Oceanogr.*, in press.
- Müller-Karger, F. E., J. J. Walsh, R. H. Evans, and M. B. Meyers (1991), On the seasonal phytoplankton concentration and sea surface temperature cycles of the Gulf of Mexico as determined by satellites, *J. Geophys. Res.*, *96*, 12,645–12,665.
- Myers, V. B., and R. Iverson (1981), Phosphorus and nitrogen limited phytoplankton productivity in northeastern Gulf of Mexico coastal estuaries, in *Estuaries and Nutrients*, edited by B. J. Watson and L. E. Cronin, pp. 569–582, Humana Press, Clifton, N. J.
- Nagasawa, S., and R. Marumo (1967), Taxonomy and distribution of *Trichodesmium* in Kuroshio water, *Inf. Bull.*, 139–144.
- Negri, R. M., J. I. Carreto, H. R. Benavides, V. A. Lutz, and R. Akelsman (1992), An unusual bloom of *Gyrodinium cf. aureolum* in the Argentine Sea: Community structure and conditioning factors, *J. Plankton Res.*, *14*, 261–269.
- Negri, R. M., N. G. Montoya, J. I. Carreto, R. Akelsman, and D. Inza (2004), *Pseudonitzschia australis*, *Mytilus edulis*, *Engraulis anchoita*, and domoic acid in the Argentine Sea, in *Harmful Algae 2002*, edited by K. A. Steidinger et al., pp. 139–141, Fla. Fish and Wildlife Comm., St. Petersburg.
- Neuhard, C. A. (1994), Phytoplankton distributions across the Texas-Louisiana shelf in relation to coastal physical processes, M. S. thesis, Tex. A&M Univ., College Station.
- Nicholls, N., G. V. Gruza, J. Jouzel, T. R. Karl, L. A. Ogallo, and D. E. Parker (1996), Observed climate variability and change, in *Climate Change 1995*, pp. 137–192, Cambridge Univ. Press, New York.
- Nordlie, F. G. (1990), Florida rivers, in *Ecosystems of Florida*, edited by R. L. Myers and J. J. Ewel, pp. 392–428, Univ. of Cent. Fla. Press.
- Odum, H. T., J. B. Lackey, J. Hynes, and N. Marshall (1955), Some red tide characteristics during 1953–54, *Bull. Mar. Sci.*, *5*, 247–258.
- Orcutt, K. M., F. J. Lipschultz, K. Gundersen, R. Arimoto, A. F. Michael, A. H. Knap, and J. R. Gallon (2001), A seasonal study of the significance of nitrogen-fixation by *Trichodesmium* at the Bermuda Atlantic Time-series (BATS) site, *Deep Sea Res.*, *48*, 1583–1608.
- Ottway, B. M., M. Parker, D. McGrath, and M. Crowley (1979), Observations of a bloom of *Gyrodinium aureolum* Hulbert on the south coast of Ireland, summer 1976, associated with mortalities of littoral and sublittoral organisms, *Ireland Fish. Invest.*, *18*, 1–9.
- Paerl, H. W., C. Guo, and L. E. Prufert-Bebout (1994), Iron-stimulated N₂ fixation and growth in natural and cultured populations of the planktonic marine cyanobacterium *Trichodesmium*, *Appl. Environ. Microbiol.*, *60*, 1044–1047.
- Pakulski, J. D., R. Benner, T. E. Whittedge, R. M. W. Amon, B. Eadie, L. A. Cifuentes, J. Ammerman, and D. Stockwell (2000), Microbial metabolism and nutrient cycling in the Mississippi and Atchafalaya river plumes, *Estuarine Coastal Shelf Sci.*, *50*, 173–184.
- Paytan, A., B. J. Cade-Menun, K. McLaughlin, and K. L. Faul (2003), Selective phosphorus regeneration of sinking marine particles: Evidence from 31P-NMR, *Mar. Chem.*, *82*, 55–70.
- Pewe, T. L. (1981), Desert dust: An overview, *Geol. Soc. Am. Spec. Pap.*, *186*, 1–10.
- Philips, E. J., and S. Badylak (1996), Spatial variability in phytoplankton standing crop and composition in a shallow inner-shelf lagoon, Florida Bay, Florida, *Bull. Mar. Sci.*, *58*, 203–216.
- Pilson, M. E., and S. B. Betzer (1973), Phosphorus flux across a coral reef, *Ecology*, *54*, 581–588.

- Porter, J. V. (1879), On the destruction of fish by poisonous water in the Gulf of Mexico, *Proc. U.S. Nat. Mus.*, 4, 121–122.
- Prospero, J. M. (1981), Arid regions as sources of mineral aerosols in the marine atmosphere, *Geol. Soc. Am. Spec. Pap.*, 186, 71–86.
- Prospero, J. M. (1996), Saharan dust transport over the North Atlantic Ocean and Mediterranean: An overview, in *The Impact of Desert Dust Across the Mediterranean*, edited by S. Guerzoni and R. Chester, pp. 133–151, Springer, New York.
- Prospero, J. M., and R. T. Nees (1986), Impact of the North African drought and El Niño on mineral dust in the Barbados trade winds, *Nature*, 320, 735–738.
- Prospero, J. M., R. T. Nees, and M. Uematsu (1987), Deposition rate of particulate and dissolved aluminum derived from Saharan dust in precipitation at Miami, Florida, *J. Geophys. Res.*, 92, 14,723–14,731.
- Prufert-Bebout, L., H. W. Paerl, and C. Lassen (1993), Growth, nitrogen-fixation, and spectral attenuation in cultivated *Trichodesmium* species, *Appl. Environ. Microbiol.*, 59, 1367–1375.
- Redfield, A. C., B. H. Ketchum, and F. A. Richards (1963), The influence of organisms on the composition of seawater, in *The Sea*, vol. 2, pp. 26–77, Wiley-Interscience, Hoboken, N. J.
- Reid, D. F. (1984), Radium variability produced by shelf-water transport and mixing in the western Gulf of Mexico, *Deep Sea Res.*, 31, 1501–1510.
- Remsen, A., S. Samson, and T. Hopkins (2004), What you see is not what you catch: A comparison of concurrently collected net, optical plankton counter, and SIPPER data from the northeast Gulf of Mexico, *Deep Sea Res.*, 51, 129–151.
- Revelante, N., and M. Gilmartin (1982), Dynamics of phytoplankton in the Great Barrier Reef Lagoon, *J. Plankton Res.*, 4, 47–76.
- Revelante, M. W., W. Williams, and J. S. Bunt (1982), Temporal and spatial distribution of diatoms, dinoflagellates, and *Trichodesmium* in waters of the Great Barrier Reef, *J. Exp. Mar. Biol. Ecol.*, 63, 24–45.
- Rhodes, L. L., A. J. Haywood, W. J. Ballentine, and A. L. MacKenzie (1993), Algal blooms and climate anomalies in north-east New Zealand, August–December 1992, *N. Z. J. Mar. Freshw. Res.*, 27, 419–430.
- Rhodes, L. L., A. J. Haywood, J. Adamson, K. Ponika, and C. Scholin (2004), DNA probes for the detection of *Karenia* species in New Zealand's coastal waters, in *Harmful Algae 2002*, edited by K. A. Steidinger et al., pp. 273–275, Fla. Fish and Wildlife Comm., St. Petersburg.
- Rieglman, R., W. Stolte, A. M. Noordeloos, and D. Slezak (2000), Nutrient uptake and alkaline phosphatase (ec 3:1:3:1) activity of *Emiliania huxleyi* (prymnesiophyceae) during growth under N and P limitation in continuous cultures, *J. Phycol.*, 36, 87–96.
- Riley, G. A. (1937), The significance of the Mississippi River drainage for biological conditions in the northern Gulf of Mexico, *J. Mar. Res.*, 1, 60–74.
- Roenneberg, T., and E. J. Carpenter (1993), Daily rhythm of O₂ evolution in the cyanobacterium *Trichodesmium thiebautii* under natural and constant conditions, *Mar. Biol.*, 117, 693–697.
- Romans, K. M., E. J. Carpenter, and B. Bergman (1994), Buoyancy regulation in the colonial diazotrophic cyanobacterium *Trichodesmium tenue*: Ultrastructure and storage of carbohydrate, polyphosphate, and nitrogen, *J. Phycol.*, 30, 935–942.
- Rosa, Z. M., and T. C. Busetelo (1981), Sobre ocorrência de floracio de *Gyrodinium aureolum* Hulburt (*Dinophyceae*) no litoral sul do Estado do Rio Grande do Sul, Brazil, *Iberingia*, 28, 169–179.
- Rubio, C. F., F. G. Camancho, J. M. Fernandez Sevilla, Y. Chisti, and E. M. Grima (2003), A mechanistic model of photosynthesis in microalgae, *Biotechnol. Bioeng.*, 81, 459–473.
- Rudnick, D. T., Z. Chen, D. L. Childers, J. N. Boyer, and T. D. Fontaine (1999), Phosphorus and nitrogen inputs to Florida Bay: The importance of the Everglades watershed, *Estuaries*, 22, 398–416.
- Rueter, J. G., K. Ohki, and Y. Fujita (1990), The effect of iron nutrition on photosynthesis and nitrogen fixation in cultures of *Trichodesmium* (Cyanophyceae), *J. Phycol.*, 24, 30–35.
- Rueter, J. G., D. A. Hutchins, R. W. Smith, and N. L. Unsworth (1992), Iron nutrition of *Trichodesmium*, in *Marine Pelagic Cyanobacteria: Trichodesmium and Other Diazotrophs*, edited by E. J. Carpenter, D. A. Capone, and J. G. Rueter, pp. 289–306, Springer, New York.
- Ryder, P. D. (1985), Hydrology of the Florida aquifer system in west-central Florida, *U. S. Geol. Surv. Prof. Pap.*, 1403-F, 63 pp.
- Sanudo-Wilhelmy, S. A., A. B. Kustka, C. J. Gobler, D. A. Hutchins, M. Yang, K. Lwiza, J. Burns, D. G. Capone, and E. J. Carpenter (2001), Phosphorus limitation of nitrogen fixation by *Trichodesmium* in the central Atlantic Ocean, *Nature*, 411, 66–69.
- Sarthou, G., et al. (2003), Atmospheric iron deposition and sea-surface dissolved iron concentrations in the eastern Atlantic Ocean, *Deep Sea Res.*, 50, 1339–1352.
- Schutz, L., R. Jaenicke, and H. Pietrek (1981), Saharan dust transport over the North Atlantic Ocean, *Geol. Soc. Am. Spec. Pap.*, 186, 87–100.
- Shanley, E., and G. A. Vargo (1993), Cellular composition, growth, photosynthesis, and respiration rates of *Gymnodinium breve* under varying light levels, in *Toxic Phytoplankton Blooms in the Sea*, edited by T. J. Smayda and Y. Shimizu, pp. 831–836, Elsevier, New York.
- Sheng, L. T., G. X. Fei, A. Z. Sheng, and F. Y. Xiang (1981), The dust fall in Beijing, China on April 18, 1980, *Geol. Soc. Am. Spec. Pap.*, 186, 149–157.
- Slobodkin, L. B. (1953), A possible initial condition for red tides off the coast of Florida, *J. Mar. Res.*, 12, 148–155.
- Snyder, G. H., and J. M. Davidson (1994), Everglades agriculture: Past, present, and future, in *Everglades: The Ecosystem and Its Restoration*, edited by S. M. Davis and J. C. Ogden, pp. 85–115, St. Lucie Press, Delray Beach, Fla.
- Steidinger, K. A. (1983), A re-evaluation of toxic dinoflagellate biology and ecology, *Prog. Phycol. Res.*, 2, 147–188.
- Steidinger, K. A., G. A. Vargo, P. A. Tester, and C. R. Tomas (1998a), Bloom dynamics and physiology of *Gymnodinium breve* with emphasis on the Gulf of Mexico, in *Physiological Ecology of Harmful Algal Blooms*, edited by D. M. Anderson, A. D. Cembella, and G. M. Hallegraeff, pp. 135–153, Springer, New York.
- Steidinger, K. A., D. A. Stockwell, E. W. Truby, W. J. Wardle, Q. Dortch, and F. M. VanDolah (1998b), Phytoplankton blooms off Louisiana and Texas, May–June 1994, in *Characteristics and Causes of Texas Marine Strandings*, Tech. Rep. NMFS 143, edited by R. Zimmerman, pp. 13–18, NOAA, Seattle, Wash.
- Stovall-Leonard, A. (2003), Characterization of CDOM for the study of carbon cycling in aquatic systems, M. S. thesis, Univ. of South Fla., Tampa.
- Subramanian, A., E. J. Carpenter, and P. G. Falkowski (1999), Bio-optical properties of the marine diazotrophic cyanobacteria *Trichodesmium* spp. II. A reflectance model for remote sensing, *Limnol. Oceanogr.*, 44, 618–627.
- Sunda, W. G., and S. A. Huntsman (1995), Iron uptake and growth limitation in oceanic and coastal phytoplankton, *Mar. Chem.*, 50, 189–206.
- Sutton, T., T. Hopkins, A. Remsen, and S. Burghart (2001), Multisensor sampling of pelagic ecosystem variables in a coastal environment to estimate zooplankton grazing impact, *Cont. Shelf Res.*, 21, 69–87.
- Taylor, F. J. (1966), Phytoplankton of the southwestern Indian Ocean, *Nova Hedwig.*, 12, 433–467.
- Tester, P. A., and K. A. Steidinger (1997), *Gymnodinium breve* red tide blooms: Initiation, transport, and consequences of surface circulation, *Limnol. Oceanogr.*, 42, 1039–1051.
- Tester, P. A., K. Wiles, S. M. Varnam, G. V. Ortega, A. M. Dubois, and V. A. Fuentes (2004), Harmful algal blooms in the western Gulf of Mexico: *Karenia brevis* is messin' with Texas and Mexico, in *Harmful Algae 2002*, edited by K. A. Steidinger et al., pp. 41–43, Fla. Fish and Wildlife Comm., St. Petersburg.
- Tomas, C. R., B. Bendis, and K. Johns (1999), Role of nutrients in regulating plankton blooms in Florida Bay, in *The Gulf of Mexico Large Marine Ecosystem*, edited by H. Kumpf, K. Steidinger, and K. Sherman, pp. 323–337, Blackwell Sci., Malden, Mass.
- Tomczak, M., and J. S. Godfrey (1994), *Regional Oceanography: An Introduction*, 422 pp., Elsevier, New York.
- Trebatoski, B. (1988), Observations on the 1986–1987 Texas red tides *Ptychodiscus brevis*, Rep. 88-02, 48 pp., Tex. Water Comm., Austin.
- Tullet, M. T. (1984), Saharan dust-fall in northern Ireland, *Weather*, 39, 151–152.
- Turner, R. E., and N. R. Rabalais (1994), Coastal eutrophication near the Mississippi river delta, *Nature*, 368, 619–621.
- Turner, R. E., and N. N. Rabalais (1999), Suspended particulate and dissolved nutrient loadings to Gulf of Mexico estuaries, in *Biogeochemistry of Gulf of Mexico Estuaries*, edited by T. S. Bianchi, J. R. Pennock, and R. R. Twilley, pp. 89–107, John Wiley, Hoboken, N. J.
- Twilley, R. R., J. Cowan, T. Miller-Way, P. A. Montagna, and B. Mortazavi (1999), Benthic nutrient fluxes in selected estuaries in the Gulf of Mexico, in *Biogeochemistry of Gulf of Mexico Estuaries*, edited by T. S. Bianchi, J. R. Pennock, and R. R. Twilley, pp. 163–209, John Wiley, New York.
- U.S. Department of Energy (2003), Uranium industry annual 2002, Washington, D.C. (Available at <http://www.eia.doe.gov/fuelnuclear.html>)
- Vallino, J., C. S. Hopkinson, and J. E. Hobbie (1996), Modeling bacterial utilization of dissolved organic matter: Optimization replaces Monod growth kinetics, *Limnol. Oceanogr.*, 41, 1591–1609.
- Van Dolah, F. M., and T. A. Leighfield (1999), Diel phasing of the cell-cycle in the Florida red tide dinoflagellate, *Gymnodinium breve*, *Phycology*, 35, 1404–1411.
- Vargo, G. A., and D. Howard-Shamblott (1990), Phosphorus requirements in *Ptychodiscus brevis*: Cell phosphorus, uptake and growth requirements, in *Toxic Marine Phytoplankton*, edited by E. Graneli et al., pp. 324–329, Elsevier, New York.

- Vargo, G. A., C. A. Heil, D. Spence, M. B. Neely, R. Merkt, K. Lester, R. H. Weisberg, J. J. Walsh, and K. Fanning (2001), The hydrographic regime, nutrient requirements, and transport of a *Gymnodinium breve* Davis red tide on the West Florida shelf, in *Proceedings of the IX International Symposium on Harmful Algal Blooms, Feb 7–11, 2000, Hobart, Australia*, edited by G. M. Hallegraeff et al., pp. 157–160.
- Vargo, G. A., et al. (2004), Four *Karenia brevis* blooms: A comparative analysis, in *Harmful Algae 2002*, edited by K. A. Steidinger et al., pp. 14–16, Fla. Fish and Wildlife Comm., St. Petersburg.
- Villareal, T. A., and H. A. Magana (2001), A red tide monitoring program for Texas coastal waters, final report, 56 pp., Tex. Parks and Wildlife Dept., Austin.
- Villareal, T. A., M. A. Brainard, and L. W. McEachron (2001), *Gymnodinium breve* (DINOPHYCEAE) in the western Gulf of Mexico: Resident versus advected populations as a seed stock for blooms, in *Proceedings of the IX International Symposium on Harmful Algal Blooms, Feb 7–11, 2000, Hobart, Australia*, edited by G. M. Hallegraeff et al., pp. 153–156.
- Vose, R. S., R. L. Schmoyer, P. M. Steurer, T. C. Peterson, R. Heim, T. R. Karl, and J. Eischeid (1992), The global historical climatology network: Long-term monthly temperature, precipitation, sea level pressure, and station pressure data, *Rep. ORNL/CDIAC-53, NDP-041*.
- Walsby, A. E. (1992), The gas vesicles and buoyancy of *Trichodesmium*, in *Marine Pelagic Cyanobacteria: Trichodesmium and Other Diazotrophs*, edited by E. J. Carpenter, D. A. Capone, and J. G. Rueter, pp. 141–161, Springer, New York.
- Walsh, J. J. (1978), The biological consequences of the interaction of the climatic, El Nino, and event scales of variability in the eastern tropical Pacific, *Rapp. P.V. Reun. Cons. Int. Explor. Mer*, 173, 182–192.
- Walsh, J. J. (1988), *On the Nature of Continental Shelves*, 520 pp., Elsevier, New York.
- Walsh, J. J. (1996), Nitrogen fixation within a tropical upwelling ecosystem: Evidence for a Redfield budget of carbon/nitrogen cycling by the total phytoplankton community, *J. Geophys. Res.*, 101, 20,607–20,616.
- Walsh, J. J., and K. A. Steidinger (2001), Saharan dust and Florida red tides: The cyanophyte connection, *J. Geophys. Res.*, 106, 11,597–11,612.
- Walsh, J. J., G. T. Rowe, R. L. Iversen, and C. P. McR (1981), Biological export of shelf carbon is a neglected sink of the global CO₂ cycle, *Nature*, 291, 196–201.
- Walsh, J. J., E. T. Premuzic, J. S. Gaffney, G. T. Rowe, G. Harbottle, R. W. Stoenner, W. L. Balsam, P. R. Betzer, and S. A. Macko (1985), Organic storage of CO₂ on the continental slope off the Mid-Atlantic Bight, the southeastern Bering Sea, and the Peru coast, *Deep Sea Res.*, 32, 853–883.
- Walsh, J. J., et al. (1999), Numerical simulation of carbon-nitrogen cycling during spring upwelling in the Cariaco Basin, *J. Geophys. Res.*, 104, 7807–7825.
- Walsh, J. J., B. Penta, D. A. Dieterle, and W. P. Bissett (2001), Predictive ecological modeling of harmful algal blooms, *Hum. Ecol. Risk Assess.*, 7, 1369–1383.
- Walsh, J. J., K. D. Haddad, D. A. Dieterle, R. H. Weisberg, Z. Li, H. Yang, F. E. Muller-Karger, C. A. Heil, and W. P. Bissett (2002), A numerical analysis of landfall of the 1979 red tide of *Karenia brevis* along the west coast of Florida, *Cont. Shelf Res.*, 22, 15–38.
- Walsh, J. J., et al. (2003), Phytoplankton response to intrusions of slope water on the West Florida shelf: Models and observations, *J. Geophys. Res.*, 108(C6), 3190, doi:10.1029/2002JC001406.
- Walsh, J. J., G. J. Kirkpatrick, B. P. Darrow, G. A. Vargo, K. A. Fanning, E. B. Peebles, C. A. Heil, J. Havens, and K. A. Steidinger (2006), Fish farming by *Karenia brevis*: A nutrient source for large red tides, *Cont. Shelf Res.*, in press.
- Weisberg, R. H., and R. He (2003), Local and deep-ocean forcing contributions to anomalous water properties on the West Florida Shelf, *J. Geophys. Res.*, 108(C6), 3184, doi:10.1029/2002JC001407.
- Weisberg, R. H., B. D. Black, and Z. Li (2000), An upwelling case study on Florida's west coast, *J. Geophys. Res.*, 105, 11,459–11,469.
- Weisberg, R. H., Z. Li, and F. E. Muller-Karger (2001), West Florida shelf response to local wind forcing: April 1998, *J. Geophys. Res.*, 106, 31,239–31,262.
- Weiss, R. F. (1970), The solubility of nitrogen, oxygen, and argon in water and seawater, *Deep Sea Res. Oceanogr. Abstr.*, 17, 721–735.
- Whitledge, T. E. (1989), Data synthesis and analysis—Nitrogen process studies (NIPS): Nutrient distributions and dynamics in Lavaca, San Antonio, and Nueces/Corpus Christi Bays in relation to freshwater inflow, *Tech. Rep. 89-007*, Mar. Sci. Inst. Univ. of Tex., Austin.
- Wilson, W. B. (1966), The suitability of sea-water for the survival and growth of *Gymnodinium breve* Davis; and some effects of phosphorus and nitrogen on its growth, *FSU Prof. Pap. Ser.*, 7, 1–42.
- Wilson, W. B., and A. Collier (1955), Preliminary notes on the culturing of *Gymnodinium breve* Davis, *Science*, 121, 394–395.
- Wilson, W. B., and S. M. Ray (1956), The occurrence of *Gymnodinium brevis* in the western Gulf of Mexico, *Ecology*, 37, 388.
- Wozniak, B., J. Derza, D. Ficek, and R. Majchrowski (2002), Dependence of the photosynthesis quantum yield in the oceans on environmental factors, *Oceanologia*, 44, 439–459.
- Yanagi, T., T. Yamamoto, Y. Koizumi, T. Ikeda, M. Kamazono, and H. Tamori (1995), A numerical simulation of red tide formation, *J. Mar. Syst.*, 6, 269–285.
- Yang, H., and R. H. Weisberg (1999), Response of the West Florida Shelf circulation to climatological wind stress forcing, *J. Geophys. Res.*, 104, 5301–5320.
- Yang, Z. B., and I. J. Hodgkiss (2001), Early 1998 massive fish kills and associated phytoplankton in Port Shelter water, Hong Kong, in *Proceedings of the IX International Symposium on Harmful Algal Blooms, Feb 7–11, 2000, Hobart, Australia*, edited by G. M. Hallegraeff et al., pp. 70–73.
- Yentsch, C. M., and C. S. Yentsch (1982), The attenuation of light by marine phytoplankton with special reference to the absorption of near-UV radiation, in *The Role of Solar Ultraviolet Radiation in Marine Ecosystems*, edited by J. Calkins, pp. 691–706, Springer, New York.
- Yentsch, C. M., C. S. Yentsch, and J. P. Perras (1972), Alkaline phosphatase activity in the tropical marine blue-green alga *Oscillatoria erythraea* ('*Trichodesmium*'), *Limnol. Oceanogr.*, 17, 772–774.
- Young, R. W., et al. (1991), Atmospheric iron inputs and primary productivity: Phytoplankton responses in the North Pacific, *Global Biogeochem. Cycles*, 5, 119–134.
- Zepp, R. G., and D. M. Cline (1977), Rates of direct photolysis in aquatic environments, *Environ. Sci. Technol.*, 11, 359–366.
- Zepp, R. G., and P. F. Schlotzhauer (1981), Comparison of photochemical behavior of various humic substances in water: Spectroscopic properties of humic substances, *Chemosphere*, 10, 479–486.

P. S. Bontempi, Department of Marine Science, University of Southern Mississippi, Stennis Space Center, MS 39529, USA.

K. L. Carder, F. R. Chen, B. P. Darrow, D. A. Dieterle, K. A. Fanning, J. M. Lenes, S. P. Milroy, F. E. Muller-Karger, A. Remsen, E. Shinn, G. A. Vargo, J. J. Walsh, and R. H. Weisberg, College of Marine Science, University of South Florida, St. Petersburg, FL 33701-5016, USA. (jwalsh@seas.marine.usf.edu)

C. A. Heil and K. A. Steidinger, Florida Marine Research Institute, Florida Fish and Wildlife Conservation Commission, St. Petersburg, FL 33701, USA.

A. E. Jochens, Department of Oceanography, Texas A&M University, College Station, TX 77843, USA.

J. K. Jolliff, Naval Research Laboratory, Stennis Space Center, MS 39529, USA.

G. J. Kirkpatrick, Mote Marine Laboratory, Sarasota, FL 34236, USA.

T. N. Lee and J. S. Prospero, Rosenstiel School of Marine and Atmospheric Science, University of Miami, Miami, FL 33149, USA.

D. A. Stockwell and T. E. Whittedge, School of Fisheries and Ocean Sciences, University of Alaska, Fairbanks, AK 99775, USA.

C. R. Tomas, Center for Marine Science, University of North Carolina, Wilmington, NC 28409, USA.

T. A. Villareal, Department of Marine Science, University of Texas, Port Aransas, TX 78373, USA.